Universitat Autònoma de Barcelona

Departament d'Enginyeria Química

Escola d'Enginyeria

TOWARDS GRANULAR BIOMASS IMPLEMENTATION FOR URBAN WASTEWATER TREATMENT

PhD Thesis

Supervised by:

Dr. Julián Carrera Muyo and Dr. Julio Pérez Cañestro

Eduardo Isanta Monclús

Bellaterra, September 2014

JULIÁN CARRERA MUYO i JULIO PÉREZ CAÑESTRO, professors agregats doctors, del Departament d'Enginyeria Química de la Universitat Autònoma de Barcelona,

CERTIFIQUEM:

Que l'enginyer químic EDUARDO ISANTA MONCLÚS ha realitzat sota la nostra direcció, el treball que amb títol "Towards granular biomass implementation for urban wastewater treatment", es presenta en aquesta memòria, i que constitueix la seva Tesi per optar al Grau de Doctor per la Universitat autònoma de Barcelona.

I per a què se'n prengui coneixement i consti als afectes oportuns, presentem a l'Escola d'Enginyeria de la Universitat Autònoma de Barcelona l'esmentada Tesi, signant el present certificat a

Bellaterra, 14 de Juliol de 2014

Dr. Julián Carrera Muyo

Dr. Julio Pérez Cañestro

Acknowledgments

Cuando se acerca el final de una etapa, es inevitable mirar hacia atrás y darse cuenta de que un proyecto tan grande como este es imposible realizarlo sin la aportación de mucha gente. Es por ello, que quiero dedicar estas primeras líneas a todas esas personas que, de manera directa o indirecta, han hecho posible que esto llegara buen puerto. Ya sabéis que soy muy despistado, así que pido perdón por adelantado por si me olvido de alguien!

En primer lugar, quiero dar las gracias a mis directores de tesis, Julio y Julián. Si hoy estoy redactando estos agradecimientos es gracias a la confianza que depositasteis en mi por allá en verano de 2008, gracias a la beca que me ofrecisteis, y sobretodo, gracias a vuestra paciencia, dedicación e ideas, durante todos estos años. Por todo esto, gracias.

Quiero extender el agradecimiento al resto de profesores de GENOCOV, empezando por Mª Eugenia, por su inestimable ayuda con multitud de técnicas de laboratorio, y siguiendo por Javier, Juan, Albert, Javier y David.

A los compañeros de mil batallas en las plantas piloto de depuradoras, Carlota, Javi, Isaac, Torà, Mariangel, Carlos, Zulk y Clara (no me congeles los bichos! ;)). A Albert Bartolí por dejarme en herencia sus air-lifts. A Edgar, Yolanda, Nuria, y a Lore. A Tercia, por tu ayuda con la pirosecuenciación.

Especiales gracias a los primero compis de carrera, amigos después y finalmente compis de doctorado (y alguno hasta vecino de planta piloto y de despacho), Javi, Carles, Jose y Mabel. Y por supuesto, a Cris y a Olaia, y al King Luis.

A los ilustres miembros del QC-1083 y accionistas de la Nespresso más usada de la historia, Ana, Javi, Joel, Rim, Michele, Caterina, Erasmo, Juliana, Tahseen y Caterina. Nos vemos en el Pollo Rico!

Al resto de compañeros de ahora y de simpre del departamento, Marina, Andrea, Belén, Cesc, Alfred, Marc, Canet, Elena, Calleja, Xavi,... a los Rollings, Marcel, Torà, Roger, Ponsà, Jero, Edu,... (y a los muchos que me dejo!). Por esos buenos momentos en los pasillos, laboratorios, comidas y fiestas!!

Quiero extender mis agradecimientos a Anuska Mosquera y a Jose Luís Campos, por acogerme en el bio-grup de la USC durante mi corta estancia en Santiago. También a Nico, por acogerme

en su casa, y a Ángeles por tu ayuda, paciencia y consejos durante la puesta en marcha del reactor granular.

A los Hibéricos, JuanRa, Luis i Nico, agradeceros el rock'n'roll y la amistad. Esto es lo que estaba haciendo cuando decía que tenía que dejar un ensayo para ir a “regar las plantas”, jeje.

A la gente de Cerdanyola, Silvia, Anchu, Pedro, Nuria, David, Marta y Marc que os he tenido abandonados últimamente con tanta tesis!

A Juanca y a Santi, por confiar en mi para ser el prof. Bacterio de Protecmed y darme la flexibilidad necesaria para poder acabar la tesis. Mil gracias de verdad (pero no me haré del Madrid...)!! Y a los ahora compañeros de batalla Cris, Luis, David, Jose y Manel.

Por supuesto, a mis padres, a mis hermanos, Alberto y Ana. Y a la que pronto será mi familia, Silvia, Xavier, Eric, Iris y Uri. Gracias a todos por vuestro cariño. No sé si entenderéis lo que hacen las bolitas de bichos, pero si daros las gracias a todos por la paciencia que habéis tenido estos años

Y por último y no menos importante, a ti, Alba. Es difícil agradecerte solo con palabras el cariño, comprensión, apoyo y paciencia que recibido de ti todos estos años. Sin lugar a dudas, hubiera sido imposible terminar la tesis sin ti. Te debo unos cuantos fines de semana! jeje. Si alguien busca una prueba de amor, que haga una tesis!!! Te quiero!!

Edu

Summary

Granular biomass has been proposed as an alternative to activated sludge for the sewage treatment. The morphological characteristics of granular biomass (i.e. higher size and density), provides granules two main advantages over flocular biomass of the activated sludge: (i) the ability of settling faster, and (ii) the possibility of performing aerobic, anoxic and anaerobic processes simultaneously into the same bioparticle. Two different granular systems have a demonstrated potential for the treatment of urban wastewater. First, aerobic granular sequencing batch reactors (GSBR), which perform the same nutrient removal process occurring in activated sludge systems, but taking advantage of the abovementioned granular sludge properties. Second, an anammox-based sewage treatment, which could allow obtaining a more sustainable (energy-neutral or even energy-positive) wastewater treatment.

This thesis is focused in improving the knowledge of these granular biomass systems towards confirming granular biomass as a real alternative to urban wastewater treatment with activated sludge.

For urban wastewater treatment with GSBRs, two different studies were done. First, the stability of granules and their performance at pilot scale were first studied in a 100 L GSBR treating low-strength wastewater for simultaneous carbon, nitrogen and phosphorus removal was operated for eleven months. Mature granules prevailed in the GSBR during a period of five months (from days 150 to 330), with a SVI_{30} of 13±6 mL g^{-1} TSS, a granule density around 114±5 g TSS L^{-1} and an average particle size of 2.4 mm. The biological nitrogen removal with mature granules was mainly performed via nitrite, probably due to the large granule size achieved. Nitrification efficiency was higher than 75% and occurred simultaneously with denitrification during the aerobic phase of the GSBR. A progressive accumulation of P-salts (probably apatite), was found from days 150 to 300, which could enhance the destabilization of granules at the end of the experimental period.

Second, a model-based study was carried out to determine the guidelines to design an automatic control strategy with the final aim of enhancing biological N-removal in a GSBR. The model was first calibrated with experimental data from a granular sequencing batch reactor treating swine wastewater. Specific simulations were designed to elucidate the effect of DO concentration (0.5 – 8 mg O_2 L^{-1}), granule size (0.5 – 3.5 mm), influent C/N ratio (4 – 10 g O_2 g^{-1} N) and NLR (0.41 – 0.82 g N L^{-1} d^{-1}) on the nitrification-denitrification efficiency. Simulation results showed that, in general, high N-removal efficiencies (from 70 to 85 %) could be obtained

only setting the appropriate DO concentration. That appropriate DO concentration could be easily found based on effluent ammonium concentration. Those results were used to propose a control strategy to enhance N-removal efficiencies. The control strategy was based on a closed DO loop with variable DO set-point. The DO set-point was established at a constant value for the whole cycle (i.e. once per cycle), based on the on-line measurement of ammonium concentration at the end of the previous cycle.

Regarding the anammox-based sewage treatment, two additional studies were carried out. First, the feasibility of a two-step reactor system was studied. For the first step (i.e. partial nitritaion), a bench-scale granular sludge bioreactor was operated in continuous mode with a low nitrogen concentration wastewater (to mimic pretreated municipal nitrogenous wastewater) and the temperature was progressively decreased from 30 to 12.5 ºC. A suitable effluent nitrite to ammonium concentrations ratio to a subsequent anammox reactor was maintained stable during more than 450 days, including more than 365 days at temperatures equal or lower than 15ºC. The average applied nitrogen loading rate at 12.5ºC was 0.7±0.3 g N L^{-1} d^{-1}, with an effluent nitrate concentration of only 2.5±0.7 mg N-NO_3^- L^{-1}. A previously existing mathematical model was evaluated with the experimental results. The model was used to determine why partial nitritation was feasible. Simulations showed that NOB was only effectively repressed when their oxygen half-saturation coefficient was higher than that of AOB. Simulations also indicated that a lower specific growth rate of NOB was maintained at any point in the biofilm (even at 12.5ºC) due to the bulk ammonium concentration imposed through the control strategy.

Finally, changes in microbial diversity during the recovery process of an anammox granular reactor after a temperature shock were explored using 454-pyrosequencing technique. The temperature shock reduced the nitrogen removal rate up to 92% compared to that just before the temperature shock, and no specific anammox activity could be measured 7 days after temperature shock. Similar nitrogen removal rate to that before the temperature shock (ca. 0.30 g N L^{-1} d^{-1}) was obtained after day 70, but the specific anammox activity did not recover similar values until day 166 (ca. 0.4 g N g^{-1} VSS d^{-1}). Biomass samples from days 13, 45 and 166 after the temperatures shock were used for the pyrosequencing analysis. Pyrosequencing results obtained with a general primer showed that microbial diversity in the reactor decreased as the reactor progressively recovered from the temperature shock. Anammox bacteria were accounted as 6%, 35% and 46% of total sequence reads in samples taken 13, 45 and 166 days after the temperature shock. These results were in agreement with N-removal performance

results and SAA measured in the reactor during the recovery process. A specific anammox primer revealed that *Brocadia anammoxidans* was the most abundant anammox species in the recovered rector (95% overall anammox species). In contrast, just after the temperature shock, *Candidatus Kuenenia sp.* was the most abundant species (61%). The population shift could be due to the different kinetic strategies (i.e. either r or K-strategist) of *Brocadia* and *Candidatus Kuenenia* genera, respectively.

Resumen

La biomasa granular se ha propuesto como una alternativa al tratamiento de aguas residuales urbanas mediante lodos activos. Las características morfológicas de la biomasa granular (su mayor tamaño y densidad) le confieren, principalmente, dos ventajas sobre la biomasa floculenta de los lodos activos: (i) la habilidad de sedimentar más rápido, y (ii) la posibilidad de realizar procesos aerobios, anóxicos y anaerobios dentro de la misma biopartícula. Dos sistemas diferentes basados en biomasa granular han demostrado su potencial para el tratamiento de aguas urbanas. En primer lugar, los reactores secuenciales granulares (GSBR, de sus siglas en ingles), en los cuales se llevan a cabo los mismos procesos de eliminación de nutrientes que en los sistemas de lodos activos, pero con las ventajas de la biomasa granular. En segundo lugar, un tratamiento de aguas residuales urbanas basado en tecnología anammox, el cual permitiría una depuración de aguas sostenible (sin aporte o incluso productora de energía).

Esta tesis busca incrementar el conocimiento de estos sistemas de biomasa granular, con el objetivo último de confirmar si la biomasa granular puede ser una alternativa real al tratamiento de aguas residuales urbanas con lodos activos.

Para el tratamiento de aguas residuales urbanas con GSBRs, se realizaron dos estudios diferentes. En primer lugar, se estudió la estabilidad y rendimiento de los gránulos aerobios para la eliminación simultanea de materia orgánica, nitrógeno y fósforo de un agua residual de baja carga en un GSBR a escala piloto (100L) operado durante 11 meses. Se obtuvieron gránulos maduros durante 5 meses (entre los días 150 y 330), con un IVF_{30} de 13±6 mL g^{-1} SST, una densidad de 114±5 g SST L^{-1} y un diámetro promedio de 2.4 mm. La eliminación biológica de nitrógeno fue principalmente vía nitrito, probablemente debido al gran tamaño de partícula de los gránulos. La eficacia de nitrificación fue del 75% y se obtuvo desnitrificación simultánea a la nitrificación durante las fases aerobias del GSBR. Se observó una acumulación progresiva de sales de fósforo (probablemente apatita) entre los días 150 y 300, que pudo influir negativamente en desestabilización de los gránulos al final del periodo experimental.

En segundo lugar, mediante el uso de un modelo matemático, se llevó a cabo un estudio para determinar las directrices de diseño de una estrategia de control automático que permita mejorar la eficacia de eliminación biológica de nitrógeno en un GSBR. El modelo se calibró con datos experimentales obtenidos de un GSBR tratando purines diluidos. Se diseñaron simulaciones específicas para elucidar el efecto de la concentración de oxígeno disuelto (0.5 – 8 mg O_2 L^{-1}), el tamaño de gránulo (0.5 – 3.5 mm), la ratio C/N del afluente (4 – 10 g O_2 g^{-1} N) y la

carga volumétrica de nitrógeno (0.41 – 0.82 g N L^{-1} d^{-1}) sobre la eficacia de nitrificación-desnitrificación. Los resultados de las simulaciones mostraron que, en general, se pueden obtener altas eficacias de eliminación de nitrógeno (70 - 85%) simplemente fijando la consigna de oxígeno disuelto apropiada. Esa consigna apropiada se puede encontrar fácilmente en función de la concentración de amonio en el efluente. Se usaron estos resultados para proponer una estrategia de control que mejorara la eficacia de eliminación de nitrógeno. La estrategia de control se basaba en un lazo cerrado de oxígeno disuelto con una consigna variable de oxígeno disuelto. La consigna de oxígeno disuelto se fijaba, para cada ciclo (i.e. una vez por ciclo), a un valor constante en función de la concentración de amonio al final del ciclo anterior.

Respecto al tratamiento de aguas residuales urbanas basado en tecnología anammox, se realizaron dos estudios adicionales. En el primero de ellos, se estudió la factibilidad de un sistema de eliminación autótrofa de nitrógeno de dos etapas. Para la primera etapa (i.e. nitritación parcial), se operó un reactor granular de 2.5L trabajando en continuo, tratando un agua residual con una concentración de nitrógeno baja (para simular un agua residual urbana pretratada). Se disminuyó progresivamente la temperatura del agua residual desde 30ºC hasta 12.5ºC. Se obtuvo, durante más de 450 días, un efluente con una relación entre las concentraciones de nitrito y amonio adecuado para alimentar un reactor anammox posterior, incluyendo más de 365 días a temperaturas iguales o menores a 15 ºC. Con 12.5 ºC, la carga volumétrica de nitrógeno fue de 0.7±0.3 g N L^{-1} d^{-1} con una concentración de nitrato de solo 2.5±0.7 mg N-NO_3^- L^{-1}. Se usó un modelo matemático ya existente para explorar las razones que permitieron obtener nitritación parcial a temperaturas tan bajas. Primero se evaluó el modelo con los datos experimentales obtenidos en este estudio. Luego, las simulaciones mostraron que la actividad NOB era solamente reprimida de manera efectiva cuando el coeficiente de semi saturación por oxígeno de los NOB era mayor que el de los AOB. Las simulaciones también indicaron que se mantuvo, en cualquier punto de la biopelícula, una velocidad de crecimiento especifica de los NOB menor que la de los AOB (incluso a 12.5 ºC) gracias al exceso de concentración de amonio impuesto por la estrategia de control en la fase líquida del reactor.

Finalmente, se exploró el efecto de un choque térmico (i.e. 46 ºC) sobre las poblaciones microbianas de un reactor granular anammox utilizando la técnica de pirosecuenciación. Esta técnica ofrece una plataforma de secuenciación rápida, económica y con un alto rendimiento para determinar la diversidad microbiana de muestras biológicas. El choque térmico redujo un 92% la velocidad de eliminación de nitrógeno en comparación con el que había justo antes del choque térmico. Además, no se puedo detectar actividad anammox específica 7 días después del

choque térmico. Tras 70 días, se pudo recuperar un velocidad de eliminación de nitrógeno similar a la anterior del (aprox. 0.30 g N L^{-1} d^{-1}), pero la actividad anammox específica de los gránulos no recuperó valores similares a los previos al choque térmico hasta 166 días después del choque térmico. Para el análisis de la comunidad microbiana mediante la pirosecuenciación, se utilizaron muestras de biomasa de los días 13, 45 y 166 tras el choque térmico. Los resultados obtenidos con un primer general mostraron que la diversidad microbiana en el reactor disminuyó progresivamente a medida que el reactor se recuperaba del choque térmico. La población anammox sumó el 6%, 35% y el 46% del total de lecturas de secuencias en las muestras de los días 13, 45 y 166, respectivamente. Estos resultados concuerdan con los resultados de eliminación de nitrógeno y los test de actividad realizados durante el proceso de recuperación del reactor. Un primer específico para bacterias anammox mostró que la especie mayoritaria en el reactor recuperado era *Brocadia Anammoxidans* (un 95% de lecturas entre todas las especies anammox). En cambio, *Candidatus Kuenenia sp.* era la especie mayoritaria en el reactor justo después del choque térmico (61%). El cambio de población pudo deberse a la diferente estrategia cinética (i.e. estrategas de la r o de la K) de *Brocadia* y *Candidatus Kuenenia*, respectivamente.

List of symbols and abbreviations

ABBREVIATION	DEFINITION
ANFIBIO	Automatic control for partial nitrification to nitrite in biofilm reactors
AOB	Ammonia-oxidizing bacteria
ASM	Activated sludge model
C	Carbon
CANON	Completely autotrophic nitrogen removal over nitrite
C/N	Chemical oxygen demand to nitrogen ratio
COD	Chemical oxygen demand
D	Diameter
DEMON	Deammonification
DO	Dissolved Oxygen
EBPR	Enhanced-biological phosphorus removal
FA	Free ammonia
FISH	Fluorescence in-situ hybridization
FNA	Free nitrous acid
GAO	Glycogen-accumulating organisms
GSBR	Granular sequencing batch reactor
H	Height
HDP	Hydroxy-dicalcium-phosphate
HRT	Hydraulic retention time
MBR	Membrane bioreactor
N	Nitrogen
NLR	Nitrogen loading rate
NOB	Nitrite-oxidizing bacteria
OLAND	Oxygen-limited autotrophic nitrification-denitrification
P	Phosphorus
PAO	Phosphate-accumulating organisms
PHA	Poly-hydroxyalkanoates
SBR	Sequencing batch reactor
RBC	Rotating biological contactor
SHARON	High activity ammonia removal over nitrite
SNAP	Single-stage nitrogen removal using anammox and partial nitrification
SND	Simultaneous nitrification and denitrification
SRT	Sludge retention time
TAN	Total ammonia nitrogen ($NH_4^+ + NH_3$)
TNN	Total nitrite nitrogen ($NO_2^- + HNO_2$)
TSS	Total suspended solids
SVI	Sludge volumetric index
UASB	Up-flow anaerobic sludge blanket
VFA	Volatile fatty acids
VSS	Volatile suspended solids
WWTP	Wastewater treatment plant

Table of content

CHAPTER 1

GENERAL INTRODUCTION

1.1 Research motivations

Wastewater is any water that has been adversely affected in quality by anthropogenic influence. Urban wastewater is a mixture of domestic wastewater with industrial wastewater, as well as (usually) storm-water run-off. One of the problems of discharging untreated urban wastewater to aquatic environments is the potential of causing eutrophication due to the overload of biological nutrients, such as nitrogen (N) and phosphorus (P). A high concentration of these nutrients stimulates the growth of algae and phytoplankton, as well as increases the demand for dissolved oxygen (DO), both effects contributing to the deterioration of aquatic environments (EPA, 2009).

The removal of nutrients from urban wastewater is usually carried out in wastewater treatment plants (WWTP) with the so-called activated sludge process. The activated sludge process was discovered in the early 20th century, and successfully used for organic matter removal (Tchobanoglous et al., 2003). Later, the continuous research on the process allowed the removal of nitrogen and phosphorus with the activated sludge process (Gujer, 2010). In the last decades, advances on instrumentation and control have allowed the optimization of the process for delivering an effluent with the required quality reducing the operating costs (Olsson, 2012).

Despite all the advances with the activated sludge process, there are several issues related to the biomass characteristics that cannot be avoided. Low settling properties of the biomass flocs constituting the activated sludge limit the biomass retention (de Kreuk et al., 2007a). Thus, reactors with large volumes and settlers with large surfaces are needed to successfully treat wastewater. Additionally, although some energy is recovered with the biogas obtained from the anaerobic digestion of the produced sludge, nutrient removal with activated sludge is a net energy consumer process due to the aeration, pumping and mixing requirements (Kartal et al., 2010).

Granular biomass has been extensively researched in the last decade as an alternative to overcome the limitations of the activated sludge process (Adav et al., 2008; de Kreuk et al., 2007a; Liu and Tay, 2004; Van Hulle et al., 2010). The morphological characteristics of granular biomass (i.e. higher size and density) provide granules two main advantages over flocular biomass of the activated sludge: (i) the ability of settling faster, and (ii) the possibility of performing aerobic, anoxic and anaerobic processes simultaneously into the same bioparticle. Both characteristics contribute to reduce the required reactor volume and to treat higher

wastewater loading rates, producing more compact designs, when compared to conventional activated sludge systems.

Two different systems have been proposed for the treatment of urban wastewater with granular sludge. First, aerobic granular sequencing batch reactors (GSBR), which perform the same nutrient removal process occurring in activated sludge systems (nitrification-denitrification and enhanced biological phosphorus removal (EBPR)), but taking advantage of the abovementioned granular sludge properties (Beun et al., 2001; de Kreuk et al., 2005a). Second, a more sustainable (energy-neutral or even energy-positive) wastewater treatment can be achieved using the partial nitritation-anammox process (Kartal et al., 2010) in granular reactors for nitrogen removal from urban wastewater. Both granular systems have a demonstrated potential in lab-scale studies. However, there is still lack of knowledge that needs to be fulfilled in order to confirm granular biomass as a real alternative to urban wastewater treatment with activated sludge.

1.2 Biological nutrient removal processes for wastewater treatment

1.2.1 Biological nitrogen removal

The biological nitrogen removal is the conversion of the main nitrogen species found in wastewater (i.e. ammonium, nitrite and nitrate) into nitrogen gas by means of biological processes. The three main biological processes for nitrogen removal are nitrification, denitrification and anammox (see Figure 1.1).

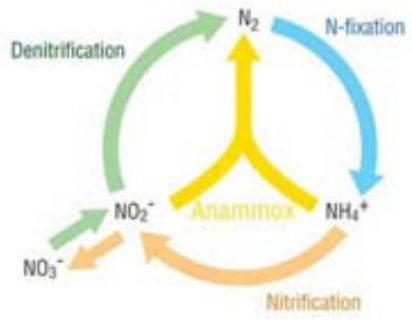

Figure 1.1: Biological transformation processes in the nitrogen cycle. Picture obtained from web page (www.waterworld.com).

1.2.1.1 Nitrification

The nitrification process is the biological oxidation of ammonium into nitrate. This process is carried out in two steps by different microorganism: first, ammonium oxidizing bacteria (AOB) oxidize ammonium into nitrite (nitritation process) and then, nitrite oxidizing bacteria (NOB) oxidize nitrite into nitrate (nitratation process).

The nitrification process has the following stoichiometry (EPA, 2009):

Nitritation: $NH_4^+ + 1.5\ O_2 \xrightarrow{AOB} NO_2^- + 2\ H^+ + H_2O$ (1.1)

Nitratation: $NO_2^- + 0.5\ O_2 \xrightarrow{NOB} NO_3^-$ (1.2)

Nitrification: $NH_4^+ + 2\ O_2 \longrightarrow NO_3^- + 2\ H^+ + H_2O$ (1.3)

Based on the above total oxidation reaction, the oxygen required for complete oxidation of ammonium is 4.57 g O_2 g^{-1} N, with 3.43 g O_2 g^{-1} N and 1.14 g O_2 g^{-1} N for nitrite and nitrate productions, respectively.

AOB are obligatory chemoautotrophic gram-negative bacteria that utilize ammonia as a source of electrons for the immobilization of inorganic carbon into biomass. They are aerobic, employing oxygen as the final or terminal electron acceptor (Ahn, 2006). Five of the best known AOB genera are *Nitrosomonas*, *Nitrosolobus*, *Nitrosovibrio*, *Nitrosococcus* and *Nitrosospira* (Ahn, 2006). AOB can grow at temperatures of 5-35 ºC with the optimum around 25-35 ºC, and at a pH range around 5.8-9.0 with 7.8 as the optimum (Watson et al., 1989).

NOB are chemoautotrophic bacteria with the ability to use nitrite as their energy source and to assimilate CO_2 as the carbon (C) source for cell growth. Some of the best known NOB genera are *Nitrobacter*, *Nitrococcus*, *Nitrospira* and *Nitrospina* (Ahn, 2006). They are not all obligate chemoautotrophs. In fact, many strains of *Nitrobacter* can grow as heterotrophs, where both energy and carbon are obtained from organic carbon sources, or mixotrophically (Watson et al., 1989). These bacteria are collectively known as facultative chemoautotrophs or lithoautotrophs. They are also aerobic although some of them can also grow in anaerobic conditions. NOB can grow in a pH range 6.5-8.6 and at temperatures between 5 ºC and 37 ºC, although the optimal growth conditions are at pH values around 7.6 - 8.0 and a temperatures between 25 and 30 ºC (Watson et al., 1989).

1.2.1.2 Partial nitrification

Partial nitrification is the oxidation of the influent ammonium into nitrite, but not to nitrate. To achieve partial nitrification, the nitratation process must be prevented. If the partial nitrification consists on the oxidation of around 50% of the influent ammonium to nitrite, it is named partial nitritation. Many parameters have been suggested for influencing nitrite accumulation, either individually or in combination with other factors. The main factors affecting AOB and NOB activities in a different degree and useful to achieve partial nitrification are temperature, oxygen affinity, free ammonia (FA) and free nitrous acid (FNA) inhibitions.

Temperature: The growth rate dependence on temperature is different in AOB and NOB (Jubany et al., 2008). At temperatures above ca. 20ºC, AOB maximum growth rate is higher than that of NOB, while at temperatures below 20ºC the trend is inverted and the maximum growth rate of NOB is higher than that of NOB. Therefore, operating a reactor above 25 ºC at an appropriate sludge retention time (SRT) would allow a selection AOB and the washout of NOB, which grow slower than AOB (Hellinga et al., 1998).

Oxygen affinity: AOB have, in general, higher oxygen affinity than NOB (Guisasola et al., 2005; Wiesmann, 1994; Wyffels et al., 2004). In biofilm reactors, due to the biofilm internal mass transfer resistance, that difference in oxygen affinity allows AOB to outcompete NOB for oxygen consumption when oxygen limiting conditions are applied, leading for partial nitrification (Brockmann and Morgenroth, 2010; Pérez et al., 2009). Furthermore, ammonium bulk liquid concentration plays an important role, since it may provide either ammonium or oxygen limiting conditions depending on the ratio of ammonium ratio with DO concentration (Jemaat et al., 2013; Sliekers et al., 2005). Accordingly, Bartrolí et al. (2010) obtained full nitration applying a DO to total ammonium nitrogen (TAN = $N\text{-}NH_4^+$ + $N\text{-}NH_3$) bulk liquid concentrations ratio (DO/TAN) of 0.25 mg O_2 mg^{-1} N in a nitrifying biofilm airlift reactor treating a high strength ammonium wastewater. This DO/TAN bulk liquid concentrations ratio ensured oxygen limiting condition inside the biofilm, which repressed NOB activity despite having high oxygen concentrations in the bulk liquid (7 mg O_2 L^{-1}). With suspended biomass, partial nitrification due to oxygen limiting conditions is harder to obtain (Wang and Yang, 2004; Wyffels et al., 2004). However, Sliekers et al. (2005) obtained partial nitrification in a suspended biomass culture by applying microaerobic condition (DO < 0.1 µM) while maintaining ammonium in excess.

FA and FNA inhibitions: AOB and NOB present inhibition for the non-ionized forms of ammonium (i.e. NH_3) and nitrite (i.e. HNO_2). Based on the results reported Anthonisen et al. (1976), NOB was more sensitive than AOB to FA and FNA, especially to FA. Accordingly, high FA concentration can repress NOB activity (Jubany et al., 2009a). Since the equilibrium between the ionized and non-ionized forms of FA and FNA depends on pH, pH is also an important factor to determine the inhibition degree. These inhibitions are only significant when dealing with high-strength ammonium-concentration wastewaters because the inhibitory concentrations of FA and FNA are more pronounced than the occurring in urban wastewaters.

1.2.1.3 Denitrification

The denitrification is the biological reduction of nitrogen-oxidized species (i.e. nitrate, nitrite) into nitrogen gas (N_2). This process is carried out by a variety of common heterotrophic bacteria

which, in anoxic conditions (i.e. absence of oxygen), use nitrite and nitrate as electron donor to oxidize organic matter. Similarly to nitrification, the denitrification involves several reduction steps (Henze et al., 2000):

$$NO_3^- \rightarrow NO_2^- \rightarrow NO \rightarrow N_2O \rightarrow N_2 \quad (1.4)$$

The stoichiometric equation for denitrification from nitrate considering acetate as carbon source is (Wiesmann 1994):

$$8\,NO_3^- + 5\,CH_3COOH \rightarrow 4\,N_2 + 10\,CO_2 + 6\,H_2O + 8\,OH^- \quad (1.5)$$

According to the stoichiometry in Eq. 1.5, denitrification requires 2.9 g COD g^{-1} $N\text{-}NO_3^-$, although the real COD requirements can vary between 3-5 g COD g^{-1} $N\text{-}NO_3^-$ depending on the carbon source (Matějů et al., 1992). Also from the stoichiometry, it can be inferred that the denitrification process increases of the alkalinity of the medium of 3.6 g of alkalinity (as $CaCO_3$) per g of $N\text{-}NO_3^-$ reduced.

1.2.1.4 Anammox

The anammox process consists in the oxidation of ammonium to nitrogen gas, using nitrite as electron donor and inorganic carbon as carbon source (Strous et al., 1998). This process is carried out by the chemolithoautotrophic microorganisms commonly named anammox (anaerobic ammonium oxidation).

The anammox process has the following stoichiometry (Strous et al., 1998):

$$1\,NH_4^+ + 1.3\,NO_2^- + 0.066HCO_3^- + 0.13H^+ \rightarrow 1.02\,N_2 + 0.26\,NO_3^- + 0.066CH_2O_{0.5}N_{0.15} + 2.03\,H_2O \quad (1.6)$$

As observed form stoichiometry, the anammox process does not require any organic carbon source to denitrify. The nitrite required for the anammox process is typically obtained by partially oxidizing the influent ammonium with the partial nitritation process.

Regarding the environmental conditions, the anammox process can only occur in the absence of oxygen, since oxygen reversibly inhibits the anammox process (Strous et al., 1997; van de Graaf et al., 1996) at DO concentrations higher than 0.042 mg O_2 L^{-1} (Kuenen, 2008; Schmidt et al., 2003). Anammox can grow at pH values between 6.7 - 9.0 (Egli et al., 2001; Strous et al., 1999), although optimum pH value around 8.

Regarding temperature, in natural environments, anammox growth has been reported to occur at temperatures as low as −2.5°C in sea ice (Dalsgaard and Thamdrup, 2002; Rysgaard and Glud, 2004) and as high as 70°C in hot springs and hydrothermal vent areas (Byrne et al., 2009; Jaeschke et al., 2009). In contrast, in wastewater treatment reactors anammox maximum growth temperature has been reported at 43 ºC (Strous et al., 1999). The optimum temperature for anammox growth is 35 ºC (Dosta et al., 2008; Strous et al., 1999).

The growth rate of anammox bacteria is very slow. Generally, doubling times around 10-14 days have been reported in bioreactors when the anammox process was operated at the optimum temperature (Fux et al., 2004; Strous et al., 1998). However, lower doubling times, around 3.6 - 7.5 days, have been reported when anammox was cultivated in a MBR (van der Star et al., 2008) or in shake flasks (Tsushima et al., 2007).

The anammox process is inhibited by high concentrations of both process substrates: ammonium and nitrite (Jin et al., 2012). Among both substances, anammox was more vulnerable to nitrite inhibition than to ammonium inhibition (Dapena-Mora et al., 2007; Isaka et al., 2007). The threshold concentration for nitrite inhibition has not been clearly defined, since different inhibition thresholds between 60 and 400 mg N L^{-1} have been reported under different experimental conditions and operating modes (Dapena-Mora et al., 2007; Fux et al., 2002; Lotti et al., 2012; Strous et al., 1999). However, increasing exposure times to high nitrite concentration increased the anammox process inhibition (Lotti et al., 2012). Regarding ammonium inhibition, to maintain a stable operation of anammox reactors, the FA concentration needs to be below 20–25 mg FA L^{-1} (Fernández et al., 2012).

1.2.2 Enhanced biological phosphorus removal

The biological method of removing P from wastewater, typically in the form of phosphate, consists of encouraging the accumulation of P in bacterial cells in the form of polyphosphate (polyP) in excess of the normal levels normally required to satisfy the metabolic demand for growth (Seviour et al., 2003). This storage process is commonly referred to as EBPR. The bacteria with the metabolic capability of performing this P uptake are known as polyP accumulating organisms (PAO).

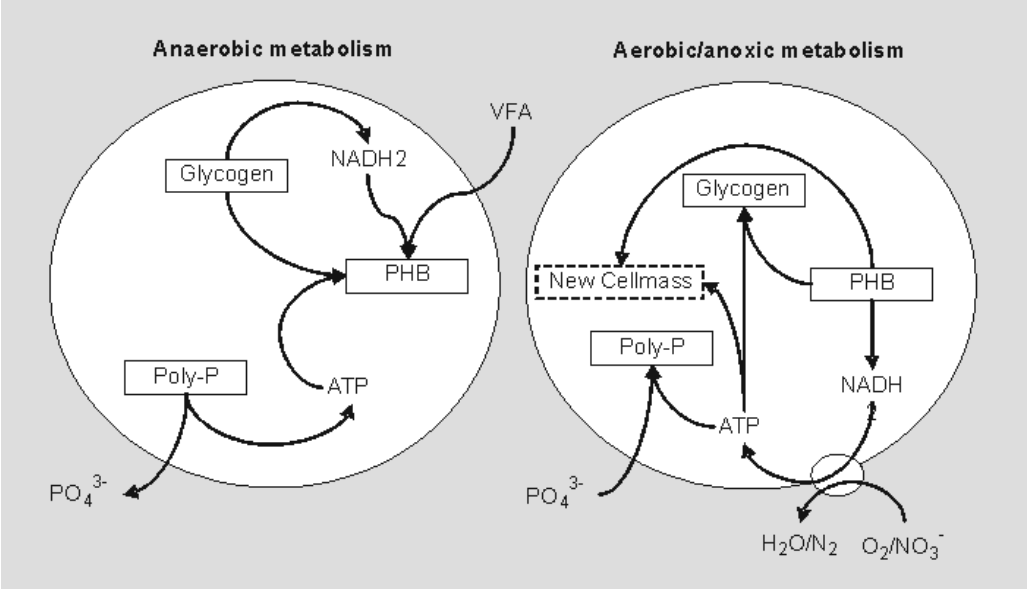

Figure 1.2: Schematic representation of PAO metabolism. On the left, the anaerobic stage; on the right, the aerobic/anoxic stage. Picture obtained from web page (www.wastewaterhandbook.com).

The metabolic activity of PAO consists of (i) first, being capable of uptaking organic substrates (preferably volatile fatty acids, VFA) and store them as poly-hydroxyalkanoates (PHA) in absence of any electron donor (anaerobic conditions) (Figure 1.2, left). The reducing power for the accumulation of PHA is obtained from the catabolism of glycogen, while the energy is obtained from the hydrolysis of previously accumulated polyP chains (Mino et al., 1998). Thus, this results in an increase of the wastewater P concentration. Then (ii), in the presence of an electron donor (in anoxic or aerobic conditions), PAO oxidize the previously accumulated PHA to obtain the carbon and energy necessary for growth, but also for the replenishment of the polyP and glycogen pools, uptaking the P from the wastewater (Figure 1.2, right). Since the P-uptake during the aerobic phase is higher than the P-release during the anaerobic phase, a net P-removal from wastewater is achieved. When biomass is removed from the system, P is so.

Apart from PAO, there is a group of bacteria capable of performing a similar metabolism than PAO, but without accumulation polyP. These bacteria are known as glycogen accumulating organisms (GAO), and are one of the main concerns in EBPR failure (Oehmen et al., 2007).

The terms 'PAO' and 'GAO' include multiple microbial groups (Oehmen et al., 2007). The most well-known PAO group is *Candidatus Accumulibacter phosphatis*, which consist of two types with metabolically distinct features such as denitrification capacity and anaerobic utilization of the tricarboxilic acid cycle. Another group of PAOs within the *Actinobacteria* group have been found to be abundant in urban wastewater (Kong et al., 2005). Regarding GAOs, two different groups have been observed, *Candidatus Competibacter* and *Defluviicoccus vanus*, both of which

have several sub-groups with varying denitrification capabilitys but similar anaerobic stoichiometry (Oehmen et al., 2007).

1.3 Conventional urban wastewater treatment

A typical urban wastewater treatment plant usually comprises the following phases of treatment: pretreatment, primary, secondary and tertiary (see Figure 1.3)

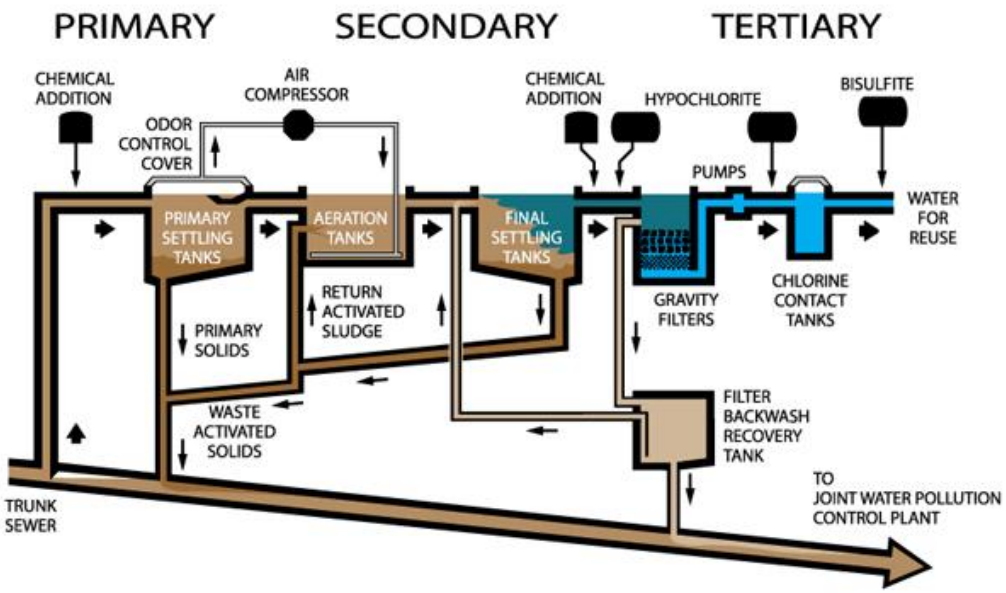

Figure 1.3: Schematic representation of the typical flows on an urban wastewater treatment plant. Picture obtained from http://www.lacsd.org/wastewater/wwfacilities/moresanj.asp.

The pretreatment consists on the removal of wastewater constituents such as ragas, sticks, floatables, grit and grease that may cause maintenance or operational problems with the posterior treatment operations. The primary treatment is the removal of a portion of the suspended solids and organic matter from the wastewater by means of chemical addition and primary settlers. The wastewater then passes to the secondary treatment, consisting of the biological removal of the biodegradable content of wastewater, typically organic matter, nitrogen and phosphorus. The conventional activated sludge process is normally used for the secondary treatment. A tertiary phase may be used to further improve the quality of the secondary effluent, by chemically removing nitrogen, phosphates, suspended solids or pathogens not removed in secondary treatment.

1.3.1 Activated sludge process

The activated sludge process is a method for treating the biodegradable content of the wastewater. Activated sludge utilizes microorganisms able to remove wastewater pollutants,

such as organic matter, nitrogen or phosphorus, transforming them into other by-products (i.e. CO_2 or N_2) and producing cell mass.

By definition, a basic activated sludge treatment system consists of the following three basic components (Tchobanoglous et al., 2003): (1) a reactor in which the microorganisms are kept in suspension; (2) a liquid-solid separation unit to remove biomass from clean water; and (3) a recycle system for returning biomass from the liquid-solid separation unit back to the reactor. This basic configuration is only capable of degrading organic matter and performing the nitrification process. Therefore, for including simultaneous nitrogen and phosphorus removal, additional anoxic and anaerobic reactors must be added to include the denitrification and the EBPR processes. Some configurations used for nutrient removal are the A^2/O process (Figure 1.4), the modified Bardenpho^{TM}, the Virginia initiative plant (VIP), the PhoStrip process and the university of Cape Town (UCT) process (Tchobanoglous et al., 2003).

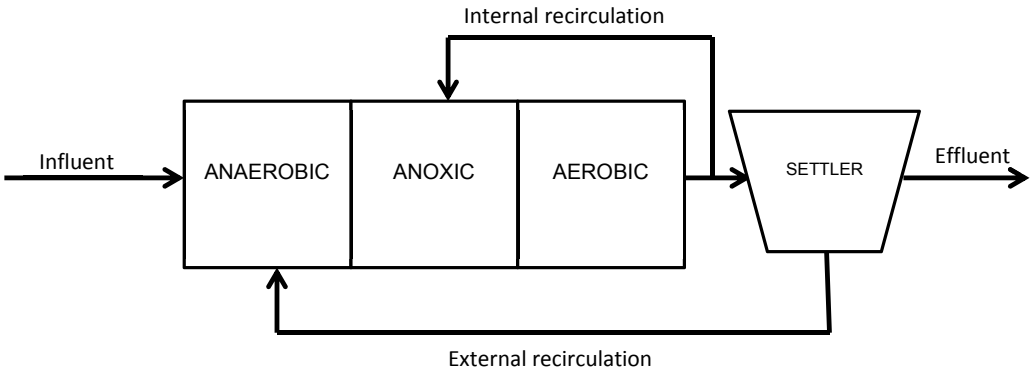

Figure 1.4: Schematic representation of the secondary treatment of a WWTP with an A^2/O configuration for C, N and P removal.

Although the activated sludge process is widely used for urban wastewater treatment, it has several limitations. A first set of limitations are devoted to the biomass retention capacity of the system. In the activated sludge, biomass grows in small biomass aggregates typically less than 0.2 mm known as flocs. The small size and density of flocs generally provides them of poor settling properties, with Sludge Volume Index (SVI) values typically above 100 mL g^{-1} TSS and settling velocities around 1 m h^{-1}. Accordingly, the biomass concentration achieved inside the aerated reactor is low (1.5 - 3.5 g VSS L^{-1}). This low biomass concentration limits the nutrient removal capacity that can be applied in conventional municipal WWTPs based on activated sludge (around 1.0 g O_2 L^{-1} d^{-1} and 0.10 g N L^{-1} d^{-1} (Tchobanoglous et al., 2003)). Also as a consequence of the poor settling properties, the space requirements to carry out the activated sludge process are high. On one side because large reactor volumes are required to compensate the low biomass concentrations, and on the other side because big settlers are needed to retain

the flocs. Additionally, problems of bulking can appear due to the proliferation of filamentous microorganisms that worsen the settling properties of the flocs and promote the formation of foams in the surface of the secondary settler, producing high concentrations of suspended solids in the effluent (Seka et al., 2001).

Second, the urban WWTP are net energy-consumers. Much of the energy consumed in an urban WWTP is associated to the aeration requirements to nitrify the influent ammonium. A lot of efforts have been done to optimize the WWTP to minimize the energy consumption (Olsson, 2012). Some energy can be recovered from the biogas generated during the digestion of the sludge. Higher energy recovery could be obtained if the influent COD was not used in the denitrification process (Kartal et al., 2010).

1.3.2 Alternatives to activated sludge process

1.3.2.1 Membrane Bioreactors (MBR)

Membrane bioreactors (MBRs) are biological reactors combining a suspended growth of biomass with solids removal via filtration. The MBR have several advantages compared to activated sludge (Tchobanoglous et al., 2003; Visvanathan et al., 2000; Yang et al., 2006): (i) the use of membranes for the solids filtration, which can be placed immersed in the biological reactor or in the outside, avoids the use of big settlers to remove solids from wastewater. (ii) The higher solids separation efficiency of MBR allows operating the reactors with higher biomass concentrations, thereby reducing the reactor volume requirements. (iii) Also devoted to the higher solids retention efficiency, MBRs have often been operated with longer solids residence times (SRTs), which results in lower sludge production; but this is not a requirement (EPA, 2009). (iv) The use of MBR reduces the footprint required for wastewater treatment.

MBRs have also some disadvantages, and the main one is the higher operation and investment costs than activated sludge for the same application (Tchobanoglous et al., 2003; Visvanathan et al., 2000). Some of the operational costs include, cleaning and fouling control, and eventually membrane replacement. Also, energy expenses are higher as a result of the requirement of extra aeration to: (i) control the bacterial growth in the membranes, (ii) large oxygen supply requirements due to the operation at large SRT values.

1.3.2.2 Granular sludge reactors

Aerobic granular biomass is composed by aggregates of microbial origin, which do not coagulate under reduced hydrodynamic shear, and which settle significantly faster than activated sludge

(de Kreuk et al., 2005b). The morphological structure of aerobic granular sludge (i.e. high particle diameter and density) provides two main advantages if compared to activated sludge processes:

(i) Granular biomass settles significantly faster than activated sludge (Adav et al., 2008; Liu and Tay, 2004), reaching to 50 – 90 m h^{-1}, depending on actual size and density, which is much larger than the 1 m h^{-1} of activated sludge. This higher settling velocity easies the biomass retention and allows operating at higher biomass concentrations. Biomass concentrations between 12 – 18 g VSS L^{-1} have been reported in GSBR (de Kreuk et al., 2005a; Yilmaz et al., 2008). Also, the faster settling velocity allows operating granular reactors without an external settler.

(ii) In granular biomass, substrate profiles across the granule radius are observed, which allows simultaneous aerobic, anoxic and anaerobic processes into the same granule, such as simultaneous COD, N and P removal (de Kreuk et al., 2005a; Yilmaz et al., 2008) or completely autotrophic nitrogen removal (Third et al., 2001; Winkler et al., 2011b).

All these characteristics contribute to reduce the required reactor volume or to treat higher wastewater loading rates, producing more compact designs, when compared to conventional activated sludge systems.

Two different systems have been proposed for the treatment of urban wastewater with granular sludge. First, granular sequencing batch reactors (GSBR), on which the nutrient removal process performed in activated sludge systems (nitrification-denitrification and EBPR) are mimicked, but taking advantage of the abovementioned granular sludge properties (Beun et al., 2001; de Kreuk et al., 2005a). This technology has been recently commercialized as NEREDA® by a Dutch company (http://www.royalhaskoningdhv.com/en/nereda). Second, a more sustainable (energy-neutral or even energy-positive) wastewater treatment can be achieved using the partial nitritation-anammox for nitrogen removal in the mainstream of urban WWTPs (Kartal et al., 2010).

1.4 Granular sequencing batch reactors

Granular sludge was first observed in up-flow anaerobic sludge blanket (UASB) reactors treating industrial wastewaters at the end of 1970s and, a decade after, it was widely applied at full scales (Hickey et al., 1991; Lettinga et al., 1980). The UASB reactors acquired popularity for fast COD removal because granular biomass presented a high settling velocity, which allowed the accumulation of high concentrations of solids inside the reactor systems. For the treatment of urban-like wastewaters, the anaerobic granular sludge presented several drawbacks that included a long start-up period, relatively high operating temperatures, unsuitability for low

strength organic wastewater and low removal efficiency of nitrogen and phosphorus form wastewater (Adav et al., 2008).

Unlikely to anaerobic granular sludge, aerobic granules present the capability not only of degrading COD but also of performing nitrification and EBPR, making them a potential technology for urban wastewater treatment. Aerobic granules were first reported by Mishima and Nakamura (1991) in a continuous aerobic up-flow sludge blanket reactor. Several years later, Morgenroth et al. (1997) used a sequencing batch reactor (SBR) to develop aerobic granular sludge. Since then, SBR have been successfully used for cultivation of aerobic granules (Beun et al., 1999; de Kreuk et al., 2005a; Tay et al., 2004). Recently, a Dutch company (DHV) has started to build-up full-scale GSBR facilities under the commercial name of NEREDA® (ww.dhv.com).

1.4.1 Cultivation of aerobic granules

The formation of aerobic granules is a complex process. Several factors, such as seed sludge, feed compositions and SBR operational parameters (e.g. pH, temperature, cycling time, and others) affect direct or indirectly to granulation process (Liu and Tay, 2004).

1.4.1.1 GSBR configuration and operation

The reactor structure and the cyclic operation of SBRs have a direct effect over the aerobic granulation process. A basic GSBR cycle configuration would include the following phases: influent filling, reaction, settling and effluent discharge (Beun et al., 2001; Mosquera-Corral et al., 2005).

During the **settling phase**, short settling times are chosen to only select particles that can settle down within the given settling time. This strategy promotes the formation of aerobic granules in detriment of suspended biomass. Full granulation is observed in SBRs operated at settling times corresponding to a minimal settling velocity of 8 m h^{-1}, while a mixture of aerobic granules and suspended sludge develops in SBRs run at longer settling times (Liu et al., 2005). Associated with the settling time, GSBR typically have large height (H) to diameter (D) ratio to enhance the separation of slow and fast setting particles (Beun et al., 2002). Furthermore a large H/D ratio can ensure a longer circular flowing trajectory, which in turn creates an optimal interactive pattern between flow and microbial aggregates for granulation (Liu et al., 2005).

Regarding the **feeding phase,** the feeding pattern plays a key role on the granulation process. Short feeding periods are normally selected (Beun et al., 1999), producing high substrate concentrations during the first minutes of the reaction phase. Accordingly, during the reaction

phase, feast and famine periods are observed, characterized by the presence or absence of organic matter in the liquid media, respectively. During the feast period, the organic matter is stored inside bacterial cells (van Loosdrecht et al., 1997), while during the famine period, the bacteria grow on the stored compounds. This periodic starvation has also a strong effect on cell hydrophobicity, which is an important factor on the formation and stability of granules (Lee et al., 2010; Liu et al., 2003, 2004). McSwain et al. (2004) studied the stability of granules in three parallel reactors with different percentage of aerated fill (0%, 33% and 66%) and maintain the rest of the feeding static (without aeration nor mixing), and found that granules stability decreased as the ratio of aerated fill increased.

Along the **reaction phase**, the aeration intensity has a direct effect over granulation, since the structure of mature aerobic granules is dependent of the hydrodynamic shear forces. Tay et al. (2001) found that aerobic granules could be formed only above a threshold shear force value in terms of superficial up-flow air velocity above 1.2 cm s^{-1} in a lab bubble column SBR. Adav et al. (2007) compared the granulation processes in three identical reactors aerated at different intensities (1–3 L air min^{-1}). At low aeration intensity (1 L min^{-1}), no granules were formed while at high aeration rate (3 L min^{-1}), mature and stable granules with a particle size around 1–1.5 mm and compact interior were formed. At intermediate intensity (2 L min^{-1}), large granules (3–3.5 mm) with overgrown filaments were formed. Therefore, it seems that enough aeration intensity should be provided to form granules.

Aeration intensity has also an indirect effect over granules stability since this parameter, in systems where the mixture is achieved by air flow, is related to the DO concentration. Mosquera-Corral et al. (2005) found that low DO concentrations negatively influenced the stability of mature granules. Also found that it was not possible to form stable granules at such low DO concentration. In fact, Liu and Liu, (2006) demonstrated that overgrowth of filamentous microorganisms could result in reactor failure when the amount of dissolved oxygen is inadequate, which commonly occurs in reactors with high OLR.

1.4.1.2 Influent characteristics

Aerobic granules have been cultivated using different substrates such as glucose, acetate, phenol, starch, ethanol, molasses, sucrose and other synthetic wastewater components (Adav et al., 2008; Liu and Tay, 2004). However, the COD loading seems to have a strong effect over granule stability. Tay et al. (2004) was unable to cultivate aerobic granules at less than 4 kg COD m^{-3} day^{-1} using glucose and peptone as substrates. Conversely, granules subjected to high OLR would disintegrate (Liu and Liu, 2006; Moy et al., 2002; Thanh et al., 2009; Zheng et al., 2006).

With urban wastewater, which has a relatively low COD concentration, de Kreuk and van Loosdrech (2006) were able to cultivate aerobic granules at lab-scale, although filamentous bacteria and irregular finger-type structures were observed. These authors pointed out that applying a high COD loading by shortening the cycle time was a necessary condition to promote aerobic granulation with urban wastewater.

1.4.2 Nutrient removal in aerobic granules

1.4.2.1 Nitrogen removal

Similarly to activated sludge, N-removal with aerobic granules is usually achieved through a combination of nitrification and denitrification processes. Two operational modes are commonly reported for N-removal with aerobic granular sludge:

(i) GSBRs with a completely aerated reaction phase (Beun et al., 2002; Figueroa et al., 2011; Mosquera-Corral et al., 2005). In this operational mode, there is lack of a specific anoxic phase in the GSBR cycle dedicated to denitrification. Thus, denitrification can only be achieved in the anoxic zones in the inner part of the granules, generated when DO is not fully penetrating the granules as a consequence of the heterotrophic or autotrophic aerobic microbial activity (see Figure 1.5). Therefore, simultaneous nitrification and denitrification (SND) is observed (Beun et al., 2002; Mosquera-Corral et al., 2005).

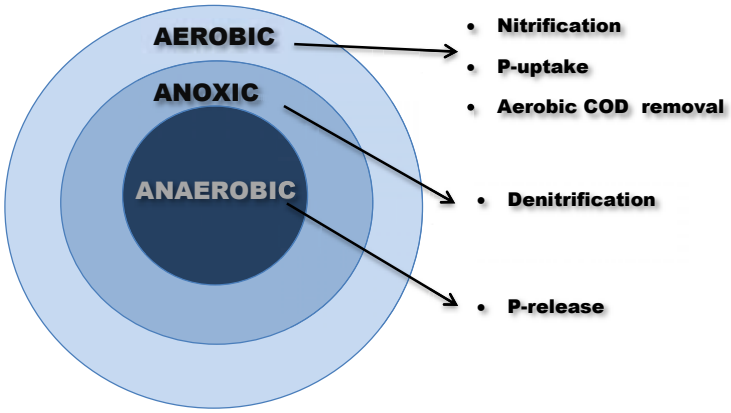

Figure 1.5: Biological processes occurring into the aerobic granule

The balance between aerobic and anoxic regions strongly determines the nitrogen removal efficiency (de Kreuk et al., 2007b; Li et al., 2008). This balance depends on many variables, some of them are associated to the granules characteristics (i.e., particle size, density, porosity),

whereas others are related to the operational conditions of the reactor (DO concentration, nitrogen loading rate (NLR) or influent C/N ratio).

(ii) GSBRs with one or several anoxic periods (Adav et al., 2009; Chen et al., 2011; Kishida et al., 2006). In these systems, anoxic periods are introduced for enhancing denitrification apart from the possible SND during the aerobic phase. Very high N-removal efficiencies have been observed with this strategy (higher than 95%), although it usually requires the addition of an external carbon source.

1.4.2.2 Phosphorus removal

EBPR needs alternating anaerobic and aerobic condition to promote the proliferation of PAO. To achieve simultaneous COD, N and P removal using aerobic granules, de Kreuk and van Loosdrecht (2004) proposed the introduction of an anaerobic feeding phase for selecting PAOs from heterotrophic bacteria. Feeding was supplied through the bottom of the reactor and passed through the bed of settled biomass in plug-flow regime. This plug-flow regime prevented the inhibition of P-release by the interaction with nitrite or nitrate remaining from previous cycle. Furthermore, stability is enhanced in PAO enriched granules due to the fact that their maximum growth rate is lower compared to conventional heterotrophic biomass (de Kreuk and van Loosdrecht, 2004; Picioreanu et al., 2000).

Other authors such as Cassidy and Belia (2005), Coma et al. (2011) or Yilmaz et al. (2008) achieved simultaneous COD, N and P removal from alternating anaerobic, anoxic and aerobic reaction phases using mechanically mixed reactors to provide mixing during anaerobic or anoxic phases.

In granular systems with EBPR, the precipitation of P-salts in the core of the granules is commonly observed (de Kreuk et al., 2005a; Mañas et al., 2011; Yilmaz et al., 2008). In those studies, it was suggested that precipitated P-salts were apatite ($Ca_5(PO_4)_3(F, Cl, OH)$) and struvite ($NH_4MgPO_4 \cdot 6H_2O$), whose formation was induced by the high P concentrations measured during P-release devoted to PAO activity. Furthermore, this precipitation can represent an important percentage of the total P-removal (de Kreuk et al., 2005a; Mañas et al., 2011). It has been proposed that the precipitation of apatite via the surface complex hydroxy-dicalcium-phosphate ($[Ca_2HPO_4(OH)_2]$, HDP) determines the solubility of phosphate in the wastewater (Maurer et al., 1999). The solubility of HDP decreases at high Ca^{2+} concentrations and high pH values.

1.5 Energy – positive WWTP

For the achievement of more sustainable wastewater treatment plants, the use of anammox for nitrogen removal from sewage treatment has been recently proposed by Kartal et al. (2010). The scheme of the anammox based WWTP configuration is shown in Figure 1.6.

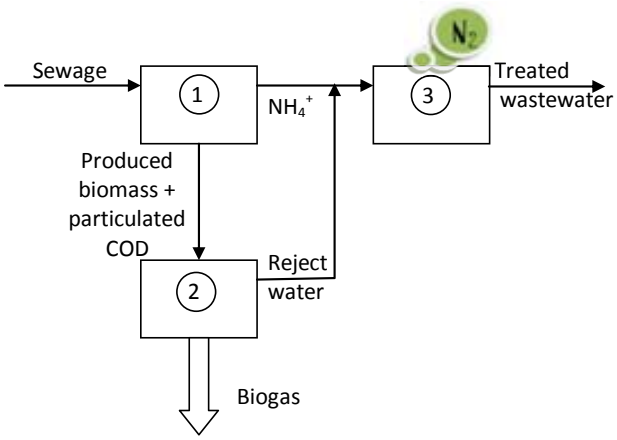

Figure 1.6: Sewage treatment with anammox, basic configuration (based on Kartal et al., 2010). **1**: Very-high-load activated sludge + settler; **2**: Anaerobic digester; **3**: Granular sludge nitritation - anammox reactor.

In this new WWTP configuration, the organic matter would be treated in a highly-loaded aerobic biological reactor (Figure 1.6, unit 1), with the aim of enhancing sludge production and reducing aeration requirements. This sludge would be later digested anaerobically together with the primary sludge to produce biogas (Figure 1.6, unit 2). The effluent wastewater from unit 1 (now mainly containing ammonium) together with the reject water from the dewatering of the digested sludge in unit 2 (a highly loaded ammonium stream) would be treated using the partial nitritation – anammox process in unit 3 (Figure 1.6). Final polishment of the treated wastewater could include a tertiary treatment with P precipitation.

Table 1.1. Calculation of net energy consumption based on mass fluxes for three wastewater treatment variants: (Case A) Conventional treatment; (Case B) Conventional treatment, with anammox used for treatment of digester effluent; (Case C) Optimized treatment, with anammox in the full main water line. Units Mass flux, grams per person per day (g p^{-1} d^{-1}); energy, Watthours per person per day (Wh p^{-1} d^{-1}). Table obtained from Kartal et al. (2010).

Oxygen and Energy needed	**Mass Flux (g p^{-1} d^{-1})**			**Energy (Wh p^{-1} d^{-1})**		
	Case A	*Case B*	*Case C*	*Case A*	*Case B*	*Case C*
Aeration for COD removal	40	30	15	-40	-30	-15
Aeration for Nitrogen removal[b]	22	22	16	-22	-22	-16
Pumping/Mixing energy	-	-	-	-20	-20	-15[a]
Methane-COD and electrical energy production form biogas	30	40	55	+38	+51	+70
Net energy	**-**	**-**	**-**	**-44**	**-21**	**+24**

[a]Lower because of absence of recirculation flows
[b]Nitrate effluent for cases A and B: 2.5 g p^{-1} d^{-1}; for case C: 1.1 g p^{-1} d^{-1}

Kartal et al. (2010) compared the energy fluxes of this new WWTP configuration (Table 1.1, Case C) with those of a conventional WWTP (Table 1.1, Case A) and those of a conventional WWTP with anammox for sidestream nitrogen removal (Table 1.1, Case B). These authors estimated that, for Case C, the wastewater treatment resulted in +24 Wh p^{-1} d^{-1} of energy production, in contrast to the -21 Wh p^{-1} d^{-1} or the -44 Wh p^{-1} d^{-1} of energy consumption for cases B and A, respectively (Table 1.1). The main energetic advantages of Case C were: (i) the lower oxygen requirements for COD and ammonium oxidation; (ii) higher electricity production by an enhancement of biogas production (Table 1.1). Therefore, if anammox is used for nitrogen removal from the mainstream of an urban WWTP, this wastewater treatment could become an energy-yielding treatment (Kartal et al., 2010).

1.5.1 Nitritation – anammox systems for high strength wastewater

As abovementioned, achieving an energy-positive urban wastewater treatment requires using the nitritation-anammox process. During the last decade, the nitritation-anammox process was successfully implemented for the treatment of high-strength ammonium wastewaters (Van Hulle et al., 2010). Two different approaches are observed in the literature:

1.5.1.1 Two-stage system

The first approach for implementing the partial nitritation – anammox process consists in separate both partial nitritation and anammox processes in two different reaction units. The first unit (i.e. the partial nitritation unit) is operated under aerobic conditions to convert approximately half of the ammonium to nitrite, whereas the second unit is operated under anaerobic conditions to obtain autotrophic denitrification which is performed by anammox bacteria.

For the first step, the patented High activity Ammonia Removal Over Nitrite (SHARON) is probably the most extended process for performing partial nitritation (Jaroszynski and Oleszkiewicz, 2011), especially for industrial wastewaters. SHARON is a suspended biomass system that works at temperatures higher than 25 ºC as a chemostat, using hydraulic retention times (HRT) lower than the doubling rate of NOB but higher than that of AOB (Hellinga et al., 1998). Accordingly, since this process has no sludge retention, NOB are not able to remain in the reactor and are easily washed out of the system. Despite SHARON has demonstrated to be a very robust process to perform partial nitritation, the main drawback of this technology is the low nitrogen loading rates obtained with this process (NLR around 0.32-0.52 g N m^{-3} d^{-1} at 30 ºC) and the need of temperatures higher than 25 ºC (Jaroszynski and Oleszkiewicz, 2011). This occurs because, since there is no retention of biomass, low biomass concentration are achieved.

Higher NLR than those in SHARON can been achieved with other partial nitrification systems with better biomass retention. Torà et al. (2014) obtained stable partial nitrification of reject water at a NLR up to 5.0 g N m^{-3} d^{-1} at 30 ºC, using a combination of pH, DO and ammonium control loops with an activated sludge system. Biofilm reactors are also a good alternative for achieving high NLR due to the good settling properties of granular biomass. Torà et al. (2013) obtained stable partial nitrification of reject water in a granular nitrifying airlift at maximum NLR of 1.75 g N m^{-3} d^{-1} at 30 ºC. The success of such a treatment relies on the use of a control strategy to maintain the adequate ratio between oxygen and ammonium concentrations in the reactor bulk liquid, as to repress NOB activity in the biofilm (automatic control for partial nitrification to nitrite in biofilm reactors, ANFIBIO) (Bartrolí et al., 2011, 2010; Jemaat et al., 2013).

The second step, i.e, the anammox process, can be carried out with different reactors. At laboratory scale, the granular SBRs are widely used due to its flexibility of operation and easy control (Arrojo et al., 2008; Dapena-Mora et al., 2004; Dosta et al., 2008). At full-scale, Internal Circulating reactors similar to those used in the anaerobic processes were first used (van der Star et al., 2007), achieving a high NLR of 9.5 g N m^{-3} d^{-1}. However, UASB reactors have even higher potential, since extremely high NLRs (up to 77 g N m^{-3} d^{-1}) have been observed at laboratory scale in this type of reactors (Jin et al., 2013; Ma et al., 2013; Tang et al., 2011).

1.5.1.2 One-stage systems

A second type of partial nitritation-anammox systems are the one-stage reactors. In these systems, a co-culture of AOB and anammox bacteria is established under microaerobic conditions to avoid inhibition of anammox bacteria by oxygen and to achieve appropriated conditions to obtain partial nitritation (Strous and Jetten, 1997).

Different commercial names were given to this process, such as CANON: Completely Autotrophic Nitrogen removal Over Nitrite process (Third et al., 2001), OLAND: Oxygen-Limited Autotrophic Nitrification-Denitrification (Kuai and Verstraete, 1998), DEMON: deammonification (Hippen et al., 1997; Wett, 2007) and SNAP: Single-stage Nitrogen removal using anammox and Partial nitritation (Furukawa et al., 2006).The difference among them mainly lies in the organisms that were originally assumed to be responsible for anaerobic ammonium oxidation. In both the OLAND-process and the aerobic/anoxic deammonification process nitrifiers were erroneously assumed to perform this ammonium oxidation under microaerobic conditions (Helmer et al., 1999; Kuai and Verstraete, 1998). In the CANON process anammox bacteria were assumed to be responsible. However, later studies confirmed with fluorescence in-situ hybridization (FISH)

analyses (Helmer et al., 2002; Pynaert et al., 2003) that anaerobic ammonium oxidation in all reactors was performed by anammox organisms, although Pynaert et al. (2003) did not exclude a specific role for the aerobic ammonium oxidizers

One-stage partial nitritation-anammox reactors have been implemented at full scale for the treatment of high-loaded ammonium industrial wastewaters at temperatures around 30-35ºC, such as reject water (Joss et al., 2009; Weissenbacher et al., 2010), landfill leachate (Hippen et al., 2001) or other industrial wastewaters (Abma et al., 2010).

Different reactor-types have been used to perform these one-stage nitritation-anammox process, such as rotating biological contactors (RBC) (Hippen et al., 2001), SBR (Joss et al., 2009; Wett, 2007), granular sludge reactors (Abma et al., 2010), activated sludge (Desloover et al., 2011) or moving bed bioreactors (MBBR) with Kaldnes rings as biomass carrier (Rosenwinkel and Cornelius, 2005).

SBR technology is the most commonly applied and, among SBR technologies, DEMON configuration is the most popular with more than 80% of all SBR systems (Lackner et al., 2014). DEMON uses hydrocyclones to adjust the SRT for ammonium oxidizing bacteria and anammox bacteria separately and to separate the slow growing anammox bacteria from incoming solids (Wett et al., 2010).

In biofilm or granular biomass, the AOB are active in the outer layers of the biofilm, producing a suitable amount of nitrite for the anammox bacteria that are active in the inner layers (see Figure 1.7). This way the anammox bacteria are protected from oxygen, which is consumed in the outer layers (Wyffels et al., 2004).

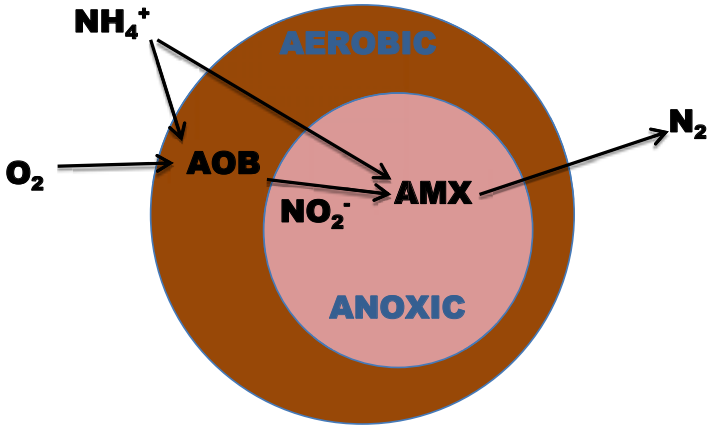

Figure 1.7: Schematic representation of CANON process in biomass aggregates. AMX stands for anammox.

1.5.2 Application of the partial nitritation - anammox process in the mainstream of urban WWTPs.

Two main factors differentiate and challenge the application of the partial nitritation – anammox process to the treatment of the mainstream of an urban WWTP: lower ammonium influent concentrations (< 100 mg $N\text{-}NH_4^+$ L^{-1}) and lower wastewater temperatures, especially in winter. On one side low temperature may lead to lower specific activities and growth rates for both anammox bacteria and AOB (Dosta et al., 2008); and in the other side, both low winter temperatures and low ammonium concentrations favors NOB proliferation, hindering to maintain stable partial nitritation. Note that specific winter wastewater temperatures will strongly depend on the geographical location of the WWTP, being around 15 ºC in Spain, or 8 ºC in northern Europe. In contrast, in equatorial regions such as Brazil or Singapore, the wastewater temperature remains quite constant during all the year (28 – 32 ºC). Therefore, in these regions temperature is not expected to be a drawback for a good partial nitritation- anammox process performance.

The performance of one-stage partial nitriation-anammox reactors with pretreated municipal nitrogenous wastewater at low temperatures (12.5 – 15 ºC) has been tested with SBR (Hu et al., 2013; Winkler et al., 2012) or RBC (de Clippeleir et al., 2013) as a first approach. In many of the studies, the known weak point of those trials is that nitrite oxidizing bacteria (NOB) develop in the long term operation, triggering the production of nitrate, and decreasing importantly the N-removal performance with anammox (de Clippeleir et al., 2013; Winkler et al., 2011b).

1.6 Mathematical modeling of biofilm reactors

The mathematical modeling can be considered a very useful tool for analyzing complex ecosystems, such as activated sludge or granular sludge systems, where lots of parameters, processes and reactions are involved. In that sense, mathematical models represent an important and fundamental tool to know in detail the processes developed inside the granules. Furthermore they can provide a solid foundation for design and operation without the time consumption and materials expense of the experimental approach.

For the conventional floc-based activated sludge systems, the International Water Association (IWA) has provided a consistent framework for the description of biological processes: the Activated Sludge Model (ASM, Henze et al. (2000)). The Activated Sludge Model no. 1 (ASM1) was developed by mid-1980s, and allowed simulating the biological organic matter removal, nitrification and denitrification processes. Later, in the mid-1990s, since the EBPR process was becoming popular and the understanding of the process was increasing, the Activated Sludge

Model no.2 (ASM2) was published including the EBPR process. However, the ASM2 model was expanded into version ASM2d model, where denitrifying PAOs were included. Finally, in late-1990s, the IWA decided to develop a new modeling platform, the ASM3, based on recent developments in the understanding of the activated sludge processes. In ASM3, the decay processes from ASM1 were replaced by an endogenous respiration processes, a more realistic approach under a microbiological point of view. The matrix structure and organization of ASM models makes an easy integration of these models into several simulation programs, such as AQUASIM, WEST or MATLAB.

Biofilm reactors are much complex systems than activated sludge, since many physical, chemical and biological processes occur simultaneously inside the biofilm. The biological process proposed in the ASM models can describe the biological reactions occurring in a biofilm reactor (i.e. nitrification, denitrification, etc.), but not other physical and chemical processes, such as substrates diffusion into the biofilm, or biofilm growth. Therefore, additional considerations must be taken into account for a correct description of the overall processes (Wanner et al., 2006).

Biofilm models typically require defining the different compartments representing the different sections of a biofilm system (i.e. bulk liquid, gas phase, boundary layer, biofilm or substratum). In each compartment, the relevant components (e.g. substrates, products, biomass, inert components, etc.) as well as their transformation, transport and transfer process are defined. Finally, all processes affecting each component in each compartment have to be mathematically linked together into a mass balance equation (Wanner et al., 2006).

The implementation of all this complexity is impractical and almost impossible without conducting simplifying assumptions. According to the simplifying assumptions conducted, the IWA Task Group on Biofilm Modelling grouped the different models into four distinct categories: analytical (Pérez et al., 2005), pseudo-analytical (Sáez and Rittmann, 1988), 1d numerical (Wanner and Reichert, 1996) and 2d/3d numerical (Eberl et al., 2004; Picioreanu et al., 2000).

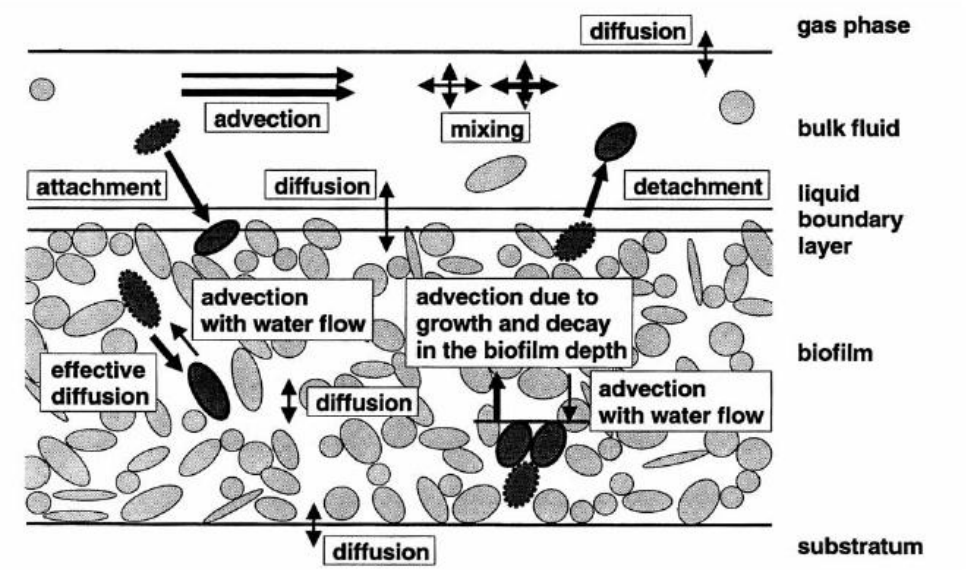

Figure 1.8: Transport processes considered in Wanner and Reichert (1996) 1d numerical biofilm model. Thick arrows refer to particulate, thin arrows to dissolved components. Picture obtained from Wanner and Reichert (1996).

Analytical and pseudo-analytical approaches contain more simplifying assumptions and, therefore, its applications are more limited. However, these models are easier to resolve and they can be implemented into a spreadsheet. Analytical and pseudo-analytical models can provide good results with simple systems (e.g. only one process, such as nitrification or COD removal, dominates de biofilm) or with moderately complex systems (e.g. multi-substrate component + multi-species biofilm systems) if significant *a priori* knowledge of biofilm composition is available (Wanner et al., 2006). In contrast, numerical models are more flexible and can provide good results in complex biofilm systems, but require higher computational power, especially for 2d/3d numerical models. The choice of the model type is dependent on the model adequacy to the modeling objectives.

For granular reactors, 1d numerical models allow for good description of the performance of these biofilm systems while simulations can be resolved in a reasonable time with current personal computers power. Perhaps for these reasons, 1d numerical model have been extensively used to model the performance of granular reactors. Beun et al. (2001) and Ni et al. (2008b) developed 1d mathematical models describing the COD and N-removal via the nitrification and heterotrophic denitrification processes. Beun et al. (2001) showed that nitrification, denitrification and COD removal can occur simultaneously in a granular sludge SBR. De Kreuk et al. (2007b) introduced the biological phosphorus removal and studied the individual influence of some parameters (i.e. temperature and granule size) over the nutrient removal. Vázquez-Padín et al. (2010) showed that the biomass characteristics could be successfully

described if a porosity profile across the granules depth was taken into account. Later, Su et al. (2012) modeled the variations in size and density of granules due to growth, detachment or breakage, to optimize the size and density of granules.

For nitrifying granular reactors, the understanding of the partial nitritation process has been deeply studied through mathematical modeling. Pérez et al. (2009) concluded that the higher oxygen affinity for AOB was the key parameter for exclusion of NOB in a biofilm reactor. They also found that inhibition of NOB by free ammonia did not substantially contribute to the compartmentalization in biofilm reactors. Brockmann and Morgenroth (2010), using Monte Carlo filtering, corroborated that competition for oxygen was the main mechanism for displacing NOB from the biofilm, and preventing re-growth of NOB in the long-term. Also found that the mechanisms for washout of NOB from biofilms are different from suspended cultures where the difference in maximum growth rate is a key mechanism. Jemaat et al. (2013) demonstrated that the use of a control strategy to maintain the adequate ratio between oxygen and ammonium concentrations in the reactor bulk liquid was convenient to repress NOB activity in the biofilm (automatic control for partial nitrification to nitrite in biofilm reactors, ANFIBIO). Also, their modeling results estimated that even at 15 ºC full nitritation could be achieved with nitrifying granules.

For anammox granular reactors, Hao et al. (2002a) first modeled the performance of a one-stage partial nitritation-anammox reactor, and later studied the effect of different process parameters over partial nitritation-anammox process (Hao et al., 2002b, 2005; Hao and van Loosdrecht, 2004). Volcke et al. (2010) studied the effect of particle size on the performance of anammox reactor, and its relation with oxygen penetration depth. Later, Volcke et al. (2012) studied also the effect of particle size but considering a particle size distribution. They observed that NOB were present in the smallest granules, while they were outcompeted by anammox bacteria in larger granules. Vangsgaard et al. (2012) calibrated a model describing nitritation-anammox process from experimental data collected during SBR cycles using a pragmatic Monte Carlo based fitting method, and found that the optimal loading ratio between oxygen and ammonia was 1.9 g O_2 g^{-1} N. For ratios above the optimum, anammox were inhibited and NOB developed, while for ratios below the optimum AOB activity was oxygen-limited.

CHAPTER 2

OBJECTIVES

As mentioned in the introduction section, two different systems have been proposed for the treatment of urban wastewater with granular sludge. First, aerobic GSBR, which perform the same nutrient removal process occurring in activated sludge systems but taking advantage of the abovementioned granular sludge properties. Second, an anammox-based sewage treatment, which could allow obtaining a more sustainable (energy-neutral or even energy-positive) wastewater treatment. The main motivation of this thesis is improving the knowledge of these granular biomass systems towards confirming granular biomass as a real alternative to urban wastewater treatment with activated sludge.

Subsequently, several specific objectives were proposed for each of the abovementioned granular systems.

For GSBR systems, the specific objectives were:

- To start-up a pilot-scale GSBR for the treatment of a low-strength wastewater.
- To evaluate the stability of granular biomass and the efficiency in C, N and P removal in the long term operation of the GSBR.
- To search for control strategies that allows enhancing the nitrogen removal in a GSBR.

For the anammox-based sewage treatment, this thesis was focused in the two-step systems, and two different specific objectives were proposed:

- To evaluate the feasibility of the partial nitritation step in with a low strength wastewater at low temperatures.
- To explore the microbial population shifts in an anammox reactor after a temperature shock using 454-pyrosequencing analysis.

CHAPTER 3

LONG TERM OPERATION OF A GRANULAR SEQUENCING BATCH REACTOR AT PILOT SCALE TREATING A LOW STRENGH WASTEWATER

This chapter is based in the following publications:

Isanta, E., Suárez-Ojeda, M.E., Val del Río, Á., Morales, N., Pérez, J., Carrera, J., 2012. Long term operation of a granular sequencing batch reactor at pilot scale treating a low-strength wastewater. Chem. Eng. J. 198-199, 163–170.

Part of this chapter was presented as oral presentation:

Isanta, E., Suárez-Ojeda, M.E., Val del Río, Á., Morales, N., Pérez, J., Carrera, J.,. Long term operation of a granular sequencing batch reactor at pilot scale treating a municipal wastewater. *IWA Biofilm Conference 2011*, Shanghai, China. October 27-30, 2011.

3.1 Introduction

Aerobic granular sludge was developed as an alternative technology to conventional activated sludge processes for the wastewater treatment. The morphological structure of aerobic granular sludge (i.e. high particle diameter and density) provides two main advantages if compared to activated sludge processes: (i) the ability of settling faster, which ease the retention of biomass (Adav et al., 2008; Liu and Tay, 2004); and (ii) the existence of substrate profiles across the granule radius, which allows simultaneous aerobic, anoxic and anaerobic processes into the same granule (de Kreuk et al., 2005a; Mosquera-Corral et al., 2005; Yilmaz et al., 2008). Both characteristics contribute to reduce the required reactor capacity producing more compact designs, or to treat higher wastewater loading rates, when compared to conventional activated sludge systems. Furthermore, since aerobic granules can be separated from wastewater in the same reactor vessel, external settling units become unnecessary (de Bruin et al., 2004).

Recently, a significant number of studies devoted to the activity, morphology and operation of aerobic granules at lab-scale have been published. High shear stress and short settling times are key parameters for selecting fast-settling biomass and to promote granulation (Beun et al., 2002; Tay et al., 2004). Also, a feast-famine regime in the reactor improves the stability of granules (de Kreuk and van Loosdrecht, 2004; Tay et al., 2001b), whereas granules become increasingly filamentous when feast periods prevail over famine periods in an SBR (McSwain et al., 2004). Dissolved oxygen (DO) concentration in granular reactors is also an important parameter, since low DO concentrations affect negatively to the formation and stability of aerobic granules due to oxygen diffusion limitation (McSwain and Irvine, 2008; Mosquera-Corral et al., 2005). To obtain simultaneous removal of nitrogen (N) and phosphorus (P) using aerobic granules, de Kreuk et al. (2005a) proposed the introduction of an anaerobic feeding phase for selecting polyphosphate-accumulating organisms (PAO) from heterotrophic bacteria. Furthermore, stability is enhanced in PAO enriched granules due to the fact that their maximum growth rate is lower compared to conventional heterotrophic biomass (Picioreanu et al., 2000). In granular systems with enhanced biological phosphorus removal (EBPR), the precipitation of P-salts in the core of the granules is commonly observed (de Kreuk et al., 2005a; Mañas et al., 2011; Yilmaz et al., 2008). In those studies, it was suggested that precipitated P-salts were apatite ($Ca_5(PO_4)_3(F,Cl,OH)$) and struvite ($NH_4MgPO_4{\cdot}6H_2O$), whose formation was induced by the high P concentrations measured during P-release devoted to PAO activity. Furthermore, this precipitation can represent an important percentage of the total P-removal (de Kreuk et al., 2005a; Mañas et al., 2011). It has been proposed that the formation of apatite passes through an intermediate, the surface complex

hidroxy-dicalcium-phosphate ($Ca_2HPO_4(OH)_2$,HDP), which determines the solubility of phosphate in the wastewater (Maurer et al., 1999). The solubility of HDP decreases at high pH values and Ca^{2+} concentrations.

Results obtained with granular aerobic reactors at lab-scale are promising but more information about the stability of granules and their performance at large scale is needed in order to establish aerobic granulation as a feasible treatment to remove nutrients from wastewater. Most of current studies at pilot or industrial scale were carried out with high-strength wastewaters (Bartrolí et al., 2010; Jungles et al., 2011; Liu et al., 2010) and only few of them treating low-strength wastewaters (Coma et al., 2010; de Kreuk and van Loosdrecht, 2006; Ni et al., 2009). However, to the best of our knowledge, there is a lack of information about long term performance of granular reactors at pilot scale, removing simultaneously carbon (C), nitrogen (N) and phosphorus (P) from low-strength wastewaters. In this context, this study presents the results of operation, during almost one year, of a pilot-scale granular sequencing batch reactor (GSBR) treating a low-strength wastewater. The stability of granules and the efficiency in C, N and P removal at long-term were also evaluated.

3.2 Materials and methods

3.2.1 GSBR pilot plant description

The GSBR consisted in a bubble column of 2 m high and of 25 cm of diameter, with a working volume of 100 L. The height (H) to diameter (D) ratio was H/D = 7.2 (Figure 3.1). The volumetric exchange ratio was 55%. Conventional operation of sequential batch reactor was applied with 180 min per cycle and with a hydraulic retention time of 5.4 h. Each cycle was divided in four phases: static feeding (60 min), aeration (114 min), settling (3 min) and discharge (3 min). The feeding phase was considered static, since there was neither aeration nor stirring. The combination of a static feeding phase followed by an aeration period has demonstrated to be suitable for removing both N and P using aerobic granules at lab-scale (de Kreuk and van Loosdrecht, 2004). During aeration phase, compressed air was supplied at a constant flow rate from the bottom of the column through a membrane aerator. The feeding was supplied through a diffuser placed in the bottom of the reactor, 6 cm above the membrane aerator. Temperature was maintained at 25 ºC. Dissolved oxygen (DO) and pH, which were online monitored but not controlled along the whole experimental period with Hach-Lange probes, ranged typically from 6 to 8 mg O_2 L^{-1} and from 7.0 to 7.7, respectively. The GSBR cycle control and monitoring was performed through specific software developed in Labview® 8.0 (National Instruments). The communication between the PC and the GSBR hardware was performed using a compact field

point (cFP) system (National Instruments, Spain), which had a cFP-1804 as the Ethernet interface and several input/output modules (cFP-AI-110 and cFP-RLY-421).

Figure 3.1. Picture of the GSBR pilot plant for the treatment of a low-strength wastewater.

The GSBR influent was a synthetic low-strength wastewater containing: 220 mg L^{-1} sodium acetate, 139 mg L^{-1} sodium propionate, 93 mg L^{-1} sucrose, 153 mg L^{-1} NH_4Cl, 14.5 mg L^{-1} KH_2PO_4, 37.1 mg L^{-1} K_2HPO_4, 44 mg L^{-1} $MgSO_4$, 70 mg L^{-1} $CaCl_2$, 19 mg L^{-1} KCl, as well as, a solution with trace elements. The resulting inflow concentrations were: Chemical oxygen demand (COD): 400 mg O_2 L^{-1}, N-NH_4^+:40 mg N L^{-1} and P-PO_4^{3-}: 10 mg P L^{-1}. The feed was kept in a refrigerated tank at 7 ºC, provided with a mechanical stirrer to guarantee homogeneity of the feed mixture.

3.2.2 Analytical methods

Total organic carbon (TOC) was measured with an OI Analytical TOC analyser (Model 1020A) equipped with a non-dispersive infrared detector and a furnace maintained at 680ºC. COD was determined spectrophotometrically using Hach Lange standard LCK COD kits. Ammonium was

analysed by means of a continuous flow analyser based on a potentiometric determination of ammonia. Nitrate and nitrite concentrations were analysed with ionic chromatography using an ICS-2000 Integrated Reagent-Free IC system (DIONEX Corporation) which performs ion analyses using suppressed conductivity detection. Phosphate was measured by a phosphate analyser (Hach Lange PHOSPHAX sc). Mixed liquor total suspended solids (TSS), mixed liquor volatile suspended solids (VSS) and sludge volumetric index (SVI) were analysed according to APHA (2008). The density of the granules was measured using the dextran blue methodology adapted from Beun et al. (2002). Photos of granules were obtained with a MZFLIII Magnifying Glass (Leica microsystems), and were used to determine the granules particle size by image analysis. The elemental composition of granules in terms of Ca, Na, P, K and Mg was performed using an Inductively Coupled Plasma Mass Spectrometer (Thermo Elemental, Xseries II).

3.2.3 2.3. Fluorescence in situ hybridization (FISH)

FISH coupled with confocal laser scanning microscopy (CLSM) was used to assess the relative abundances of ammonia-oxidizing bacteria (AOB), nitrite-oxidizing bacteria (NOB), PAO and glycogen accumulating organisms (GAO) in the granules. Crushed granules were hybridized using simultaneously the Cy3-labeled specific probe and Cy5-labeled EUBmix probe (general probe). Specific probe used for AOB detection was Nso190 (Mobarry et al., 1996) whereas for NOB detection the probe was NIT3 (Wagner et al., 1996). For PAO detection a PAOmix probe made of a mixture of AO462, PAO651 and PAO846 probes (Crocetti et al., 2000), was used. For GAO detection a GAOmix probe was used, including GAOQ431 and GAOQ989 probes (Crocetti et al., 2002). EUBmix probe consisted of the mix of probes EUB338, EUB338 II and EUB338 III (Amann et al., 1990; Daims et al., 1999). A Leica TCS SP5 AOBS microscope at a magnification of 63x (objective HCX PL APO ibd.B1 63x 1.4 oil) equipped with two He-Ne lasers with light emission at 561 and 633 nm was used for biomass quantification. For every pair of probes (general and specific), at least 40 images from different microscopic fields were taken to perform the quantification. Detailed information about FISH quantification can be found elsewhere (Jubany et al., 2009b).

3.3 Results and discussion

3.3.1 Time course of granules properties

The GSBR was inoculated with floccular activated sludge from a municipal wastewater treatment plant (WWTP) from Barcelona area. A conservative settling time (15 min) was initially used for biomass acclimation to the influent. Initial airflow rate was 25 NL min^{-1}. From day 6 to 23, the settling time was progressively reduced, from 15 min to 4 min, to increase the hydraulic

pressure selection to select fast settling biomass, favoring granules development. However, at these conditions, granules did not develop, and big flocs were the predominant biomass structures in the reactor with a high SVI_{30} (200 mL g^{-1}, Figure 3.2A, granulation start-up). It was found that the superficial air velocity in the GSBR was 0.8 cm s^{-1}, lower than the minimum required to obtain granulation, which is suggested to be 1.2 cm s^{-1}, according to Tay et al. (2004). Consequently, the aeration was doubled from 25 to 50 NL min^{-1}, meaning an increase of the superficial air velocity to 1.6 cm s^{-1}. After that, the SVI_{30} rapidly decreased from 200 mL g^{-1} on day 23 to 60 mL g^{-1} on day 28 (see Figure 3.2A) as consequence of the breakage of the flocs. Thereafter, granules started to develop. Settling time was also reduced from 4 to 3 min on day 43. Complete granulation was observed after day 51 when SVI_5/SVI_{30} was lower than 1.05 (Figure 3.2A, granulation start-up). The time required to achieve biomass granulation was close to that reported in similar GSBRs at lab-scale (43 days; (Kishida et al., 2006)) or even lower (90-100 days; (Coma et al., 2010; Mañas et al., 2011)).

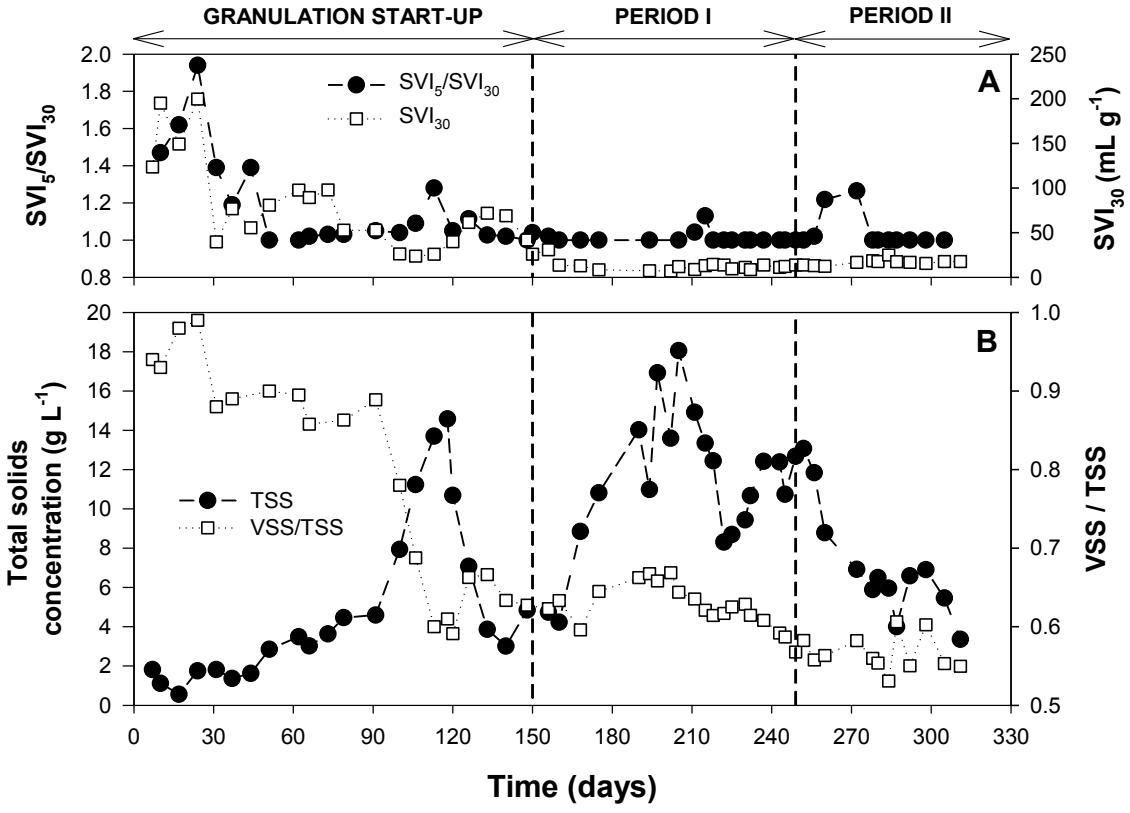

Figure 3.2. Time course profiles of sludge volumetric index (A) and solids concentration (B) during the whole experimental period.

As shown in Figure 3.2B, from day 90 to 120, granules concentration in the reactor increased rapidly from 4 to 15 g TSS L^{-1}. Interestingly, the mineral fraction of the granules also increased rapidly from 11% to 41% in that period (Figure 3.2B). Furthermore, the P-removal was very high, even achieving 100% of P-removal efficiency on day 120 (Figure 3.4). The reason for this rapid increase of the mineral fraction is not completely known, however, pH could have played an important role. During those days the pH measured in the GSBR was higher, increasing from 7.5±0.1 to 8.1±0.2. At these pH conditions, and given the Ca^{2+} concentration in the influent (at least 54 mg Ca L^{-1}), the phosphate solubility was below 1 mg P L^{-1} (Maurer et al., 1999), being possible the precipitation of P-salts, and its further accumulation in the core of the granules. More details about the mineral content of the granules are given in section 3.3.2.

Besides the increase of the mineral fraction in the granules, an overgrowth of finger-type and filamentous structures over the granules (see Figure 3.3A) was observed after an accidental increase of 70% of the applied organic loading rate at day 110. During this episode, SVI_5/SVI_{30} increased from 1.05 to 1.30 (Figure 2A), since granules lost compactness, due the presence of finger-type and filamentous structures (Figure 3A). Also, the breakage of part of the granules was observed, producing a rapid decrease of biomass concentration in the reactor (Figure 3.2B, days 120 to 140).

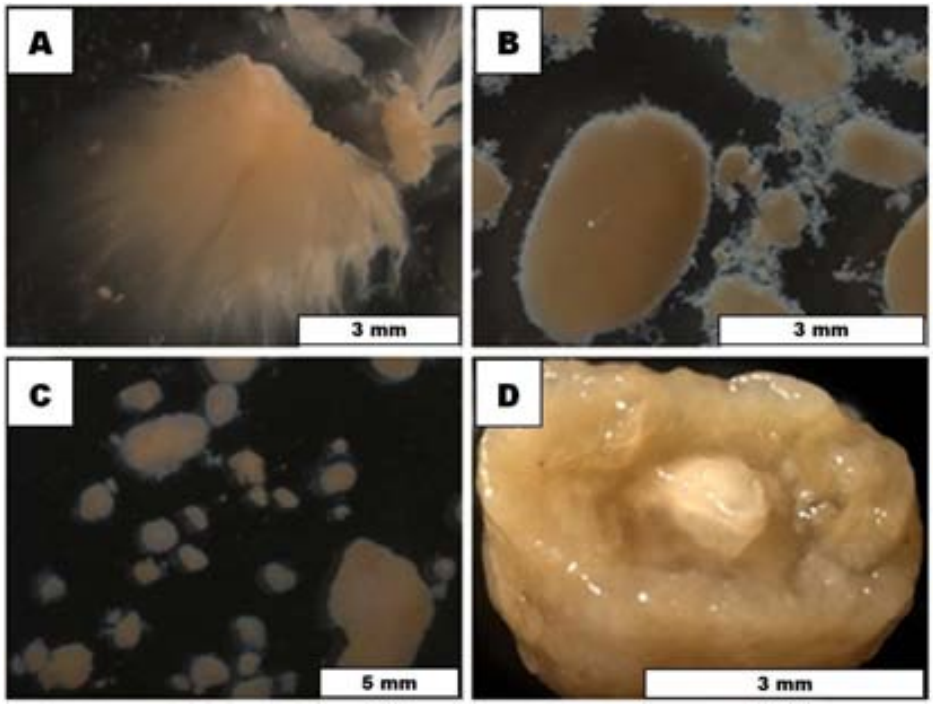

Figure 3.3. Pictures of the granules in the GSBR corresponding to: (A) finger-type and filamentous structures overgrowth at day 120; (B) granules on period I; (C) granules on period II; (D) inorganic core observed in granules. Observations were performed with a MZFLIII (Leica microsystems) magnifying glass.

According to Picioreanu et al. (2000), irregular biofilm structures tend to be formed when the values of the ratio between biomass growth rate to diffusive transport (G) are high. The organic matter overload in the reactor caused, on one side, a DO concentrations 50% lower (from 6 to 3 mg O_2 L^{-1}) during the feast phase due to higher substrate consumption, and on the other side, the TOC/O_2 bulk liquid concentrations ratio increased from 15 to 57. Consequently, higher values of G were applied favoring the tendency to form sharp-edged biofilms. Mosquera-Corral et al. (2005) observed similar overgrowth of filamentous structures onto the granules surface in a GSBR operating with similar influent concentrations when working at low DO concentrations (c.a. 3.5 mg O_2 L^{-1}) and TOC/O_2 bulk liquid concentrations ratio approximately higher than 26. After the breakage and biomass washout episode, mature granules grew and prevailed in the reactor from day 150 onwards.

To help on the discussion of the experimental data, the reactor operation with mature granules was divided in: (i) period I, from day 150 to 250 and (ii) period II, from day 250 to 330. Granular biomass properties for periods I and II are summarized in Table 3.1. On period I, the average TSS concentration was 12 ± 4 g L^{-1}. Sludge was regularly purged (from days 180 to 230) to maintain a global sludge retention time (SRT) (taking into account biomass purged and solids in effluent) around 20 days (19±4 days). Contribution of biomass purged to the SRT from days 180 to 230 was 20% whereas the rest was due to solids in the effluent. On period II the average TSS concentration was 7 ± 3 g L^{-1} and no biomass purge was carried out since an increase of the solids concentration in the effluent during this period caused a decrease of the SRT to 11 ± 3 days. The solids concentrations in the GSBR pilot plant were in the range of the TSS concentrations reported in other GSBR pilot plants treating low-strength wastewaters (9-10 g L^{-1}, (de Kreuk et al., 2005a); 8-10 g L^{-1}, (Ni et al., 2009)).

Table 3.1. Characterization of the granules developed in the GSBR for periods I and II.

	Period I	**Period II**
Average diameter (mm)	2.4	2.4
Granule density (g TSS L^{-1})	114±5	123±2
SVI_{30} (mL g^{-1})	13±6	17±4
SVI_5/SVI_{30}	1.0	1.0
Total solids concentration in the GSBR (g TSS L^{-1})	12±4	7±3
Inorganic content (%)	35-40	42-48
Apparent SRT (days)	19±4	11±3
Average diameter (mm)	2.4	2.4

The ash content of granules in period I varied from 35 to 40 %. A general increasing trend of the inorganic content of the granules was detected from day 190 onwards, since the VSS/TSS ratio progressively decreased (Figure 3.2B), this continued in period II. In fact, precipitated salts were noticed in the granules core (Figure 3.3D). To assess the nature of the precipitates found in the granules, the elemental content of some cations in the granules was determined for periods I and II (see Table 3.2). Then, the Mg/P and Ca/P mass ratios for each period were calculated and compared with the theoretical Mg/P mass ratio of struvite (0.79 g Mg g^{-1} P), and with the apatite theoretical Ca/P mass ratio (2.16 g Ca g^{-1} P). It was found that the Mg/P ratios for periods I and II were 0.03 and 0.06 g Mg g^{-1} P, respectively and the Ca/P ratios were 1.75 and 1.86 g Ca g^{-1} P, respectively (Table 3.2). Therefore, the Ca/P experimental ratios were closer to the theoretical one of apatite than the Mg/P ratios of struvite, indicating that the precipited salts in the granules could be somehow similar to apatite. Mañas et al. (2011) performed specific analysis of the mineral core of his granules and determined that the precipitate (Ca/P = 2.10 g Ca g^{-1} P) was hydroxyapatite, one particular formulation of apatite. If apatite was the main mineral found in the core of the granules, and considering that a fraction of polyphosphates will be accumulated by PAO, one would expect a Ca/P ratio in the biomass slightly lower than the Ca/P ratio for apatite (2.16 g Ca g^{-1} P), as it was indeed experimentally measured (1.75-1.86 g Ca g^{-1} P).

Table 3.2. Elemental analysis of several cations in the granules by means of an Inductively Coupled Plasma Mass Spectrometer for periods I and II. Ca/P and Mg/P weight ratios are also included.

	Period I	**Period II**
Ca (g kg^{-1})	57±5	86±5
P (g kg^{-1})	32.6±0.2	46.2±0.2
Mg (g kg^{-1})	0.93±0.01	3.00±0.01
K (g kg^{-1})	0.72±0.03	2.90±0.02
Na (g kg^{-1})	0.37±0.05	0.52±0.04
Ca/P (g Ca g^{-1} P)	1.75	1.86
Mg/P (g Mg g^{-1} P)	0.03	0.06

In contrast to biomass concentration and inorganic content, the values of SVI_{30}, density and size of granules did not change significantly between periods I and II. The SVI_{30} values ranged between 13 and 16 mL g^{-1} TSS, the granule density between 68 and 75 g VSS L^{-1} and the average size of granules was 2.4 mm (see Table 3.1). SVI_{30} of granules was similar to that obtained by other authors with lab-scale GSBR treating low-strength wastewaters (16-24 mL g^{-1}, (de Kreuk et al., 2005a); 17 mL g^{-1}, (Lin et al., 2003)) but, lower than the SVI_{30} achieved at pilot scale with low-strength wastewaters (38 mL g^{-1}, (de Kreuk and van Loosdrecht, 2006); 35 mL g^{-1}, (Ni et al.,

2009)). In both periods (I and II) granular sludge was more than 90% of the total suspended solids in the reactor. The granule density measured in the GSBR was also similar to the 78-89 g TSS L^{-1} or 62 g VSS L^{-1} reported at lab-scale by de Kreuk et al. (2005a) and Cassidy and Belia (2005), respectively. However, total density (in TSS basis) was high (114-123 g TSS L^{-1}) than those bibliographic values as a consequence of the high mineral content of the granules. In contrast, average size of granules obtained in this study (2.4 mm, Table 3.1) was higher than the diameters reported at lab-scale (1.2-1.3 mm, (de Kreuk et al., 2005a; Lin et al., 2003)) or even at pilot scale (0.2-0.8 mm, (Ni et al., 2009)). Granules size is known to be dependent on shear-stress and therefore, on aeration rate, obtaining higher particle size at lower aeration rates (Tay et al., 2004). High aeration rates are used in lab-scale granular reactors to ensure enough shear stress for granulation (2.4-2.5 cm s^{-1}, (de Kreuk et al., 2005a; Lin et al., 2003)). In our case, the shear stress was estimated at 0.087 Nm^{-2} (following the methodology established by Ren et al. (2009)). This value of shear stress was around 30% lower than that estimated for the reactor conditions in the study presented by de Kreuk et al. (2005a). Therefore, the lower air velocity (1.6 cm s^{-1}) used in this work would explain the difference in granule size.

3.3.2 Carbon and nutrients removal

Lab-scale studies have demonstrated the possibility of performing simultaneous nitrification, denitrification and phosphorus removal with granular sludge (de Kreuk et al., 2005a; Yilmaz et al., 2008). The COD storage capacity of granules, together with the oxygen penetration across the granules, will determine the capacity of performing simultaneous nitrification and denitrification (SND) during the aerobic phase. The more biological nitrogen removal (BNR) is performed through SND during aerobic phase, the less oxidized nitrogen species will remain at the end of the cycle; at the same time, less organic matter will be consumed for heterotrophic denitrification during static feeding phase and more organic matter will be available for being stored and therefore, to perform EBPR with PAO.

The TOC, N and P effluent concentrations, as well as, their removal efficiencies, calculated from the C, N and P mass balances in the reactor are presented in Figure 3.4. The TOC removal efficiencies remained, in general, higher than 80%. During the start-up or periods with significant biomass loss, the C removal efficiencies maintained higher than 70%.

For N removal, similar nitrification efficiencies were observed in both periods being, in general, higher than 75% (Table 3.3). Furthermore, this nitrification was 80% to nitrite (partial nitrification) in both periods (Table 3.3). Stable BNR via nitrite with granular biomass has not been reported in other GSBR treating low-strength wastewaters (Coma et al., 2010; de Kreuk et

al., 2005a; Ni et al., 2009). This could be due to the higher granule size obtained in the present study (2.4 mm) compared to 0.2-0.8, 0.8 and 1.3 mm reported by Ni et al. (2009), Coma et al. (2010), and de Kreuk et al. (2005a), respectively. The higher the granule size, the lower the specific granular surface; consequently, a reduced oxygen flux towards the biofilm is obtained for a given biomass amount, favoring partial nitrification due to oxygen limitation (Bartrolí et al., 2010). The DO was not controlled in the GSBR. Typically, during the feast phase at the beginning of the cycle, DO was around 6 mg O_2 L^{-1}, rising during the famine phase up to 8 mg O_2 L^{-1}, which is close to saturation. BNR via nitrite was therefore accomplished despite using high DO concentrations. Bartrolí et al. (2010) (among other studies) demonstrated the possibility of obtaining full nitritation (i.e. 100% oxidation of ammonia to nitrite) at high DO concentration in biofilm reactors by maintaining ammonium in excess. In their study, with nitrifying granules with an average size of 0.9 mm, they required a DO to ammonium concentrations ratio (DO/TAN) lower than 0.3 mg O_2 mg^{-1} $N\text{-}NH_4^+$ to obtain full nitritation. In our case, it is clear that ammonium was always in excess (Figure 3.4), and the DO/TAN ratio at the end of the cycle ranged from 0.45-0.90 mg O_2 mg^{-1} $N\text{-}NH_4^+$. This low DO/TAN concentrations ratio could be the reason why BNR via nitrite was detected. Also the distribution of AOB and NOB populations in the GSBR (Table 3.3) confirmed the partial nitrification. In both periods, the ratio of the AOB and NOB fractions was in the range 5-8, which in significantly above the theoretical ratio of growth yield coefficients (Y_{AOB}/Y_{NOB} = 2.25, from Jubany et al. (2008)), indicating that NOB were disfavoured.

Table 3.3. Performance of the GSBR for nutrient removal and quantification of the bacterial populations through FISH analysis for periods I and II.

	Period I	**Period II**
% Ammonia removal	75-90%	80-90%
Partial nitrification to nitrite	80%	80%
Complete nitrification to nitrate	20%	20%
Nitrification rate (g N L^{-1} d^{-1})	0.12-0.15	0.13-0.14
Denitrification (% of total nitrogen nitrified)	90%	60%
Occurred during static feeding phase	11%	83%
Occurred during aerobic reaction phase	89%	17%
Denitrification rate (g N L^{-1} d^{-1})	0.11-0.14	0.078-0.084
P-removal	60-70%	45-55%
P uptake rate (mmol P g^{-1} VSS h^{-1})	0.016	0.011
P release during static feeding phase (mmol P $mmol^{-1}$ C)	0.145	0.011
AOB fraction (%)	4±2	10±3
NOB fraction (%)	0.5±0.5	2±0.6
PAO fraction (%)	10±3	5±2
GAO fraction (%)	11±4	2.4±0.8

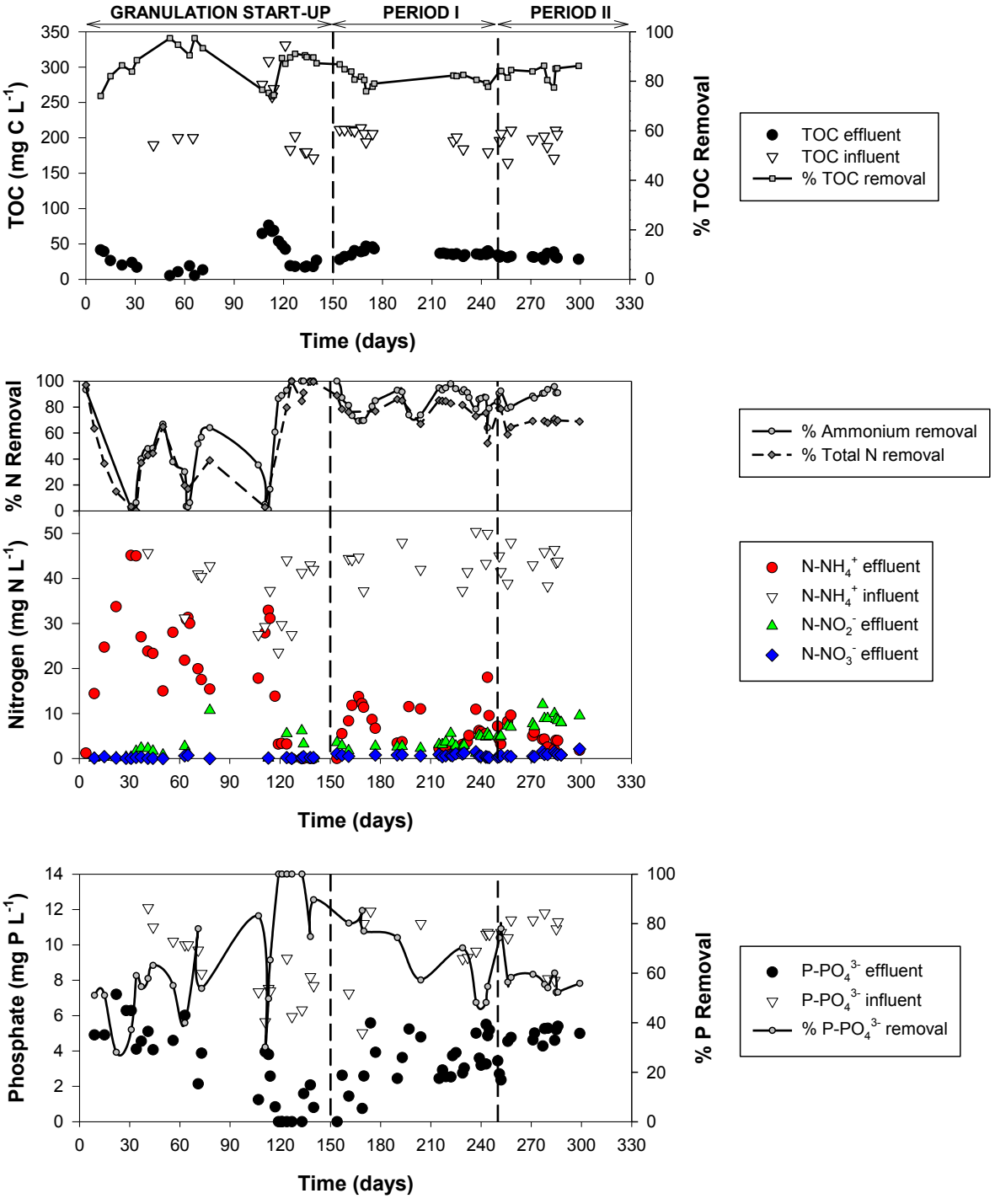

Figure 3.4. Time course profiles of the influent and effluent concentrations of carbon, nitrogen and phosphorus compounds along the whole experimental period, as well as, the removal efficiencies.

Denitrification efficiency varied from 90% in period I to 60% in period II. More detailed data about nutrients removal in the granular biomass was obtained with specific batch experiments, as well as, SBR cycle studies. Time course of COD, N and P concentrations in the bulk liquid for

two typical cycles from periods I and II are shown in Figure 3.5. In period I, 19 mg $N\text{-}NH_4^+$ L^{-1} were removed during the aeration phase. Only 2.5 mg $N\text{-}NO_2^-$ L^{-1} and less than 1 mg $N\text{-}NO_3^-$ L^{-1} remained at the end of the cycle (Figure 3.5B). In period II, 15.5 mg $N\text{-}NH_4^+$ L^{-1} were removed and 9 mg $N\text{-}NO_2^-$ L^{-1} and 3 mg $N\text{-}NO_3^-$ L^{-1} remained at the end of the cycle (Figure 3.5D). In addition, both nitrite and nitrate were fully consumed after the static feeding period, as can be expected, since there was COD addition without aeration (Figures 3.5A and 3.5C). Therefore, from the mass balance along the cycles, 89% of denitrification occurred during the aerobic phase in period I whereas only 17% of denitrification occurred in that phase in period II.

The COD and N-loading rates applied in the GSBR through the whole operational period were: 1.74 g O_2 L^{-1} d^{-1} and 0.17 g N L^{-1} d^{-1}, respectively. These loading rates are above the average loadings applied in conventional municipal WWTPs based on activated sludge (1.0 g O_2 L^{-1} d^{-1} and 0.10 g N L^{-1} d^{-1}; (Tchobanoglous et al., 2003)).

Regarding P-removal, 60-70% and 45-55% of the influent P was removed during periods I and II (Table 3.3), respectively. The P-release to C-uptake ratio is a good indicative of the EBPR activity (Pijuan et al., 2009). The experimental values were 0.145 and 0.011 mmol P $mmol^{-1}$ C for periods I and II, respectively (Table 3.3). These values are low in comparison with other EBPR systems, where this ratio was between 0.250-0.320 mmol P $mmol^{-1}$C, depending on the carbon source (Pijuan et al., 2009). The causes for those low P-release to C-uptake ratios could be: (i) the precipitation of P-salts detected in the GSBR and (ii) the COD consumption during the feeding not linked to PAO activity, (i.e. heterotrophic denitrification or GAO activity).

On the other side, the PAO and GAO fractions measured with FISH (Table 3.3) provided further information to understand the low EBPR activity, but also the denitrification in the GSBR. In period I, PAO (10% ± 3%) and GAO (11% ± 4%) populations would have competed for COD uptake, resulting in low EBPR activity, but providing SND capability to the system with the stored COD. In contrast, lower PAO fraction (5% ± 2%) was measured in period II, which is in accordance with the lower EBPR measured (Table 3.3), but also a lower GAO fraction (2.4% ± 0.8%) was detected, which would also explain the lower SND measured.

On one side, the precipitation of P-salts in the core of the granules was evident, as abovementioned. It was not possible to accurately assess the contribution of precipitation to the total P-removal, since the time course Ca^{2+} and Mg^{2+} concentrations in the bulk liquid were not measured. At the pH (7.5±0.1) and temperature (25ºC) conditions in the GSBR, and with the influent calcium concentration (at least 54 mg Ca L^{-1}), the solubility of phosphate was below 12

mg P L^{-1} (Maurer et al., 1999). Therefore, P-precipitation could occur during the P-release, especially in period I, where 19 mg P-PO_4^{3-} L^{-1} were measured at the end of the static feeding. In period II only 11 mg P-PO_4^{3-} L^{-1} were measured at the end of the static feeding, and probably the precipitation was lower than in period I. In fact, the accumulation of inorganics in period II was lower, as depicted form the slope of the VSS/TSS ratio in Figure 3.2B.

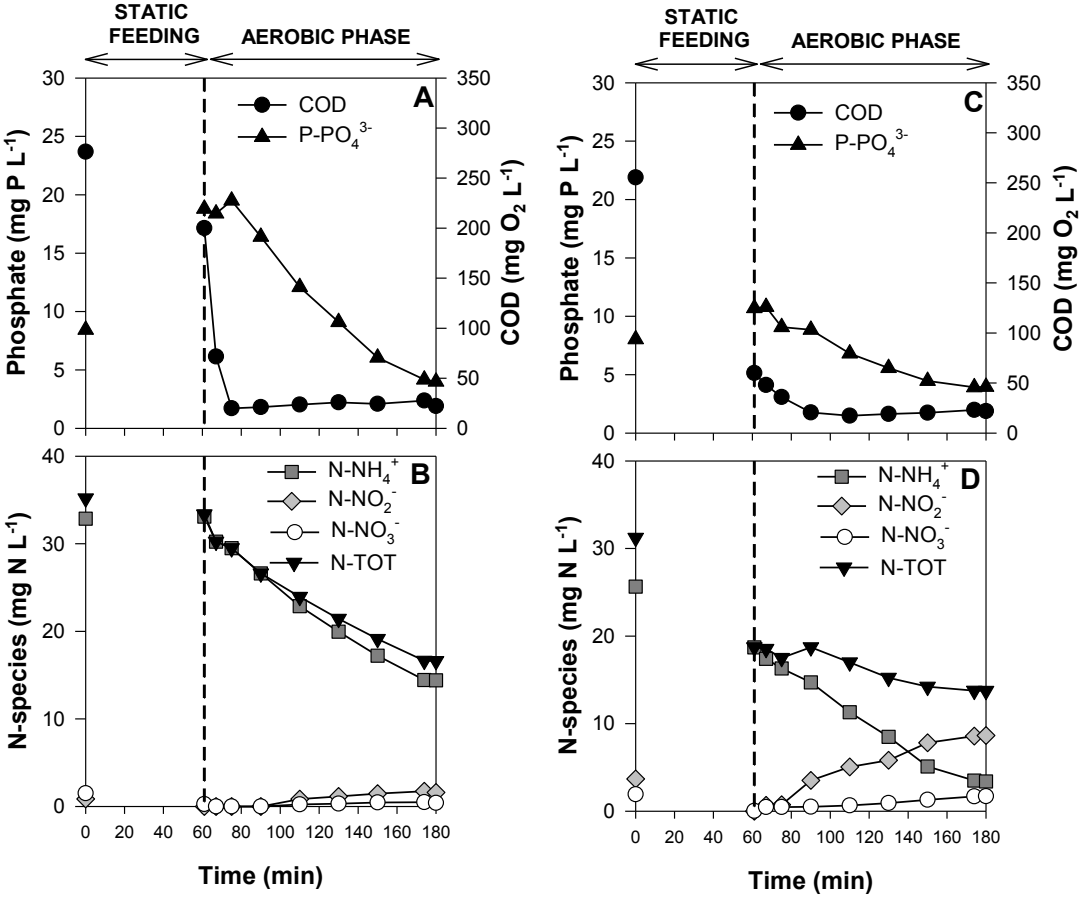

Figure 3.5. Time course profiles of COD, ammonia, nitrite, nitrate and phosphate concentrations in the bulk liquid for two typical GSBR cycles. Period I: A and B Period II: C and D. Initial values (at 0 minutes) correspond to the theoretical concentration that each compound would have after the feeding phase considering no biodegradation.

The analysis of the results of operation of the pilot-scale GSBR during almost one year suggested that the decrease of the removal efficiency at the end of the experimental period was due to a destabilization of the granules and the subsequent loss of biomass. The final cause of this destabilization is not fully understood, but the clear accumulation of inorganic P-salts in the core of the granules was probably a cause of this process. Furthermore, the presence of an inorganic core would imply a reduction of the anoxic volume of the granules, limiting the SND, as observed in the GSBR. If this hypothesis was correct, a regular purge based on the inorganic content rather than the SRT should help to avoid the destabilization of the granules. Granules with higher

mineral content could be purged selectively by performing the granules withdrawn from the bottom of the reactor, since those granules will have higher settling velocity. However, this strategy should be carefully evaluated, since could enhance GAO proliferation (no P-release, therefore, lower P-precipitation) in front of PAO population (Winkler et al., 2011a). Nevertheless, and despite granules destabilization, COD and N removal efficiencies prevailed high, being this work a step forward towards the use of granular technology for the treatment of low-strength wastewater.

3.4 Conclusions

A GSBR at pilot scale was operated during almost a year performing organic matter, N and P removal from a low-strength wastewater at high loading rates.

The BNR with mature granules in the GSBR was via nitrite, and simultaneous nitrification and denitrification was achieved.

Short COD overloading events can lead to overgrowth of filamentous structures onto the granules producing breakage of granules which ends up in a severe biomass washout.

Long term operation of granular biomass with EBPR leads to the accumulation of inorganic particles in the granules as a result of P-salts precipitation, and causing instability of the mature granules. This accumulation can be very fast at high pH values.

CHAPTER 4

A NOVEL CONTROL STRATEGY FOR ENHANCING BIOLOGICAL N-REMOVAL IN A GRANULAR SEQUENCING BATCH REACTOR: A MODEL BASED STUDY

This chapter is based on the following publication:

Isanta, E., Figueroa, M., Mosquera-Corral, A., Campos, L., Carrera, J., Pérez, J., 2013. A novel control strategy for enhancing biological N-removal in a granular sequencing batch reactor: A model-based study. Chem. Eng. J. 232, 468–477.

Part of this chapter was a patented invention:

Isanta, E., Figueroa, M., Mosquera-Corral, A., Campos, L., Carrera, J., Pérez, J., A method and a system for enhancing Nitrogen removal in a GSBR and computer program product. Priority patent application: GB 1313194.1 EP13382301 Applicant: Universitat Autònoma de Barcelona i Universidade de Santiago de Comostela.

4.1 Introduction

Recently, aerobic granular sequencing batch reactors (GSBR) have been successfully used for the treatment of municipal and industrial wastewater effluents (Arrojo et al., 2004; Beun et al., 1999; Coma et al., 2011; de Kreuk and van Loosdrecht, 2006; Figueroa et al., 2011; Wang et al., 2007; Yilmaz et al., 2008). Granules have a compact, dense and thick structure which provides good settling and retention capacities (Adav et al., 2008; Liu and Tay, 2004). Granular sludge reactors operate at higher loading rates using more compact reactor designs, if compared with activated sludge (de Kreuk et al., 2005a; Isanta et al., 2012; Jungles et al., 2011). Moreover, the morphological structure of aerobic granular sludge provides the existence of substrate profiles across the granule depth, enabling simultaneous aerobic and anoxic processes into the same bioparticle. For these reasons, GSBRs have shown a very good performance in organic matter and nitrogen (N) removal (Beun et al., 2001; de Kreuk et al., 2005a; Mosquera-Corral et al., 2005).

High N-removal is achieved when the aerobic and anoxic zones of the granules are correctly balanced (de Kreuk et al., 2007b). This balance depends on many variables, some of them are associated to the granules characteristics (i.e., particle size, density, porosity), whereas others are related to the operational conditions of the reactor (DO concentration, NLR, influent C/N ratio). Experimental campaigns devoted to study the individual effect of these variables is often very challenging and time-consuming, since a change in one of them may affect the others. For example, studying the effect of influent loading rate over nutrients removal efficiency may be affected by variations in the size of the granules. Also, changing the DO concentrations manipulating the air-flow rate may also cause a change in the density of the granules (Tay et al., 2004). Therefore, it is difficult to experimentally assess, in an independent manner, the effects of each variable on N-removal efficiency. Furthermore, some parameters, especially those related to biomass characteristics, are not easy to control and tend to fluctuate even in steady state (Chen et al., 2011; Isanta et al., 2012), hindering its study.

Automatic control strategies are a good tool both for optimization of the performance of wastewater treatments and to apply corrective actions in front of influent or biomass disturbances (Olsson, 2012). Two operational modes are commonly reported for N-removal with aerobic granular sludge: i) GSBRs with a completely aerated reaction phase (de Kreuk et al., 2005a; Figueroa et al., 2011; Isanta et al., 2012; Mosquera-Corral et al., 2005). In that operational mode, simultaneous nitrification-denitrification is the main N-removal pathway and ii) GSBRs with one or several anoxic periods (Adav et al., 2009; Chen et al., 2011; Kishida et al.,

2006; Yilmaz et al., 2008). These anoxic periods are introduced for enhancing denitrification. Although, in general, these configurations showed good N-removal performance, none of these studies used automatic control strategies. In fact, the use of automatic control strategies in GSBRs is still scarce. Some of the examples are: (i) to control the length of cycle as a function of the ammonium concentration for nitritation of high-strength ammonium wastewaters with a very low influent C/N ratio (Torà et al., 2013); (ii) to control the length of the cycle by means of ORP, DO and pH curves for winery (López-Palau et al., 2012) and synthetic wastewaters (Yuan and Gao, 2010).

To overcome the challenges associated to experimental set-ups, the mathematical modeling has been proven to be a useful tool for analyzing complex systems, such as the GSBR. In that sense, some researchers developed mathematical models describing the COD and N-removal via the nitrification and heterotrophic denitrification processes (Beun et al., 2001; Ni and Yu, 2010; Su and Yu, 2006). De Kreuk et al. (2007) introduced the biological phosphorus removal and studied the individual influence of some parameters (i.e. temperature and granule size) over the nutrient removal. Vázquez-Padín et al. (2010) showed that the biomass characteristics could be successfully described if a porosity profile across the granules depth was taken into account. Later, Su et al. (2013) modeled the variations in size and density of granules due to growth, detachment or breakage, to optimize the size and density of granules.

Most of the efforts of these studies were focused on understanding the behavior of the GSBR, but not in finding the best practical strategy to be implemented with the aim to improve the N-removal. In this study, a mathematical model describing the steady state operation of a GSBR treating diluted swine wastewater was calibrated and validated with different sets of experimental data. This model was then exploited to assess the impact of easily measurable parameters on the N-removal efficiency. The selected parameters were DO concentration, granule size, NLR and influent C/N ratio. From the results of the exploitation, a control strategy to improve the N-removal in GSBRs was proposed and evaluated through modeling.

4.2 Materials and Methods

4.2.1 Characteristics of the GSBR operation

Experimental data for the modeling were obtained from a 1.5 L GSBR treating diluted swine wastewater. The reactor cycles were distributed as fill (3 min), aeration (171 min), settling (1 min) and discharge (5 min). The hydraulic retention time was 6 h. The reactor was operated at room temperature (23 ± 2 ºC), while the pH was not controlled and ranged from 7.5 – 8.5. Air

was supplied through an air diffuser at the bottom of the reactor at a constant flow-rate (3.5 L min^{-1}), and the DO concentration varied in the range 2 – 6 mg O_2 L^{-1}.

Activated sludge collected from a municipal WWTP was used as inoculum. Five days after the start-up most of the inoculum biomass washed out from the reactor and first granules appeared. On day ten, the average diameter of the granular biomass was 1.87 mm and the volatile solids content inside the reactor was 1.27 g VSS L^{-1} (Figueroa et al., 2011).

After the start-up, the GSBR operational strategy consisted in stepwise decrease of the dilution ratio of the swine wastewater with tap water. Experimental data from the operational periods A and C from the GSBR (see Figure 4.1) were used for modeling purposes. In period A, the dilution ratio of swine wastewater with tap water was 1:25, resulting in an influent composition of 600 mg O_2 L^{-1} of readily-biodegradable chemical oxygen demand (COD), 60 mg O_2 L^{-1} of non-biodegradable COD and 103 mg N L^{-1} of ammonium (Table 4.1). For period C, the dilution ratio of swine wastewater with tap water was 1:15, resulting in an influent composition of 1000 mg O_2 L^{-1} of readily-biodegradable COD, 116 mg O_2 L^{-1} of non-biodegradable COD and 200 mg N L^{-1} of ammonium (Table 4.1). More details about the performance of the reactor can be found in Figueroa et al. (2011).

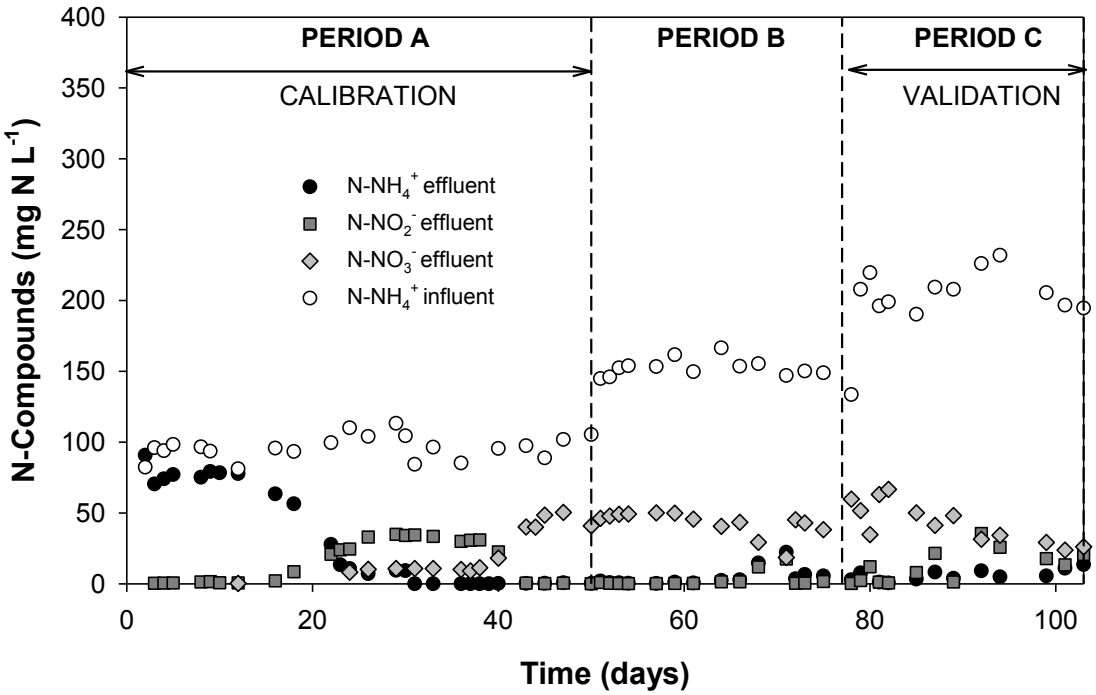

Figure 4.1. Time course concentrations of ammonium, nitrite and nitrate as experimentally measured in the lab-scale GSBR. Experimental data obtained in period A were used for the calibration of the model. Results of the model at the operating conditions established in period C were used to validate the model.

Table 4.1. Experimental data related to the influent composition and biomass characteristics in Periods A and C, used as model inputs to simulate the GSBR operation for the calibration and validation.

	Period A (Calibration)	**Period C (Validation)**
Influent characteristics		
Readily-biodegradable COD (mg O_2 L^{-1})	600	1000
Non–biodegradable COD (mg O_2 L^{-1})	60	116
Ammonium (mg N L^{-1})	103	200
Influent C/N ratio (g O_2 g^{-1} N)	5.8	5
Granules characteristics		
Volume-weighted average granule size (mm)	3.55	3.13
Biomass concentration (g VSS L^{-1})	5	11.5
Density (g VSS $L^{-1}_{granule}$)	25	37
Number of granules	12806	29301

4.3 Model development

The modeling platform used to develop the mathematical model was AQUASIM (Reichert, 1998). The biofilm reactor compartment (based on Reichert (1998) mixed-culture biofilm model) provided by AQUASIM was used to simulate the mass transfer and biological conversion processes occurring in the granules. The description of the biofilm in AQUASIM is one-dimensional, and only the perpendicular direction to the substratum is resolved (Reichert, 1998).

4.3.1 Biological processes

The model included six soluble compounds: oxygen (S_{O2}), ammonium (S_{NH4}), nitrite (S_{NO2}), nitrate (S_{NO3}), readily-biodegradable organic substrate (S_S) and non-biodegradable organic substrate (S_I); and five types of particulate compounds: ammonium-oxidizing bacteria (X_A), nitrite-oxidizing bacteria (X_N), heterotrophic bacteria (X_H), storage products (X_{STO}) and inert particulate organic material (X_I). Kinetics and stoichiometry of the biological processes were defined using the Activated Sludge Model No.3 (ASM3) platform (Henze et al., 2000). However, the ASM3 presents several limitations for describing systems operating in batch mode or with nitrite accumulation. To overcome these limitations, two modifications were introduced: (i) the model considered simultaneous growth and storage of organic matter by heterotrophic bacteria (Sin et al., 2005), (ii) nitrite was included as nitrification intermediate (Jubany et al., 2008), since there was an evident accumulation of nitrite in the GSBR (Figure 4.1). Therefore, nitrification becomes a two-step process. Firstly, ammonium is oxidized to nitrite by ammonium-oxidizing bacteria (AOB),

and secondly, nitrite is oxidized to nitrate by the nitrite-oxidizing bacteria (NOB). Furthermore, since nitrite was included in the model, all the anoxic processes, heterotrophic and autotrophic, (i.e. AOB and NOB endogenous respiration) were possible either from nitrite or from nitrate (Kaelin et al., 2009). Separate anoxic reduction factors were used for X_A, X_N and X_H (Kaelin et al., 2009). Additionally, the anoxic processes from nitrate had a lower reduction factor to avoid an overall denitrification rate higher than the aerobic consumption rate of COD (Kaelin et al., 2009).

The hydrolysis of slowly biodegradable COD (X_S) to S_S by X_H was not taken into account. Given that the raw swine wastewater was stored several weeks without continuous mixing before being diluted and entering the reactor, it was considered that most of X_S decanted in the storage tank. Therefore, the overall impact of the hydrolysis of the remaining X_S on the behavior of the GSBR was considered negligible. Further details of kinetics and stoichiometry of the developed model are summarized in Tables A4.1, A4.2 and A4.3 in the Aappendix of this chapter.

4.3.2 SBR operation

To simulate the feeding and effluent withdrawal periods of the GSBR, the biofilm reactor compartment was linked to a completely mixed liquid compartment whose volume can vary during the simulation (see Figure 4.2 and Vázquez-Padín et al. (2010) for further details). The completely mixed compartment received the feeding and effluent withdrawal operations. The biofilm reactor had a constant volume (0.75 L) and contained the total amount of granules and part of the bulk liquid. The rest of the bulk liquid was in the completely mixed reactor compartment (0.76 L). Both compartments were interconnected with a recirculation flow-rate to ensure good liquid mixing.

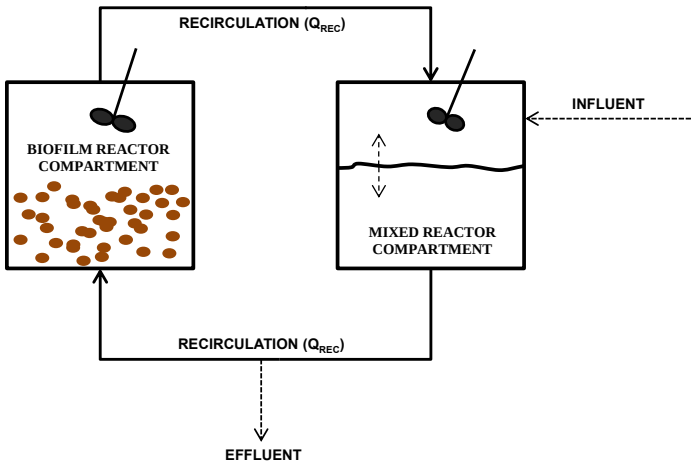

Figure 4.2. Schematic diagram of the GSBR set-up as implemented with the AQUASIM compartments. A biofilm reactor compartment reactor was connected to a mixed reactor compartment with a high recirculation flow to ensure same bulk liquid concentration of dissolved and particulate compounds. Feeding and discharge operations are performed through the mixed reactor compartment.

In the experimental set-up, during the periods without mixing (settling, discharge and feeding), the mass transfer of soluble compounds from the bulk liquid to the biofilm pore water becomes reduced, resulting in a lower biological activity of the granules. Furthermore, the GSBR was fed from the top of the reactor; therefore, the settled granules did not mix with the new media until the aeration started. To mimic the real operation of the reactor, a reduction factor applied to the diffusivity of soluble compounds into the pore water of granules, similarly to de Kreuk et al. (2007), was used with the aim to minimize the biological reactions during the non-aerated periods. This reduction factor was noted as μ_D.

4.3.3 Granules description

Biofilm area was described as a function of the granule radius, to correctly simulate the biofilm geometry. Total biofilm area was defined as a function of granule size and number of granules (see Jemaat et al. (2013) for further details). The granule size used as model input was the volume-weighted average diameter experimentally determined in the lab-reactor. The number of granules was determined dividing the total volume of granules by the volume of a single granule, taking into account the experimentally determined density and total solids concentration. As in Vázquez-Padín et al. (2010), a detachment rate (u_{Det}) was used to keep a constant biofilm thickness in steady state at a predefined value (Eq. 1).

$$u_{Det} = \left(\frac{r - R_m}{R_m} 100 + 85\right) u_F, \text{ if } u_F > 0, \text{otherwise } u_{Det} = 0 \qquad (4.1)$$

Being u_F the growth velocity of the granules (m d^{-1}), r the simulated granule radius (m) and R_m the experimental mean radius (m). Attachment of biomass onto the biofilm surface has been neglected. For the sake of simplicity external mass transfer has been neglected. The porosity of the biofilm was fixed as 80% and kept constant during all the simulations.

4.3.4 Model calibration and validation strategy

The operational conditions applied for period A as well as the biomass characteristics at the end of that period were used to calibrate the model (Table 4.1). Then, the concentrations of N-compounds and COD of a simulated cycle in steady-state were compared with an experimental cycle of the GSBR at the end of this period. To ensure steady conditions, each simulation lasted for at least 148 days, corresponding to 20 h of computing time on an Intel Core2Quad CPU at 2.66GHz. Results in terms of biofilm (biofilm thickness and biomass fractions in the biofilm depth) and N-compounds concentrations in the bulk liquid were inspected to check that constant values were achieved.

The same procedure was applied for validation, but using the experimental conditions and biomass characteristics of period C (Table 4.1) and the same kinetic and stoichiometric parameters than in calibration (Table A4.2 in Apendix of this chapter). The wastewater treated in period C had a slightly lower influent C/N ratio to that in the calibration (period A) but the NLR and organic loading rate were almost double. Due to these differences, the selection of this operational period for validation purposes is justified.

4.3.5 N-removal assessment strategy

For the assessment of the N-removal in the GSBR, four relevant and easily measurable parameters at industrial scale (DO concentration, granule size, NLR and influent C/N ratio) were selected, seeking to improve operational strategies. With that purpose, five scenarios were defined: Period A, C/N_Low, C/N_High, NLR_1.5 and NLR_2.0 (Table 4.2). Period A scenario presented the characteristics of the GSBR operation in the experimental period A (Figure 4.1). For scenarios C/N_Low, C/N_High, the conditions of Period A were taken as a basis, and the influent COD was modified to obtain an influent C/N ratio of 4 g O_2 g^{-1} N (C/N_Low) and 10 g O_2 g^{-1} N (C/N_High). For scenarios NLR_1.5 and NLR_2.0, the conditions of period A were also taken as modeling basis, and the length of the cycle time was modified to 120 min (NLR_1.5) and 90 min (NLR_2.0) to increase the applied NLR. The reduction of the cycle time was applied to the aerobic phase, keeping the same feeding, settling and discharge times used in period A.

Table 4.2. Characteristics of the scenarios used for the model exploitation

	$COD_{influent}$ (mg O_2 L^{-1})	$NH_4^+{}_{influent}$ (mg N L^{-1})	C/N (g O_2 g^{-1} N)	VSS (g L^{-1})	HRT (h)	NLR_V (g N L^{-1} d^{-1})	NLR_S (g N g^{-1} VSS d^{-1})
Period A	600	103	5.8	5	6	0.41	0.082
C/N_High	1030	103	10	5	6	0.41	0.082
C/N_Low	412	103	4	5	6	0.41	0.082
NLR_1.5	600	103	5.8	5	4	0.61	0.123
NLR_2.0	600	103	5.8	5	2	0.82	0.164

The conditions of each scenario were simulated until steady state for different DO concentrations and granule sizes. Four different granule sizes were used (0.5, 1.0, 2.0 and 3.5 mm) to cover the typical range of granule sizes found in the literature (Chen et al., 2011; de Kreuk et al., 2005a; Figueroa et al., 2011; Isanta et al., 2012). Regarding the DO variations, six different DO concentrations, between 0.5 and 8 mg O_2 L^{-1}, were tested. DO concentrations lower than 0.5 mg L^{-1} were not used since they are not expected to be applied in a real GSBR (Beun et

al., 2002; Mosquera-Corral et al., 2005). The combination of both variables resulted in 24 different simulations for every scenario. For easy comparison between scenarios, the simulations were performed with the same volume (and mass) of granules. Therefore, the number of granules used in each simulation was set according to the selected granule size.

4.4 Results and Discussion

4.4.1 Model calibration

All kinetic parameters were obtained from the bibliography with the exception of the maximum growth rate of X_H ($\mu_{max,H}$), the maximum growth rate of X_A ($\mu_{max,A}$) and the storage rate constant (k_{STO}), that were determined to provide a good description of N-compounds and COD concentration. For the sake of simplicity, the maximum growth rate of X_N ($\mu_{max,N}$) was assumed to be equal to $\mu_{max,A}$, as expected at the temperature used in the experiments (23 ± 2 ºC) (Sin et al., 2008). Best results were obtained for a $\mu_{max,H}$ of 5.2 d^{-1}, a $\mu_{max,A}$ of 1.32 d^{-1} and a k_{STO} of 13.2 d^{-1}. All three values were slightly higher than the typical values found in the literature for conventional wastewater treatment plants (2 – 3 d^{-1}, 0.8 – 1.1 d^{-1} and 5 – 12 d^{-1}, respectively (Henze et al., 2000; Kaelin et al., 2009)). However, maximum growth rates are known to be higher in reactors with alternating feast-famine conditions, as the GSBR here modeled. In fact, Munz et al. (2011b) found that $\mu_{max,A}$ ranged from 0.9 - 1.4 d^{-1} at 20 ºC for an SBR with the abovementioned conditions. Apart from these three kinetic parameters, the diffusivity reduction factor (μ_D, section 4.3.2) was also calibrated. Several values of μ_D were tested in previous simulations and best results were obtained for a μ_D of 0.01 (Figure 4.3).

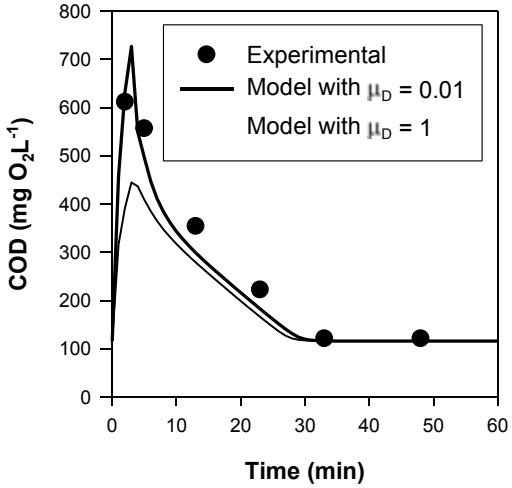

Figure 4.3. Example of the effect of using a reduction factor on the diffusion coefficient of soluble compounds on model COD predictions during the first 60 minutes of a cycle. The reduction factor (μ_D) is only active during the first 3 minutes of each cycle (minute 0 to 3 in the graph), which corresponds to the static (non-aerated) feeding phase of the GSBR.

The profiles of COD, ammonium, nitrite and nitrate predicted by the calibrated model are shown in Figures 4A and 4B. During the first 20 min of the cycle, COD was consumed (feast phase) and the nitrate remaining from the previous cycle was denitrified. The use of the μ_D factor was crucial for a correct description of the COD concentration just after the feeding phase (Figure 4.3). During the famine phase (after the COD consumption), the nitrification became the main biological process. Nitrate was the nitrification product, although a slight accumulation of nitrite occurred from minute 30 to 150 (Figure 4.4A).

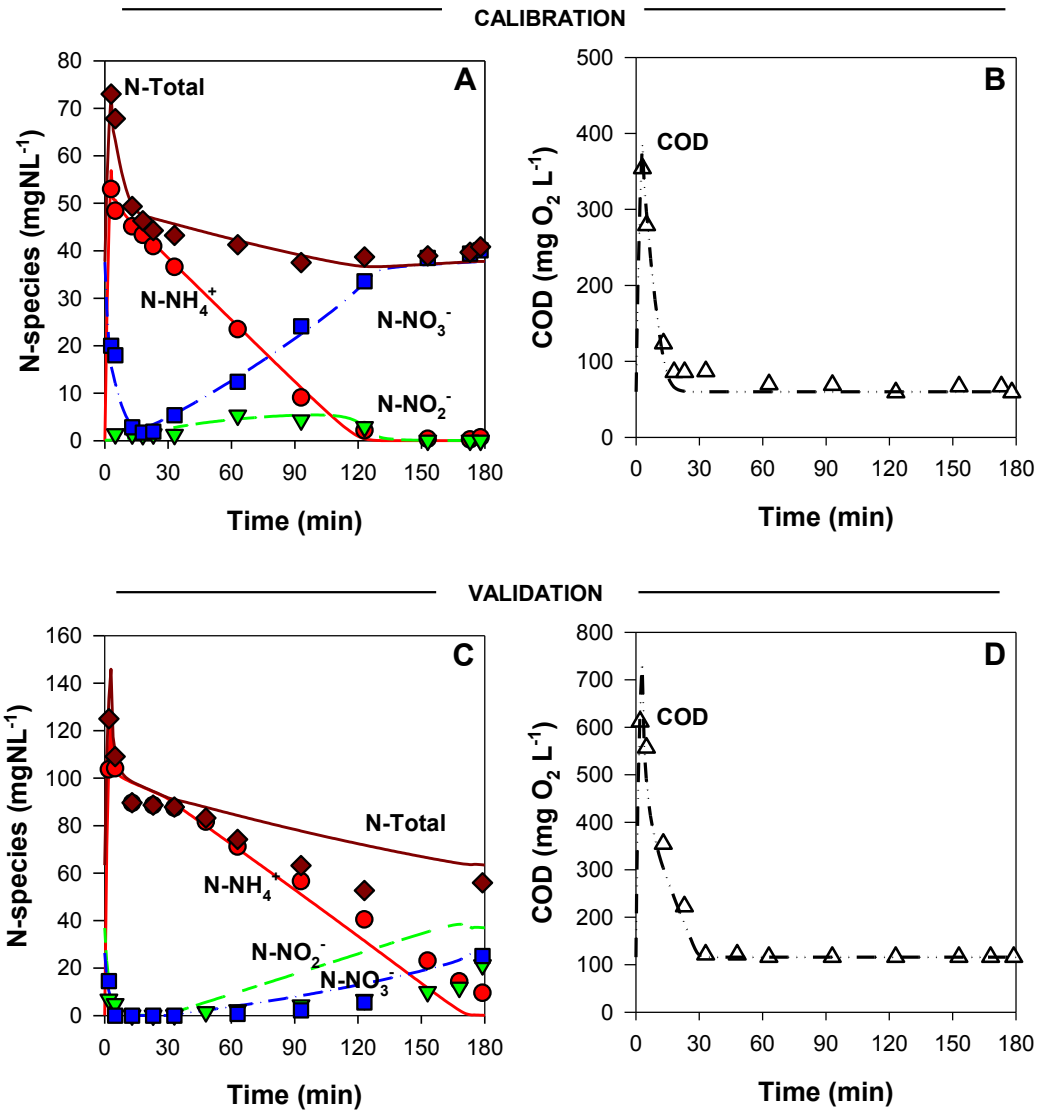

Figure 4.4. Time course concentrations of N-species (A,C) and COD (B,D) in a cycle as measured experimentally (symbols) compared to those predicted by the model (lines). A and B Figures correspond to the calibration and C and D Figures correspond to the validation.

The model was able to correctly describe all the processes occurring during the cycle. First, the COD consumption and subsequent denitrification of the nitrate occurring during the feast phase. And second, the nitrification and nitrate accumulation during the famine phase. Also the nitrite accumulation was adequately predicted by the model, although this accumulation was slightly higher than the experimentally observed. However, the N-total was correctly described by the model.

4.4.2 Model validation

In the experimental cycle from period C used for the model validation, COD was consumed during the first minutes of the cycle and all the nitrate and nitrite remaining from the previous cycle were denitrified. However, this feast phase was longer than in period A, since lasted for 30 min (Figure 4.4D). During the famine phase, ammonium was not fully consumed, since a final accumulation of 10 mg $N\text{-}NH_4^+ L^{-1}$ was observed. Nitrate and nitrite at the end of the cycle were similar. The model correctly described the feast phase, since the predicted COD, ammonium, nitrite and nitrate concentrations were similar to the experimental ones (Figure 4.4C). During the famine phase, the COD and nitrate profiles were also adequately predicted by the model. In contrast, the model did not completely describe the ammonium and nitrite profiles of the famine phase. The model overestimated the nitrite concentrations and underestimated the ammonium concentration (see Figure 4.4C). However, the general trends of both compounds were correctly predicted with the simulation results.

Considering the complexity of the system and the uncertainty of some of the experimental data used as model inputs (e.g. granule size distribution, granules density) it could be considered that the model satisfactorily described the performance of a GSBR treating swine wastewater. Moreover, it is noteworthy that only three kinetic parameters were calibrated while the rest were obtained from literature and, of course, none of these parameters was changed in the validation. Therefore, the model was ready to start performing other simulations to gain deeper insight into the treatment process.

4.4.3 Assessment of Nitrogen removal

4.4.3.1 Effect of the DO and the granule size

The coupled effect of DO and granule size over N-removal was studied using Period A scenario (see details in Table 4.2). The model results for Period A are presented in Figure 4.5. For each granule size tested, there was a DO concentration at which N-removal was maximized (DO_{opt}). At DO concentrations higher than the DO_{opt}, ammonium was completely oxidized at the end of the cycle and the N-removal efficiency decreased as DO concentration was increased. N-removal

efficiencies at the same DO concentration were higher as higher was the granule size. At DO concentrations below the DO_{opt}, the N-removal efficiency decreased rapidly for lower values of the DO concentration, and ammonium was not completely oxidized at the end of the cycle and accumulated in the effluent.

The DO_{opt} was 2 and 1 mg O_2 L^{-1} for the granule size of 3.5 and 2.0 mm, respectively, and 0.5 mg O_2 L^{-1} for the 1.0 or 0.5 mm, indicating that the DO_{opt} value increased with granule size. Note that for two of the granule sizes (1.0 and 0.5 mm), the DO_{opt} was obtained at the lowest DO concentration used (0.5 mg O_2 L^{-1}), so the decrease of the N-removal at DO concentration lower than the DO_{opt} could not be observed, although it probably occurred at lower DO concentrations.

At the conditions of period A, granules with a granule size between 1 and 2 mm presented better N-removal efficiencies (76 – 80%) than granules with larger (74%) or smaller sizes (71%) at their DO_{opt} (Figure 4.5). Noticeably, the variations in N-removal at the DO_{opt} of the different granule sizes were lower than 9%, despite the large range of granule sizes tested (0.5 – 3.5 mm). Hence, in Period A conditions, applying the adequate DO_{opt} concentration resulted in high N-removal efficiencies independently of the granule size.

4.4.3.2 Effect of the influent C/N ratio

Two different scenarios, C/N_Low and C/N_High (see Table 4.2), were used to study the effect of the influent C/N ratio over the N-removal. In general, the N-removal efficiencies in both scenarios showed similar trends than those found in period A (Figure 4.6). Similarly to Period A, a different DO_{opt} value was determined for each granule size. The values of DO_{opt} for each granule size in C/N_High and C/N_Low scenarios were very similar to those determined in Period A (Figure 4.7A). The limitation of the nitrification occurred at a DO concentration close to the DO_{opt}, since, at DO concentration above the DO_{opt}, ammonium was not completely oxidized at the end of the cycle (Figure 4.6). Therefore, the influent C/N ratio scarcely influenced the conditions at which N-removal was enhanced. However, the N-removal efficiencies obtained at the same granule size and DO concentrations were, in C/N_High scenario, higher than those in Period A (Figure 4.6). In contrast, the N-removal efficiencies in C/N_Low scenario were lower than the corresponding ones in Period A. Therefore, the higher the influent C/N ratio, the higher the N-removal efficiency.

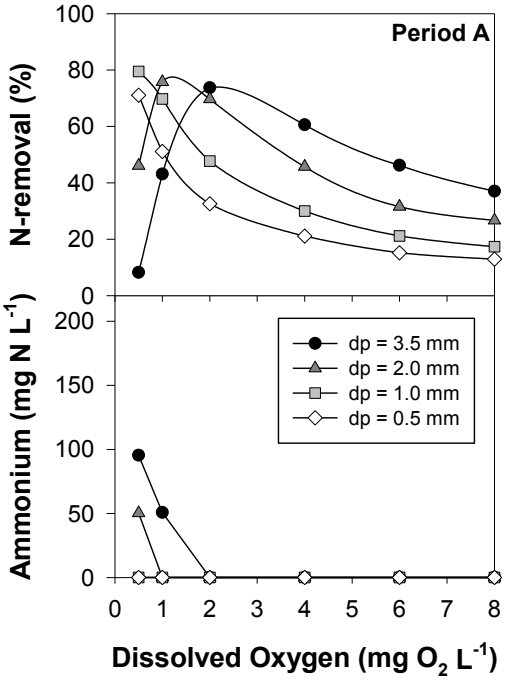

Figure 4.5. Simulated N-removal efficiencies and effluent ammonium concentrations predicted by the model at different DO concentrations in the bulk liquid and at different granule sizes (dp). Simulations were performed under the operating conditions defined for Period A scenario, as detailed in Table 4.2.

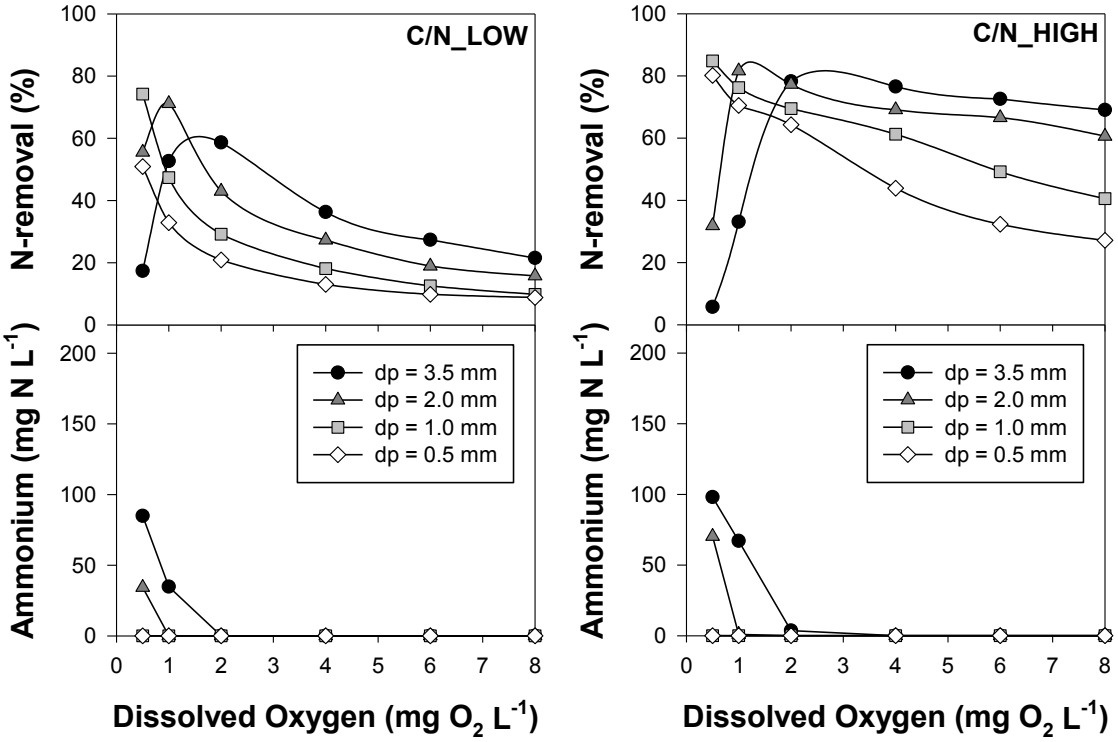

Figure 4.6. Simulated N-removal efficiencies and effluent ammonium concentrations predicted by the model at different DO concentrations in the bulk liquid and at different granule sizes (dp). Simulations were performed under the GSBR conditions defined for C/N_Low (left) and C/N_High (right) scenarios, as detailed in Table 4.2.

For C/N_High scenario, the higher influent C/N ratio also allowed for good N-removal efficiencies at DO concentrations higher than the DO_{opt}. In fact, granules with a granule size higher than 2 mm and DO concentrations higher than 4 mg O_2 L^{-1} presented N-removal efficiencies higher than 60% (Figure 4.6). Maximum N-removal efficiencies of the different granule sizes ranged between 79 and 85% and, similarly to Period A, granules with sizes between 1 and 2 mm presented the best N-removal efficiency (Figure 4.7A). In that case, the differences in maximum N-removal at different granule sizes were even lower than those found for period A, being only 6%. Therefore, with a high influent C/N ratio, there is no need to pay attention to the granule size if the adequate DO_{opt} was applied.

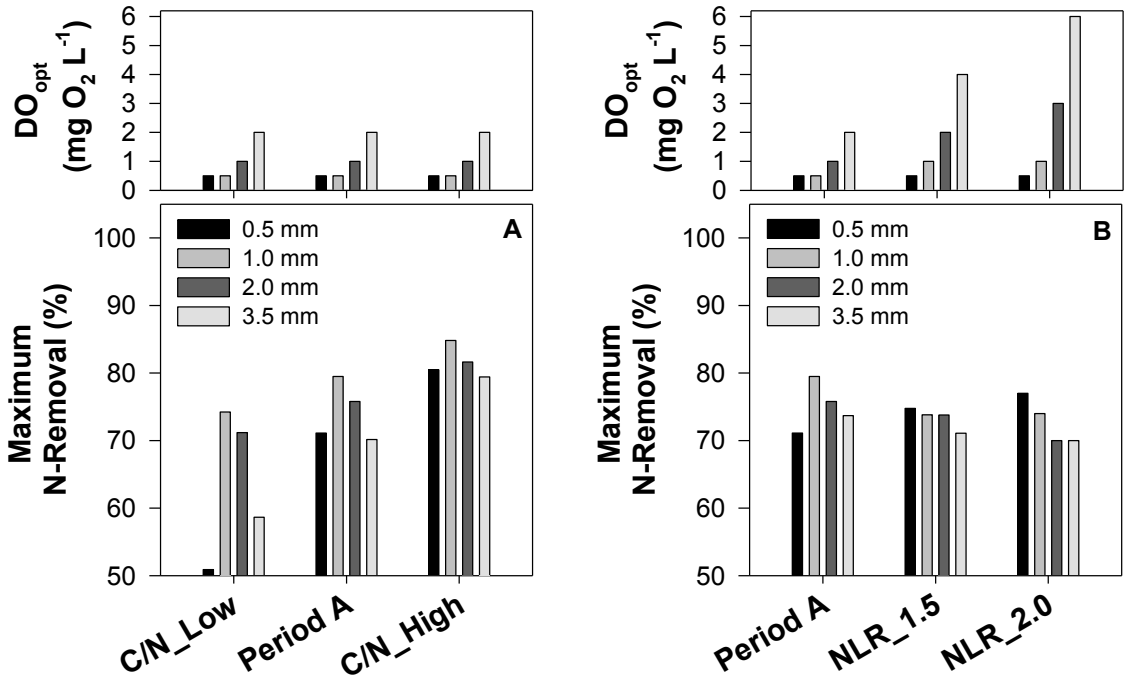

Figure 4.7. Comparison of the maximum N-removal efficiencies and DO_{opt} obtained at the different granule sizes for C/N_Low, C/N_High and Period A scenarios (A); and NLR_1.5, NLR_2.0 and Period A scenarios (B).

In the C/N_Low scenario, good N-removal efficiencies (71 – 74%) were obtained only for granule sizes between 1 and 2 mm at its corresponding DO_{opt} (0.5 - 1 mg O_2 L^{-1}, Figures 4.6 and 4.7A). For granule sizes 0.5 and 3.5 mm, the N-removal was lower than 60% even at the DO_{opt}. At DO concentrations higher than 4 mg O_2 L^{-1}, N-removal was lower than 36% for all the granule sizes tested (Figure 4.6). Note that, even though the low influent C/N ratio negatively affected the N-removal efficiency, good N-removal efficiencies could be obtained applying the adequate DO_{opt} if

granule size was between 1 and 2 mm. The maximum N-removal efficiency was only 6 % lower than that in Period A.

4.4.3.3 Effect of the NLR

The effect of the NLR on the N-removal was also evaluated with the model. One of the advantages of granular reactors is their ability to treat high loading rates due to their high biomass retention capacity (de Kreuk et al., 2005a; Figueroa et al., 2011; Isanta et al., 2012). For this reason, the effect of the NLR on the N-removal capacity was studied in two scenarios of 1.5 and 2-fold higher NLR than that applied in period A, maintaining a constant influent C/N ratio (see Table 4.2).

Simulations results of scenarios NLR_1.5 and NLR_2.0 are presented in Figure 4.8. In general, the N-removal performance after increasing the NLR presented similar trends than those found in Period A (see Figure 4.8). A DO_{opt} was found for each granule size, where the N-removal was enhanced, and nitrification was limited at a DO concentration close to the DO_{opt} value (Figure 4.8). However, the higher the NLR applied, the higher the DO concentration at which the maximum N-removal for each granule size was achieved (i.e., for granule size of 2 mm, the DO_{opt} values were 1, 2 and 3 mg O_2 L^{-1} for scenarios Period A, NLR1.5 and NLR_2.0, respectively, Figure 4.7B). Therefore, for a given granule size, the value of DO_{opt} increased with NLR. This was reasonable, since a reduction of the cycle length resulted in a reduction of the time available for nitrification. Accordingly, higher DO concentrations were needed to increase the thickness of the aerobic layer and, thus, increase the nitrification capacity.

Regarding N-removal efficiencies, the increase of the NLR affected differently the N-removal according to the granule size. At the DO_{opt}, the N-removal efficiency of granules larger than 1 mm decreased with NLR (Figure 4.7B). This decrease of N-removal was (4 – 6 %), depending on granule size, but the N-removal efficiency at the DO_{opt} maintained higher than 70% in all cases (Figure 4.7B). In contrast, for a granule size of 0.5 mm the N-removal at the DO_{opt} increased with NLR, achieving 80% of N-removal efficiency in the NLR_2.0 scenario. Therefore, in case of an increase of NLR, the lower the granule size, the better the achieved N-removal. Nevertheless, if the DO concentration is maintained at a value close to the DO_{opt}, good N-removal efficiencies could be obtained independently of the granule size.

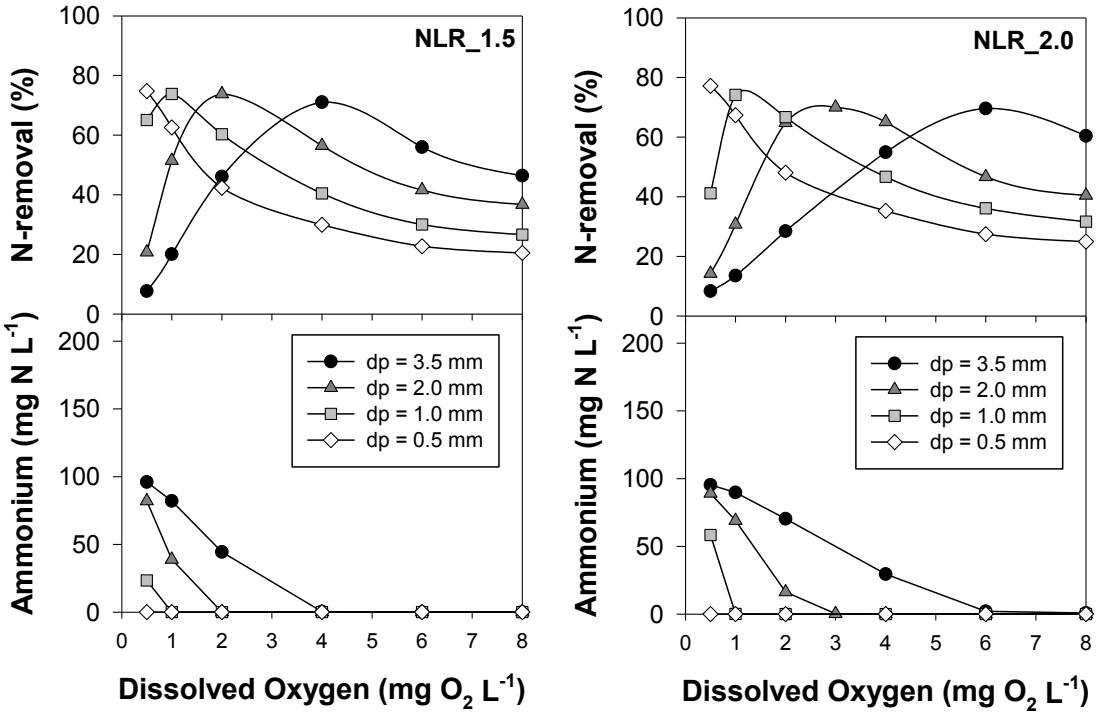

Figure 4.8. Simulated N-removal efficiencies and effluent ammonium concentrations predicted by the model at different DO concentrations in the bulk liquid and at different granule sizes (dp). Simulations were performed under the GSBR conditions for NLR_1.5 (left) and NLR_2.0 (right) scenarios, as detailed in Table 4.2.

4.4.4 Practical implications

4.4.4.1 Operating guidelines to improve N-removal

The simulation results showed that all the factors taken into account in this study (i.e. DO concentration, particle size, influent C/N ratio and NLR) affected the N-removal. Interestingly, in most of the scenarios tested, the N-removal efficiency could be highly enhanced independently of the rest of the factors, only by applying the adequate DO concentration (i.e. DO_{opt}), thus obtaining N-removal efficiencies higher than 70% (Figure 4.7). The only exception was in case of low influent C/N ratio. In that scenario, in addition to apply the DO_{opt}, a granule size between 1 and 2 mm was needed to obtain good N-removal efficiencies (Figure 4.7).

The simulation results also showed that, in all scenarios, the ammonium was completely oxidized at DO concentrations above the DO_{opt}. In contrast, at DO concentrations below the DO_{opt}, ammonium always accumulated in the effluent. This suggested that the limitation of nitrification occurred at a DO concentration close to the DO_{opt} (Figures 6.6 and 6.8). Accordingly, a slight accumulation of ammonium at the end of the cycle (i.e. a slight limitation of the nitrification) would indicate that the DO concentration was close to DO_{opt} and thus, that N-

removal was enhanced (Figure 4.9). Therefore, it is possible to enhance N-removal simply controlling DO concentration and effluent ammonium concentration. This is very interesting from an operational point of view, since both, DO and ammonium concentrations, are two variables commonly measured on full scale wastewater treatment plants (Olsson, 2012) and could easily be controlled. In contrast, granule size is practically uncontrollable in current systems (de Kreuk et al., 2007b), and influent C/N ratio and NLR are related to the wastewater, and therefore subject to variability.

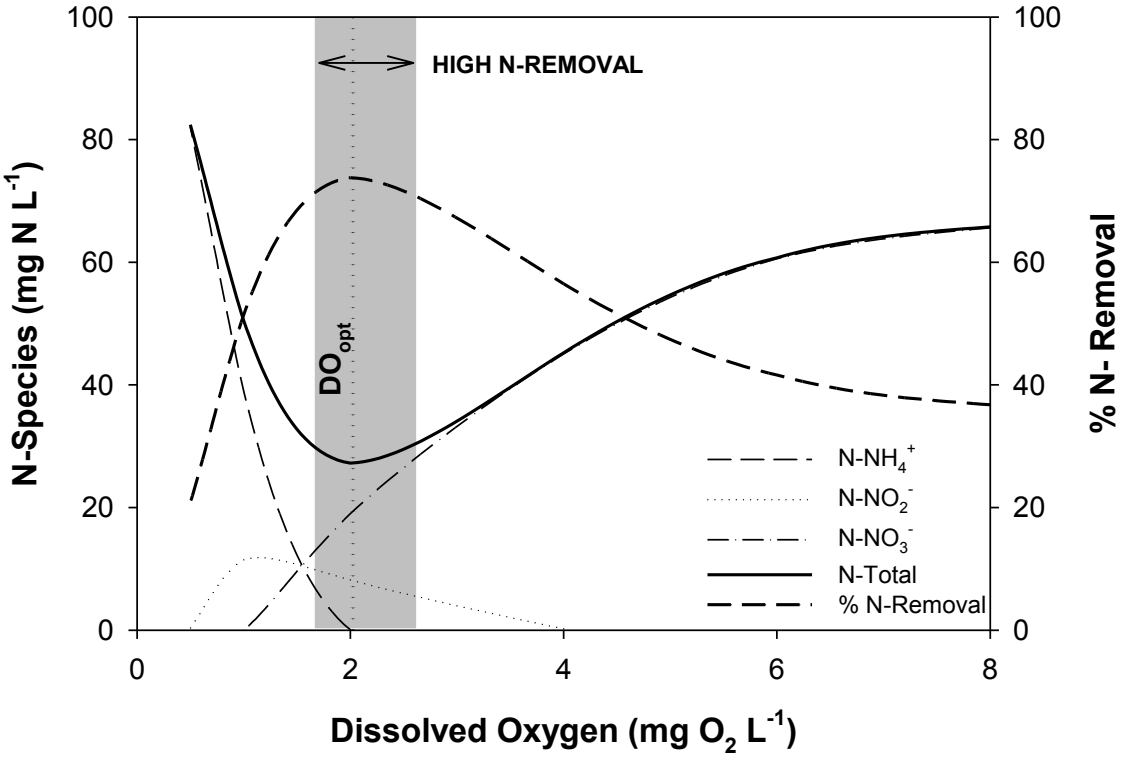

Figure 4.9. Schematic representation of the effluent concentration of N-species and N-removal obtained at different DO concentrations. The DO_{opt} value and the DO range with high N-removal efficiency are highlighted with a dotted line and grey band, respectively.

4.4.4.2 A novel control strategy for enhancing N-removal

A control strategy was proposed based on determining the DO concentration ensuring a slight accumulation of ammonium at the end of each GSBR cycle, which have been found the key to achieve high N-removal efficiencies. The proposed control strategy had a cascade control structure, with a primary control loop of ammonium concentration at the end of the cycle, and a secondary control loop of DO concentration along the aerobic phase of the GSBR (Figure 4.10). The manipulated variable of the primary control loop was, consequently, the DO set-point of the secondary loop (Stephanopoulos, 1984). The particularity of this control strategy was that the

primary ammonium control loop would only act once per cycle. Therefore, after measuring the ammonium concentration at the end of the cycle, the control loop would establish the DO set-point for the next cycle. The ammonium set-point for the primary loop was set to 5 mg $N\text{-}NH_4^+$ L^{-1}. This set-point was justified by the precision of the current on-line ammonium measurement devices, but also by the importance of having enough range to measure the error between the on-line and set-point ammonium concentrations, in order to calculate the control action (Figure 4.9). DO concentration in the reactor should be sufficiently close to the value of DO_{opt} as to obtain high N-removal efficiencies when using 5 mg $N\text{-}NH_4^+$ L^{-1} as ammonium set-point.

The short term effectiveness of the proposed control strategy over the N-removal efficiency was simulated with the model using the conditions applied in Period A with a granule size of 2 mm. To simulate the primary ammonium control loop (Figure 4.10), a proportional (P) controller was used (Stephanopoulos, 1984). The gain of the P controller was set to 0.25 mg O_2 mg^{-1} $N\text{-}NH_4^+$. The secondary control loop (Figure 4.10) was assumed to have a fast response because the control of DO in the model was described with a high gas-liquid oxygen transfer rate (see the details Jemaat et al. (2013)).

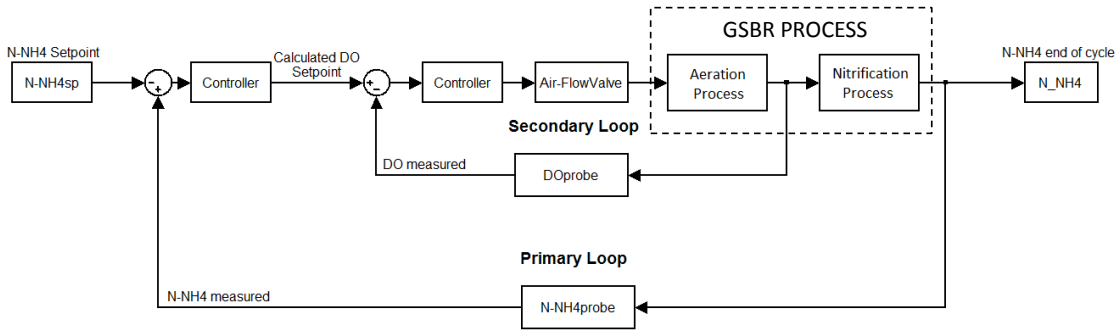

Figure 4.10. Block-diagram of the cascade control strategy proposed to enhance the N-removal. The primary loop only acts once per cycle, using the ammonium concentration at the end of one cycle (effluent concentration) to establish the DO set-point value of the next cycle. The secondary loop is only active during the aerobic phase of the GSBR cycle, and DO set-point is maintained constant during the whole aerobic phase.

Before applying the control strategy, the model was run until steady state with a DO concentration of 4 mg O_2 L^{-1}, obtaining complete nitrification at the end of the cycle and 48% of N-removal efficiency (see Figure 4.11). Then the control strategy was activated. During the first 36 h after the control activation (12 cycles) the primary ammonium control loop progressively reduced the DO set-point of the secondary DO control loop, until 1 mg O_2 L^{-1}. At that DO

concentration, ammonium concentration started to accumulate for the first time in the effluent (Figure 4.11). During the next 36 h, the ammonium in the effluent oscillated in the range 1 – 9 mg $N\text{-}NH_4^+$ L^{-1}, producing DO set-point variations between 0.75 and 1.1 mg O_2 L^{-1} (Figure 4.11). Seventy-two hours after the start-up of the control strategy, the ammonium concentration in the effluent was finally stabilized at 5 mg $N\text{-}NH_4^+$ L^{-1}, with a DO concentration of 1.0 mg O_2 L^{-1}. N-removal efficiency after the activation of the control strategy increased from 48% to 75% during the first 36 h (Figure 4.11), showing the effectiveness of the control strategy. Moreover, the N-removal efficiency remained stable at 75 ±2 % during the next 36 h (Figure 4.11), despite the oscillations of the ammonium in the effluent, showing the robustness of the control strategy.

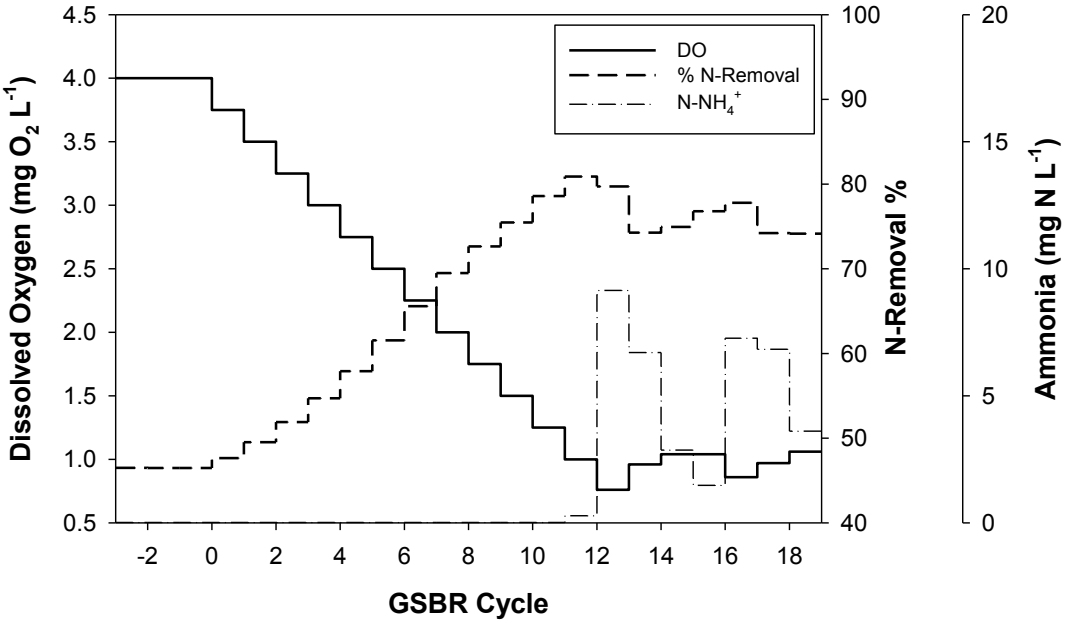

Figure 4.11. DO concentration during aerobic phase, effluent ammonium concentration (end of the cycle) and N-removal efficiencies before and after applying the proposed cascade control strategy in the GSBR. The ammonium set-point was 5 mg $N\text{-}NH_4^+$ L^{-1}. Since the secondary DO control loop was supposed to be fast and efficient, the represented DO concentration after the control strategy activation is equal to the DO set-point value.

The most successful approaches to improve N-removal in GSBR previously reported (Chen et al., 2011; de Kreuk et al., 2007b) were based on changing the cycle structure of the reactor (i. e. adding anoxic periods, dividing the feeding, etc). Here, the proposed control strategy was much simpler, because its implementation maintains the cycle structure, and only the DO set-point was directly manipulated. Furthermore, since the ammonium set-point was established independently of the influent or granular sludge characteristics (e.g. size), automation of the control system is possible and robust, providing stability to the long term operation of the GSBR.

4.4.4.3 Microbiological risks

The experimental results showed that the enhancement of the N-removal implied, in most cases, to impose low DO concentrations (lower than 2 mg O_2 L^{-1}). Working at such low DO concentrations is advantageous, since the aeration costs could be reduced considerably. However, low DO concentrations may lead to some risks associated to the granules stability. Many authors have pointed out that working at such low DO concentrations may induce an overgrowth of filamentous microorganisms over the granules, which in most cases ended up in granules breakage (Isanta et al., 2012; Mosquera-Corral et al., 2005). Also the use of low aeration rates induced granules instability and final breakdown (Tay et al., 2004). Thus, it may be necessary to further study the stability of the granular sludge at the optimal conditions for N-removal.

4.5 Conclusions

A mathematical model able to describe the operation of a GSBR was successfully calibrated and validated. The subsequent model exploitation revealed that N-removal was always enhanced when the DO applied produced a slight ammonium accumulation in the effluent (e.g. 5 mg N-NH_4^+ L^{-1}). Furthermore, this occurred independently of granule size, influent C/N ratio or NLR. Accordingly, we proposed a cascade ammonium and oxygen control strategy that successfully automates finding the adequate DO concentration to enhance N-removal. The control strategy will set the appropriate DO set-point at whatever values of granule size, influent C/N ratio or NLR. Therefore, high N-removal efficiencies (between 70 – 85%, in most cases) will be assured by the control strategy against disturbances in those variables, which are common during the reactor operation. This is one of the first control strategies proposed for aerobic granular reactors and future research in pilot plant to confirm these results would be desirable.

4.6 Appendix

Table A4.1: kinetic equations.

Process	***Equation***
1. Aeration	$k_L a \left(S_{O2}^{*} - S_{O2}\right)$
Heterotrophic bacteria	
2. Aerobic growth on S_S	$\mu_{H,max} \frac{S_{O2}}{K_{O2}^{H} + S_{O2}} \frac{S_S}{K_S + S_S} \frac{S_{NH4}}{K_{NH4}^{H} + S_{NH4}} X_H$
3. Aerobic growth on X_{STO}	$\mu_{H,max} \frac{S_{O2}}{K_{O2}^{H} + S_{O2}} \frac{S_{TAN}}{K_{TAN}^{H} + S_{TAN}} \frac{X_{STO}/X_H}{K_{STO} + X_{STO}/X_H} X_H$
4. Anoxic growth on S_S with S_{NO2}	$\mu_{H,max} \eta_H \frac{K_{O2}^{H}}{K_{O2}^{H} + S_{O2}} \frac{S_{NO2}}{K_{NO2}^{H} + S_{NO2}} \frac{S_S}{K_S + S_S} \frac{S_{NH4}}{K_{NH4}^{H} + S_{NH4}} X_H$
5. Anoxic growth on S_S with S_{NO3}	$\mu_{H,max} \eta_{H,NO3} \frac{K_{O2}^{H}}{K_{O2}^{H} + S_{O2}} \frac{S_{NO3}}{K_{NO3}^{H} + S_{NO3}} \frac{S_S}{K_S + S_S} \frac{S_{NH4}}{K_{NH4}^{H} + S_{NH4}} X_H$
6. Anoxic growth on X_{STO} with S_{NO2}	$\mu_{H,max} \eta_H \frac{K_{O2}^{H}}{K_{O2}^{H} + S_{O2}} \frac{S_{NO2}}{K_{NO2}^{H} + S_{NO2}} \frac{S_{NH4}}{K_{NH4}^{H} + S_{NH4}} \frac{X_{STO}/X_H}{K_{STO} + X_{STO}/X_H} X_H$
7. Anoxic growth on X_{STO} with S_{NO3}	$\mu_{H,max} \eta_{H,NO3} \frac{K_{O2}^{H}}{K_{O2}^{H} + S_{O2}} \frac{S_{NO3}}{K_{NO3}^{H} + S_{NO3}} \frac{S_{NH4}}{K_{NH4}^{H} + S_{NH4}} \frac{X_{STO}/X_H}{K_{STO} + X_{STO}/X_H} X_H$
8. Aerobic endogenous respiration	$b_H \frac{S_{O2}}{K_{O2}^{H} + S_{O2}} X_H$
9. Anoxic endogenous respiration on S_{NO2}	$b_H \eta_H \frac{K_{O2}^{H}}{K_{O2}^{H} + S_{O2}} \frac{S_{NO2}}{K_{NO2}^{H} + S_{NO2}} X_H$
10. Anoxic endogenous respiration on S_{NO3}	$b_H \eta_{H,NO3} \frac{K_{O2}^{H}}{K_{O2}^{H} + S_{O2}} \frac{S_{NO3}}{K_{NO3}^{H} + S_{NO3}} X_H$
11. Aerobic formation of X_{STO}	$k_{STO} \frac{S_{O2}}{K_{O2}^{H} + S_{O2}} \frac{S_S}{K_{Ss} + S_S} X_H$
12. Anoxic formation of X_{STO} on S_{NO2}	$k_{STO} \eta_H \frac{K_{O2}^{H}}{K_{O2}^{H} + S_{O2}} \frac{S_{NO2}}{K_{NO2}^{H} + S_{NO2}} \frac{S_S}{K_S + S_S} X_H$
13. Anoxic formation of X_{STO} on S_{NO3}	$k_{STO} \eta_{H,NO3} \frac{K_{O2}^{H}}{K_{O2}^{H} + S_{O2}} \frac{S_{NO3}}{K_{NO3}^{H} + S_{NO3}} \frac{S_S}{K_S + S_S} X_H$
14. Aerobic respiration of X_{STO}	$b_{STO} \frac{S_{O2}}{K_{O2}^{H} + S_{O2}} X_{STO}$
15. Anoxic respiration of X_{STO} on S_{NO2}	$b_{STO} \eta_H \frac{K_{O2}^{H}}{K_{O2}^{H} + S_{O2}} \frac{S_{NO2}}{K_{NO2}^{H} + S_{NO2}} X_{STO}$
16. Anoxic respiration of X_{STO} on S_{NO3}	$b_{STO} \eta_{H,NO3} \frac{K_{O2}^{H}}{K_{O2}^{H} + S_{O2}} \frac{S_{NO3}}{K_{NO3}^{H} + S_{NO3}} X_{STO}$
Ammonium-oxidizing bacteria (AOB)	
17. Aerobic growth	$\mu_{A,max} \frac{S_{O2}}{K_{O2}^{A} + S_{O2}} \frac{S_{NH4}}{K_{NH4} + S_{NH4}} X_A$
18. Aerobic endogenous respiration	$b_A \frac{S_{O2}}{K_{O2}^{A} + S_{O2}} X_A$

Table A4.1: (continued).

Process	***Equation***
19. Anoxic endogenous respiration on S_{NO2}	$b_A \, \eta_A \frac{K_{O2}^A}{K_{O2}^A + S_{O2}} \frac{S_{NO2}}{K_{NO2}^A + S_{NO2}} X_A$
20. Anoxic endogenous respiration on S_{NO3}	$b_A \, \eta_{A,NO3} \frac{K_{O2}^A}{K_{O2}^A + S_{O2}} \frac{S_{NO3}}{K_{NO3}^A + S_{NO3}} X_A$
Nitrite-oxidizing bacteria (NOB)	
21. Aerobic growth	$\mu_{N,max} \frac{S_{O2}}{K_{O2}^N + S_{O2}} \frac{S_{NO2}}{K_{NO2}^N + S_{NO2}} X_N$
22. Aerobic endogenous respiration	$b_N \frac{S_{O2}}{K_{O2}^N + S_{O2}} X_N$
23. Anoxic endogenous respiration on S_{NO2}	$b_N \, \eta_N \frac{K_{O2}^N}{K_{O2}^N + S_{O2}} \frac{S_{NO2}}{K_{NO2}^N + S_{NO2}} X_N$
24. Anoxic endogenous respiration on S_{NO3}	$b_N \, \eta_{N,NO3} \frac{K_{O2}^N}{K_{O2}^N + S_{O2}} \frac{S_{NO3}}{K_{NO3}^N + S_{NO3}} X_N$

Table A4.2: Kinetic and stoichiometric parameters

Symbol	Definition	Value	Units	Reference
b_A	Aerobic endogenous respiration rate of X_A	0.18	d^{-1}	Jubany et al. (2008)
b_N	Aerobic endogenous respiration rate of X_N	0.16	d^{-1}	Jubany et al. (2008)
b_H	Aerobic endogenous respiration rate of X_H	0.26	d^{-1}	Henze et al. (2000)
b_{STO}	Aerobic respiration rate for X_{STO}	0.26	d^{-1}	Henze et al. (2000)
D_{NH4}	Diffusion coefficient of S_{NH4} in water	$1.9 \cdot 10^{-4}$	$m^2\ d^{-1}$	Pérez et al. (2005)
D_{NO2}	Diffusion coefficient of S_{NO2} in water	$1.47 \cdot 10^{-4}$	$m^2\ d^{-1}$	Assumed
D_{NO3}	Diffusion coefficient of S_{NO3} in water	$1.47 \cdot 10^{-4}$	$m^2\ d^{-1}$	Assumed
D_{O2}	Diffusion coefficient of S_{O2} in water	$1.72 \cdot 10^{-4}$	$m^2\ d^{-1}$	Assumed
D_S	Diffusion coefficient for S_S	$1 \cdot 10^{-4}$	$m^2\ d^{-1}$	Perez et al. (2005)
f_X	Production of X_I in endogenous respiration	0.2	-	Henze et al. (2000)
$i_{N,Xi}$	N content of X_I	0.04	kg N kg^{-1} COD	Reichert et al. (2001)
$i_{N,BM}$	N content of biomass, X_H, X_A, X_N	0.07	kg N kg^{-1} COD	Koch et al. (2000)
η_H	Reduction factor for anoxic activity for X_H	0.6	-	Henze et al. (2000)
$\eta_{H,NO3}$	Reduction factor for anoxic activity over nitrate for X_H	0.3	-	Assumed
η_A	Reduction factor for anoxic activity for X_A	0.25	-	Munz et al. (2011b)
$\eta_{A,NO3}$	Reduction factor for anoxic activity for X_A	0.125	-	Assumed
η_N	Reduction factor for anoxic activity for X_N	0.16	-	Munz et al. (2011b)
$\eta_{N,NO3}$	Reduction factor for anoxic activity for X_N	0.08	-	Assumed
k_La	Oxygen mass transfer coefficient	1.5	min^{-1}	Assumed
K_{STO}	Saturation constant for X_{STO}	1	kg COD kg^{-1} COD	Henze et al. (2000)
K_{O2}^{A}	S_{O2} saturation constant for X_A	0.4	g O_2 m^{-3}	Munz et al. (2011b)

Table A4.2: (continued)

Symbol	Definition	Value	Units	Reference
K^{A}_{NH4}	S_{NH4} saturation constant for X_A	1	g N-NH_4^+ m^{-3}	Henze et al. (2000)
K^{A}_{NO2}	S_{NO2} saturation constant for X_A	1	g N-NO_2^- m^{-3}	Henze et al. (2000)
K^{A}_{NO3}	S_{NO3} saturation constant for X_A	0.5	g N-NO_3^- m^{-3}	Henze et al. (2000)
K^{N}_{NO2}	S_{NO2} saturation constant for X_N	1	g N-NO_2^- m^{-3}	Henze et al. (2000)
K^{N}_{O2}	S_{O2} saturation constant for X_N	0.61	g O_2 m^{-3}	Munz et al. (2011b)
K^{N}_{NO3}	S_{NO3} saturation constant for X_N	1	g N-NO_3^- m^{-3}	Henze et al. (2000)
K_{Ss}	Saturation constant for S_S	10	g COD m^{-3}	Koch et al. (2000)
K^{H}_{O2}	S_{O2} saturation constant for X_H	0.2	g O_2 m^{-3}	Henze et al. (2000)
K^{H}_{NO2}	S_{NO2} saturation constant for X_H	0. 5	g N-NO_2^- m^{-3}	Henze et al. (2000)
K^{H}_{NO3}	S_{NO3} saturation constant for X_H	0. 5	g N-NO_3^- m^{-3}	Henze et al. (2000)
K^{H}_{NH4}	S_{NH4} saturation constant for X_H	0.01	g N-NH_4^+ m^{-3}	Henze et al. (2000)
$\mu_{A,max}$	Maximum growth rate of X_A	1.32	d^{-1}	Calibrated
$\mu_{N,max}$	Maximum growth rate of X_N	1.32	d^{-1}	Assumed
$\mu_{H,max}$	Maximum growth rate of X_H	5.2	d^{-1}	Calibrated
k_{STO}	Storage rate constant	13.2	d^{-1}	Calibrated
ρ_A	Maximum density for X_A	350	kg COD m^{-3}	de Kreuk et al. (2007)
ρ_N	Maximum density of X_N	350	kg COD m^{-3}	de Kreuk et al. (2007)
ρ_H	Maximum density for X_H	150	kg COD m^{-3}	Xavier et al. (2007)
ρ_{STO}	Maximum density of X_{STO}	$1 \cdot 10^8$	kg COD m^{-3}	de Kreuk et al. (2007)
ρ_I	Maximum density of X_I	400	kg COD m^{-3}	Assumed
Y_A	Yield of X_A per S_{NH4}	0.18	kg COD kg^{-1} N	Jubany et al. (2008)
Y_N	Yield of X_N per S_{NO2}	0.08	kg COD kg^{-1} N	Jubany et al. (2008)
Y_H	Yield of X_H per S_S	0.57	kg COD kg^{-1} COD	Sin et al. (2005)
Y_{HSTO}	Yield of X_H per X_{STO}	0.68	kg COD kg^{-1} COD	Sin et al. (2005)
Y_{STO}	Yield coefficient for storage on substrate	0.80	kg COD kg^{-1} COD	Sin et al. (2005)

Table A4.3: Stoichiometric matrix of soluble and particulate components

	S_S COD kg m^{-3}	S_{O2} O_2 kg m^{-3}	S_{NH4} N kg m^{-3}	S_{NO2} N kg m^{-3}	S_{NO3} N kg m^{-3}	X_H COD kg m^{-3}	X_{STO} COD kg m^{-3}	X_A COD mg L^{-1}	X_N COD kg m^{-3}	X_I COD kg m^{-3}
1. Aeration	0	1	0	0	0	0	0	0	0	0
Heterotrophic bacteria										
2. Aerobic growth on S_S	$-1/Y_H$	$-(1/Y_H-1)$	$-i_B$	0	0	+1	0	0	0	0
3. Aerobic growth on X_{STO}	0	$-(1/Y_{HSTO}-1)$	$-i_B$	0	0	+1	$-1/Y_{HSTO}$	0	0	0
4. Anoxic growth on S_S with S_{NO2}	$-1/Y_H$	0	$-i_B$	$-(1/Y_H-1)/1.71$	0	+1	0	0	0	0
5. Anoxic growth on S_S with S_{NO3}	$-1/Y_H$	0	$-i_B$	$+(1/Y_H-1)/1.14$	$-(1/Y_H-1)/1.14$	+1	0	0	0	0
6. Anoxic growth on X_{STO} with S_{NO2}	0	0	$-i_B$	$-(1/Y_{HSTO}-1)/1.71$	0	+1	$-1/Y_{HSTO}$	0	0	0
7. Anoxic growth on X_{STO} with S_{NO3}	0	0	$-i_B$	$+(1/Y_{HSTO}-1)/1.14$	$-(1/Y_{HSTO}-1)/1.14$	+1	$-1/Y_{HSTO}$	0	0	0
8. Aerobic endogenous respiration	0	$-(1-f_X)$	$i_B-i_{XI}\cdot f_X$	0	0	-1	0	0	0	f_X
9. Anoxic endogenous respiration on S_{NO2}	0	0	$i_B-i_{XI}\cdot f_X$	$-(1-f_X)/1.71$	0	-1	0	0	0	f_X
10. Anoxic endogenous respiration on S_{NO3}	0	0	$i_B-i_{XI}\cdot f_X$	$+(1-f_X)/1.14$	$-(1-f_X)/1.14$	-1	0	0	0	f_X
11. Aerobic formation of X_{STO}	$-1/Y_{STO}$	$-(1/Y_{STO}-1)$	0	0	0	0	+1	0	0	0
12. Anoxic formation of X_{STO} on S_{NO2}	$-1/Y_{STO}$	0	0	$-(1/Y_{STO}-1)/1.71$	0	0	+1	0	0	0
13. Anoxic formation of X_{STO} on S_{NO3}	$-1/Y_{STO}$	0	0	$+(1/Y_{STO}-1)/1.14$	$-(1/Y_{STO}-1)/1.14$	0	+1	0	0	0
14. Aerobic respiration of X_{STO}	0	-1	0	0	0	0	-1	0	0	0
15. Anoxic respiration of X_{STO} on S_{NO2}	0	0	0	-1/1.71	0	0	-1	0	0	0
16. Anoxic respiration of X_{STO} on S_{NO3}	0	0	0	+1/1.14	-1/1.14	0	-1	0	0	0

Table A4.3: (continued)

	S_S COD kg m^{-3}	S_{O2} O_2 kg m^{-3}	S_{NH4} N kg m^{-3}	S_{NO2} N kg m^{-3}	S_{NO3} N kg m^{-3}	X_H COD kg m^{-3}	X_{STO} COD kg m^{-3}	X_A COD mg L^{-1}	X_N COD kg m^{-3}	X_I COD kg m^{-3}
Ammonium-oxidizing bacteria										
17. Aerobic growth	0	$-(3.43/Y_A-1)$	$-(i_B+1/Y_A)$	$1/Y_A$	0	0	0	1	0	0
18. Aerobic endogenous respiration	0	$-(1-f_X)$	$i_B-i_{Xi}\cdot f_X$	0	0	0	0	-1	0	f_X
19. Anoxic endogenous respiration on S_{NO2}	0	0	$i_B-i_{Xi}\cdot f_X$	$-(1-f_X)/1.71$	0	0	0	-1	0	f_X
20. Anoxic endogenous respiration on S_{NO3}	0	0	$i_B-i_{Xi}\cdot f_X$	$+(1-f_X)/1.14$	$-(1-f_X)/1.14$	0	0	-1	0	f_X
Nitrite-oxidizing bacteria										
21. Aerobic growth	0	$-1.14/(Y_N-1)$	$-i_B$	$-1/Y_N$	$1/Y_N$	0	0	0	1	0
22. Aerobic endogenous respiration	0	$-(1-f_X)$	$i_B-i_{Xi}\cdot f_X$	0	0	0	0	0	-1	f_X
23. Anoxic endogenous respiration on S_{NO2}	0	0	$i_B-i_{Xi}\cdot f_X$	$-(1-f_X)/1.71$	0	0	0	0	-1	f_X
24. Anoxic endogenous respiration on S_{NO3}	0	0	$i_B-i_{Xi}\cdot f_X$	$+(1-f_X)/1.14$	$-(1-f_X)/1.14$	0	0	0	-1	f_X

CHAPTER 5

STABLE PARTIAL NITRITATION FOR LOW STRENGH WASTEWATER AT LOW TEMPERATURE IN AN AEROBIC GRANULAR REACTOR

Part of this chapter is being prepared for publishing as:

Isanta, E., Reino, C., Carrera, J., Pérez, J., 2013. Stable partial nitritation for low strength wastewater at low temperature in an aerobic granular reactor. *Environ. Sci. Technol*.

Part of this chapter has been applied for a patent:

Isanta, E., Carrera, J., Pérez, J., A method and a system for wastewater nitrogen removal. Priority patent application: GB1317957.7 EP13382401. Applicant: Universitat Autànoma de Barcelona.

5.1 Introduction

For the achievement of sustainable (energy-neutral or even energy-positive) wastewater treatment plants the use of anammox for sewage treatment has been proposed (Kartal et al., 2010). The performance of one-stage nitrogen (N) removal of pretreated municipal nitrogenous wastewater has been tested with sequencing batch reactors (SBR) as a first approach (Hu et al., 2013; Winkler et al., 2011b). In many of the studies, the known weak point of those trials is that nitrite-oxidizing bacteria (NOB) develop in the long term operation, triggering the production of nitrate, and decreasing importantly the N-removal performance with anammox (de Clippeleir et al., 2013; Winkler et al., 2011b). Even in the treatment of the sidestream (reject water), with more advantageous conditions for anammox-based N-removal, the development of NOB in one-stage granular reactors was a problematic issue during the maintenance routines, like short-term aeration pulses, which are thought to lead to healthy NOB population (Joss et al., 2011).

A two-stage N-removal system operating in continuous mode could be thought also as an appealing solution for sewage treatment (Regmi et al., 2014). In fact, a two-stage N-removal system was proposed as a potential alternative (nitritation with activated sludge (Ma et al., 2011); nitritation with granular reactor (Torà et al., 2013)). In the past, poor results were reported, and little attention had been paid to partial nitritation with biofilm reactors either because such a process was thought difficult to be maintained in the long term (Fux et al., 2004; Garrido et al., 1997) or because trials yielded not the expected results (Bernet et al., 2005). However, stable nitritation in biofilm reactors operating in continuous mode have been reported for the specific treatment of the sidestream (Torà et al., 2013) and other types of rich ammonium wastewaters (Bartrolí et al., 2010; Bougard et al., 2006; Tokutomi, 2004) at temperatures over 20ºC. Also the process have been deeply studied through mathematical modeling (Brockmann and Morgenroth, 2010; Jemaat et al., 2013; Pérez et al., 2009). The success of such a treatment relays in the use of a control strategy to maintain the adequate ratio between oxygen and ammonium concentrations in the reactor bulk liquid, as to repress NOB activity in the biofilm (automatic control for partial nitrification to nitrite in biofilm reactors, ANFIBIO; Bartrolí et al. (2010); Jemaat et al. (2013)). However, when applying such a strategy to the mainstream, two different challenges could be outlined: (i) the partial nitritation reactor would need to produce the adequate ratio between ammonium and nitrite concentrations as to feed a subsequent anammox reactor and (ii) to the best of our knowledge, a stable partial nitritation reactor (achieving an effluent with a nitrite/ammonium ratio of 1), with floccular, attached or granular biomass, at temperatures lower than 15 ºC and treating low-strength

ammonium wastewaters has not been reported. Only some studies achieved stable full nitritation in SBRs at these conditions but treating low nitrogen loading rates (NLR: 0.05-0.10 g N L^{-1} d^{-1}, Gu et al. (2012); Yuan and Oleszkiewicz (2011)). Other reactors operated at higher NLRs showed sudden deterioration of the nitritation at temperatures lower than 15 ºC (Yamamoto et al., 2006).

Here, we would like to demonstrate the feasibility of partial nitritation in a granular reactor operating in continuous mode at low temperatures, treating a wastewater with low N concentrations. Microbiological analyses and mathematical modeling tools will be used to better understand the experimental results.

5.2 Materials and Methods

5.2.1 Reactor set-up, inoculum and wastewater

An airlift reactor with working volume of 2.5 L was used in this study (see scheme in Figure 5.1.). Compressed air was supplied through an air diffuser placed at the bottom of the reactor and manually manipulated to maintain the dissolved oxygen (DO) concentration in the bulk liquid in the range 1 – 5 mg O_2 L^{-1}. The DO concentration in the bulk liquid was measured on-line by means of a DO electrode (DO 60-50, Crison Instruments, Spain). The pH was measured online with a pH probe (pH 52-10, Crison Instruments, Spain) and automatically controlled at 8.0±0.1 by dosing a Na_2CO_3 0.5 M solution. Temperature was controlled at different values in the experiments, 30.0±0.1, 20.0±0.1, 15.0±0.1 and 12.5±0.1 ºC by means of a cooling system (E100, LAUDA, Germany) and an electric heater (HBSI 0.8m, HORST, Germany) connected to a temperature controller (BS-2400, Desin Instruments, Spain). The total ammonia nitrogen (TAN = $N\text{-}NH_4^+$ + $N\text{-}NH_3$) in bulk liquid was controlled varying the inflow rate. Before day 71, the TAN control was made manually based on the off-line bulk liquid TAN concentration measurement. From day 71 to day 250, the TAN control was automated by using an on-line TAN probe (NH4Dsc probe with a Cartrical cartridge, Hach Lange, Germany) using a proportional controller. From day 250 onwards, the TAN control was again made manually to check the feasibility of implementing this technology without a TAN on-line sensor.

The airlift reactor was inoculated with nitrifying granular sludge that had been stored at 4ºC for 7 months after collection from a granular sludge pilot reactor treating the sidestream of a municipal WWTP through nitritation in stable conditions for several months. The nitrifying granules had an average particle size of 0.5 mm (Torà et al., 2013).

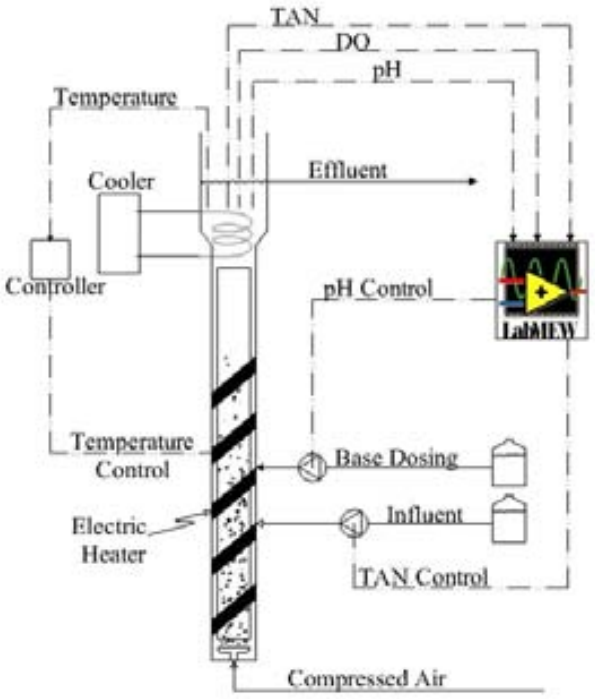

Figure 5.1. Schematic diagram of the reactor set-up showing the peripheral instrumentation and control loops.

The biofilm airlift reactor was fed with a synthetic influent mimicking the pretreated municipal wastewater from an anammox-based WWTP (Kartal et al., 2010). The pretreatment of the wastewater would consist of a classical WWTP primary treatment followed by the removal of the organic matter in a very high-loaded activated sludge reactor. The ammonium concentration of the wastewater also accounts for the ammonium coming from the sidestream produced after the digested sludge dewatering. Therefore, the resulting mineral medium contained, in average, 70 mg $N\text{-}NH_4^+$ L^{-1} (Hu et al., 2013), added as NH_4Cl. The synthetic wastewater also contained 45 mg L^{-1} KH_2PO_4, 90 mg L^{-1} $MgSO_4$, 40 mg L^{-1} $CaCl_2$ and 1 mL of trace elements solution per L of influent (Guerrero et al., 2011).

5.2.2 Analytical methods

Liquid samples were periodically withdrawn from the reactor effluent to determine the concentrations of TAN, total nitrite nitrogen (TNN = $N\text{-}NO_2^-$ + $N\text{-}HNO_2$) and nitrate. Ammonium concentration was measured with an ammonium analyzer (AMTAX sc, Hach Lange, Germany). Nitrate and TNN concentrations were analyzed with ionic chromatography using an ICS-2000 Integrated Reagent-Free IC system (DIONEX Corporation, USA) which performs ion analyses using suppressed conductivity detection. Mixed liquor total suspended solids (TSS) and mixed liquor volatile suspended solids (VSS) were analyzed according to Standard Methods (APHA,

2008). Average particle size was measured by a laser particle size analysis system (Malvern MasterSizer Series 2600, Malvern instruments Ltd., UK). The average settling velocity was measured by recording the time taken for at least 40 individual granules to fall from a certain height in a measuring cylinder filled with the synthetic medium described in the previous section.

5.2.3 Fluorescence in situ hybridization (FISH)

FISH technique coupled with confocal laser scanning microscopy was used to determine the relative abundances of ammonia-oxidizing bacteria (AOB), NOB and anammox bacteria (AMX) in the granules. Hybridizations were carried out using at the same time a Cy3-labeled specific probe and Cy5-labeled general bacteria probe. The general probe was a 1:1:1 mixture of EUB338I, EUB338II, and EUB338III for all Bacteria (Table 5.1). Specific and general probe sequences are also listed Table 5.1. A Leica TCS SP2 AOBS confocal laser scanning microscope at a magnification of x63 (objective HCX PL APO ibd.B163 x1.4 oil) equipped with two HeNe lasers with light emission at 561 and 633nm was used for biomass quantification. The detailed procedure and additional information related to FISH quantification can be found elsewhere (Jubany et al., 2009b).

Table 5.1. 16S rRNA-targeted oligonucleotide probes, target microorganisms, and references used in this study to determine the relative abundance of microbial population with the FISH technique.

Probe	Sequence (from ‘5 to ‘3)	Specificity	Reference
EUB338 I	GCTGCCTCCCGTAGGAGT	Most bacteria	Amann et al. (1990)
EUB338 II	GCTGCCTCCCGTAGGAGT	Planctomycetales	Daims et al. (1999)
EUB338 III	CGCCATTGTATTACGTGTGA	Verrucomicrobiales	Daims et al. (1999)
NSO190	CGATCCCCTGCTTTTCTCC	All AOB	Mobarry et al. (1996)
NIT3	CCTGTGCTCCATGCTCCG	*Nitrobacter* spp.	Wagner et al. (1996)
NTSPA662	GGAATTCCGCGCTCCTCT	genus *Nitrospira*	Daims et al. (2001)
AMX368	CCTTTCGGGCATTGCGAA	All Anammox bacteria	Schmid et al. (2005)

5.2.4 Mathematical modeling

A one-dimensional biofilm model was developed to simulate the nitrifying biofilm airlift reactor performance based on Wanner and Reichert (1996) and implemented in the software package AQUASIM (Reichert, 1998), v.2.1d.

5.2.4.1 Biological Processes

The biomass species described as particulate compounds in the biofilm matrix were three: AOB, NOB and inert biomass. Nitrification was defined as a two-step process with a first oxidation of ammonium to nitrite by ammonia-oxidizing bacteria (AOB) and a subsequent oxidation of nitrite to nitrate by nitrite-oxidizing bacteria (NOB). The kinetics for each of the processes considered in this model i.e. growth and decay of each kind of bacteria (Table A5.1), the stoichiometry of the process (Table A5.2) and the kinetic parameter values (Table A5.3) are presented in the Appendix of this chapter. All the kinetic parameters were taken from literature.

The values corresponding to the maximum specific growth rates of autotrophic bacteria ($\mu_{max,AOB}$ and $\mu_{max,NOB}$) were calculated with the equations proposed by Jubany et al. (2008):

$$\mu_{\max,AOB}(pH,T) = \frac{1.28 \cdot 10^{12} e^{-8183/(273+T)}}{1 + (2.05 \cdot 10^{-9} / 10^{-pH}) + (10^{-pH} / 1.66 \cdot 10^{-7})} \quad (5.1)$$

$$\mu_{\max,NOB}(pH,T) = \frac{6.69 \cdot 10^{7} e^{-5295/(273+T)}}{1 + (2.05 \cdot 10^{-9} / 10^{-pH}) + (10^{-pH} / 1.66 \cdot 10^{-7})} \quad (5.2)$$

On the other hand, the decay rate expression for both AOB and NOB were calculated with the equations proposed by Munz et al. (2011a) and modified with a temperature correction:

$$b_{AER,AOB}(T) = 3.21 \cdot 10^{11} e^{-8183/(273+T)} \quad (5.3)$$

$$b_{ANAER,AOB}(T) = 1.34 \cdot 10^{10} e^{-8183/(273+T)} \quad (5.4)$$

$$b_{AER,NOB}(T) = 9.71 \cdot 10^{6} e^{-5295/(273+T)} \quad (5.5)$$

$$b_{ANAER,NOB}(T) = 4.66 \cdot 10^{5} e^{-5295/(273+T)} \quad (5.6)$$

5.2.4.2 Granules description

Biofilm area was described as a function of the granule radius, to correctly simulate the biofilm geometry (for further details see Jemaat et al. (2013)). Total biofilm area was defined as a function of granule size and number of granules. A detachment rate was used to keep a constant biofilm thickness in steady state at a predefined value. Detached biomass from the biofilm was considered as active following the same kinetics defined for the biomass in the biofilm. Attachment of biomass onto the biofilm surface has been neglected. For the sake of simplicity

external mass transfer has been neglected. The porosity of the biofilm was fixed as 80% and kept constant during all the simulations. Initial fractions of particulate compounds were 10% AOB, 8% NOB, 2% heterotrophic biomass. Other parameters related to the biofilm and used in the model are detailed in Appendix of this chapter (Table A5.5).

5.2.4.3 Process control modeling

The control strategy was also described by the model. Two different closed-loops were used: (i) one to maintain the TAN concentration in the bulk liquid of the nitritation reactor (i.e., the reactor effluent, considering a well-mixed liquid phase in the reactor) and (ii) a second one to control the DO concentration in the bulk liquid.

TAN concentration was maintained by regulating the inflow rate (as done experimentally in the reactor). In the model TAN control loop, an *ad hoc* expression was developed, because the control loop has the inflow rate (Q_{in}) as manipulated variable (Jemaat et al., 2013):

$$Q_{side} = Q_{side,0} \cdot \left(1 + \frac{[TAN]_{SP} - [TAN]}{[TAN]_{SP}} \cdot a \right) \tag{5.7}$$

where $Q_{in,0}$ is known as the bias of the control action, i.e. the default value of flow-rate. The controller will always act either increasing or decreasing Q_{in} around $Q_{in,0}$. [TAN] is the total TAN concentration in the bulk liquid phase. $[TAN]_{SP}$ is the TAN concentration set point. The proportional gain of the controller (*a*), could be easily tuned depending on the particular operating conditions. The principle of the performance of the expression is similar to that applied in a conventional proportional control law.

The closed DO control loop was used to keep in the simulations the same DO applied in the experiments. For the mathematical description of the DO control loop, aeration was introduced as a dynamic process only active in the bulk liquid phase. A high value for the volumetric gas-liquid oxygen transfer coefficient ($k_La = 10^4\ d^{-1}$) was selected. The oxygen solubility used was equal to the DO set point (Jemaat et al., 2013; Pérez et al., 2009):

$$\frac{d[DO]}{dt} = k_L a \cdot \left([DO]_{SP} - [DO] \right) \tag{5.8}$$

where [DO] is the dissolved oxygen concentration in the bulk liquid, and $[DO]_{SP}$ is the DO concentration set point. As a set point the experimental DO was used.

5.2.4.4 Modeling strategy

For the description of the experiments, experimental data like pH, temperature, reactor volume, biomass concentration, granule size and characteristics of the influent were input to the model. Also the TAN set point imposed in the experiments and the measured DO concentration were inputs for the model. The main model outputs are the values of TNN and nitrate concentrations in the effluent for each of the temperatures tested (20, 15 and 12.5 ºC) and flow-rate. To adequately simulate the start-up period, first a granular sludge was developed in the reactor for a period of 600 days at 30 ºC. To simulate the storage of the granular sludge before inoculation of the reactor, the reactor temperature was set to 5.5 ºC for 200 days (i.e. equivalent to the 7 months the granular sludge has been stored). DO was maintained at 0.01 mg O_2 L^{-1} and the TAN in the bulk was set to only 0.05 mg N L^{-1}, to simulate the conditions in the storing fridge. After this period, the conditions used in the real start-up were imposed in the simulation, pursuing a fully dynamic description of the experiments.

To investigate the mechanisms leading to stable partial nitritation at low temperatures, additional simulations were run. The impact of the oxygen affinity constant of NOB ($K_{O2,NOB}$) was investigated. NOB repression was investigated when (i) the oxygen affinity constants of NOB and AOB were assumed equal ($K_{O2,NOB}$ = $K_{O2,AOB}$ = 0.74 mg N L^{-1}), and (ii) assuming NOB with a higher oxygen affinity, $K_{O2,NOB}$ < $K_{O2,AOB}$ (0.16 and 0.74 mg N L^{-1}, respectively). Also, the model predictions at lower bulk ammonium concentration were explored to determine the importance of the ammonium concentration in NOB repression.

5.3 Results and Discussion

5.3.1 Reactor start-up

After the inoculation, the reactor was first left overnight in batch mode with an initial TAN concentration of 192 mg N L^{-1} and the temperature was set to 30 ºC to wake up the biomass. The day after, the continuous operation was started with an initial NLR of 0.27 g N L^{-1} d^{-1}. During the first 36 days, the temperature was progressively reduced from 30 to 20 ºC, whereas the NLR was increased from 0.27 to 1.4 g N L^{-1} d^{-1} (Figure 5.2). Only during the first days of operation a significant amount of the ammonium was oxidized to nitrate (up to 18 mg N-NO_3^- L^{-1} on day 2, see Figure 5.2C). However, the nitrate production progressively decreased to only 0.4 mg N-NO_3^- L^{-1} on day 35. From day 35 onwards, stable partial nitritation to nitrite was maintained in the reactor (Figure 5.2), see details in the next section.

From day 0 to 16, a fast decrease of the biomass concentration from 2.9 to 1.3 g VSS L^{-1} occurred, while the particle size increase from 0.5 on day 0 to 1.2 mm on day 45 (Figure 5.2A).

5.3.2 Reactor performance at low temperatures

On day 36 the reactor temperature was decreased first to 20 ºC for a period of 40 days, then to 15 ºC during 70 days and finally to 12.5 ºC during 300 days. Therefore, the reactor was operated during more than 12 months at a temperature equal than or below 15 ºC.

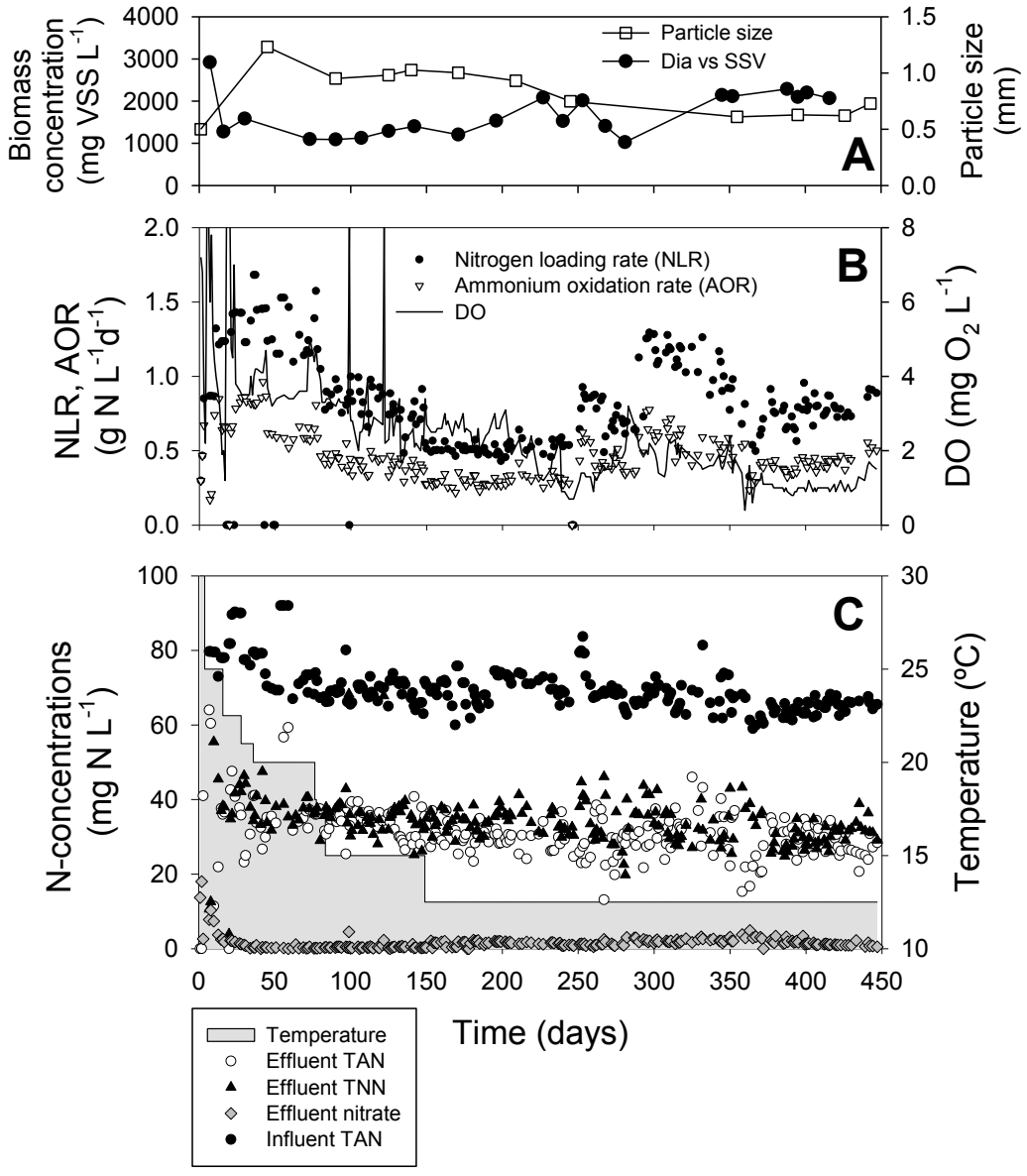

Figure 5.2. Performance of the continuous granular airlift reactor treating a synthetic municipal mainstream wastewater. (A) Biomass concentration and particle size; (B) Nitrogen Loading Rate (NLR) and Ammonium Oxidation Rate (AOR); (C) Nitrogen compounds concentrations throughout the operational period and temperature.

As shown in Figure 5.2, stable partial nitritation was successfully maintained at any of the temperatures tested by maintaining a very low DO/TAN concentrations ratio in the bulk liquid of the reactor (i.e. very strong oxygen limiting conditions) to repress NOB activity (Bartrolí et al., 2010; Jemaat et al., 2013). Low effluent nitrate concentrations were measured; 0.3±0.1 and 0.4±0.1 mg $N\text{-}NO_3^-$ L^{-1} at 20 and 15 ºC, respectively. When the temperature was decreased to 12.5 ºC, the effluent nitrate concentration slightly increased to an average value of 2.5±0.7 mg $N\text{-}NO_3^-$ L^{-1}. Interestingly, the nitrate production did not increase further and remained rather stable. Note how an effluent nitrate concentration of 2.5±0.7 mg $N\text{-}NO_3^-$ L^{-1} only means a 3.6 % of the influent ammonium oxidized to nitrate.

The average TNN/TAN concentrations ratio in the reactor effluent was 1.0±0.2 from days 40 to 150 and 1.2±0.3 from days 150 to 450. This ratio is suitable for a subsequent anammox step.

The ammonium oxidation rate (AOR) showed a decreasing trend with temperature during the first 200 days but AOR slightly increased after 100 days operating at 12.5 ºC (Figure 5.2B). This gain was probably due to the increase of the biomass concentration from day 200 onwards (Figure 5.2A). The specific ammonium oxidation rate (sAOR) achieved at 12.5 ºC (0.2±0.1 g N g^{-1} VSS d^{-1}) was considerably high compared with other reported nitrifying systems (Gu et al., 2012; Yuan and Oleszkiewicz, 2011). The sAOR at 12.5 ºC, 15 ºC (0.32±0.06 g N g^{-1} VSS d^{-1}) and 20 ºC (0.55±0.04 g N g^{-1} VSS d^{-1}) are comparable with the sAOR achieved in other nitrifying granular reactors also operated with a similar control strategy at 20 ºC (0.63±0.05 g N g^{-1} VSS d^{-1}; Jemaat et al. (2013)) and 30 ºC (1.4±0.1 g N g^{-1} VSS d^{-1}; Bartrolí et al. (2010)), and much higher than the 0.03 g N g^{-1} VSS d^{-1} reported by Hu et al. (2013) in a one-stage anammox reactor at 12ºC. The influence of the temperature in the nitritation process can be fitted to an Arrhenius-type equation ($r_{nitT1} = r_{nitT2} \cdot \theta^{(T1-T2)}$), achieving a temperature coefficient of θ=1.13±0.03 which is in the range of the coefficients for nitrifying reactors in two-stage systems (Carrera et al., 2003).

The size of the nitrifying granules quickly increased from the initial 0.5 mm to more than 1.2 mm in only 45 days. After that, the particle size showed a decreasing trend to a stable size around 0.7 mm (Figure 5.2A). The biomass concentration progressively increased from 1.1 g VSS L^{-1} on day 77 to 2.1 g VSS L^{-1} on day 450 (Figure 5.2A). The settling velocity of the granules had a rather constant value at ca. 25±2 m h^{-1} at any of the temperatures tested.

On day 99 (at 15 ºC) a failure of the feeding pump left the reactor without feeding for 6h. Also on day 115, an electricity cut left the reactor with neither feeding nor pH control during 3h, but with the aeration and temperature control correctly working. Those days have been plotted with

a NLR of 0 g N L^{-1} d^{-1} (Figure 5.2B). In both cases, the DO concentration in the reactor increased to 8 mg O_2 L^{-1} for 1-2 h after the accident due to the decrease of the AOB activity once ammonium was consumed. Both the high oxygen concentration and the ammonium depletion enhanced the nitrate production during the accidental periods, consequently, 4.5 and 2.6 mg N-NO_3^- L^{-1} were measured on days 99 and 115, respectively. However, in all cases, the day after the restoring the operational conditions, the nitrite and nitrate concentrations in the reactor were very similar to those measured before the operational accident, indicating that the operational strategy of applying a low DO/TAN concentrations ratio to repress NOB activity was robust.

From day 250 onwards, the TAN control was switched from automatic to manual mode but the process remained stable. The slight oscillations in the TNN/TAN concentrations ratio around days 260 and 360 (Figure 5.2C) can be attributed to changes in the biomass concentration rather than control problems. The successful operation of the partial nitritation process with manual control at 12.5 ºC during more than 200 days demonstrated the high stability of this technology.

5.3.3 Microbial characterization of granules

Biomass samples from days 72 (20 ºC), 147 (15 ºC), 211 (12.5 ºC) and 391 (12.5 ºC) were analyzed using the FISH-CLSM technique to quantify the AOB, NOB and anammox biomass fractions at the different temperatures at which the reactor was operated. AOB was found to be the predominant microbial population at all temperatures with similar biomass fractions, around 70±8 %, in biomass samples from day 72, 147 and 211, while slightly increased to 81±12 % on day 391 (Table 5.2).

Table 5.2. Microbial fractions of AOB, NOB and anammox at the different temperatures tested, as determined by using the FISH technique. n/d=not detectable.

	20 ºC	**15 ºC**	**12.5 ºC**	
Day	72	147	211	391
AOB sp. (%)	74±11	67±13	72±8	81±12
***Nitrobacter* spp. (%)**	17±6	18±8	19±4	1±1
***Nitrospira* spp. (%)**	n/d	n/d	n/d	n/d
Anammox (%)	n/d	n/d	n/d	n/d

The NOB biomass fraction determined by FISH was relatively high and constant, around 18±8%, in biomass samples from day 72, 147 and 211 (Table 5.2) despite the NOB activity was effectively repressed. However, on day 391, NOB fraction decreased to 1±1, indicating that NOB were almost washed out from the nitrifying granules.

Therefore, the long term application of a low DO/TAN concentrations ratio at low temperatures tended to wash out NOB, similarly to what Bartrolí et al. (2010) observed at 30ºC in a similar nitrifying granular reactor, although this process was much slower at 12.5 ºC (more than 7 months, Table 5.2) than that at 30ºC (ca. one month, Bartrolí et al. (2010)).

The main NOB genus at all the temperatures was *Nitrobacter*, whereas *Nitrospira* was not detected through FISH (Table 5.2). *Nitrobacter* are r-strategist microorganisms and they have higher maximum growth rate and nitrite half-saturation constants than those of *Nitrospira* which are K-strategist microorganisms (Blackburne et al., 2007; Downing and Nerenberg, 2008). Hence, *Nitrobacter* are favored in environments with accumulation of nitrite in the bulk liquid (Kim and Kim, 2006; Schramm et al., 2000), such as that in the granular reactor of this study (nitrite concentration ca. 30±5 mg N L^{-1}). In contrast, *Nitrospira* are favored in nitrite limiting environments, such as those in one-stage partial nitritation-anammox reactors (de Clippeleir et al., 2013; Winkler et al., 2011b) or nitrifying reactors with low nitrite concentration in the bulk liquid (Regmi et al., 2014).

Finally, anammox could not be detected in any of the analyzed samples, neither in the sample on day 391, which was taken more than 12 months after the start-up of the nitrifying airlift reactor (Table 5.2).

5.3.4 Model-based assessment of NOB repression at low temperatures

As it was demonstrated in previous studies, the NOB repression in granular reactors is achieved due to the strong oxygen limitation, assured by the control strategy, in which a low DO/TAN concentrations ratio is maintained in the bulk liquid assuring an excess of ammonium in the biofilm (Bartrolí et al., 2010; Jemaat et al., 2013). Reasons behind the efficiency of this control strategy have been already discussed in depth in those publications (Bartrolí et al., 2010; Jemaat et al., 2013), as well as the fundamental aspects of how NOB repression is achieved in biofilm reactors (Brockmann and Morgenroth, 2010; Pérez et al., 2009). However, all those studies were carried out at temperatures above 20ºC and it is not clear if the same reasons are valid at the experimental conditions of this study, because at temperatures below 20ºC, the specific NOB growth rate is higher than that of AOB (Hunik et al., 1994). A mathematical model was used to confirm the NOB repression mechanism in granular reactors at low temperatures postulated in this study.

5.3.4.1 Model evaluation

The first 240 days of operation were used for model evaluation. This period was chosen since both, the biomass concentration and the granular size achieved stable values (Figure 5.2A). The

simulated effluent concentrations of TAN, TNN and nitrate were directly compared with those obtained in the experiments (Figure 5.3). The model predicted no nitrate accumulation for the three temperatures, as obtained experimentally. The second major output of the model is the NLR applied to the reactor, model predictions showed agreement with the experiments as shown in the direct comparison of experimental and predicted flow-rates (Figure 5.3).

Maintaining the same operating conditions at 12.5ºC in long term simulation (i.e. steady state) NOB were washed out from the reactor, in agreement with the experimental trend (see NOB biomass fraction at day 391 in Table 5.2).

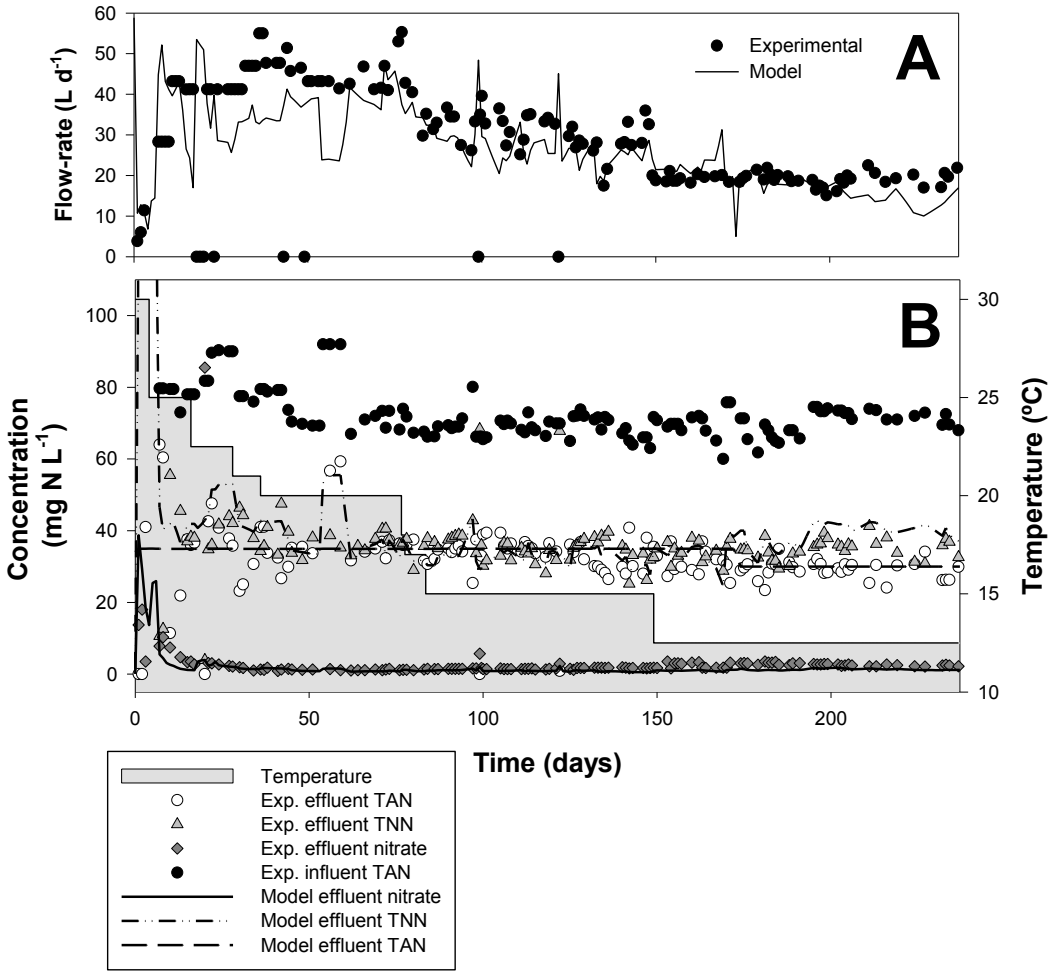

Figure 5.3. (A) Experimental and simulated flow-rate in the influent of the granular airlift reactor throughout the first 240 days. (B) Experimental and simulated nitrogen compounds concentrations throughout the first 240 days at the different temperatures tested.

5.3.4.2 Importance of the difference in oxygen affinity between AOB and NOB for effective NOB repression

When the oxygen affinity constants of NOB and AOB were assumed equal ($K_{O2,NOB}$ = $K_{O2,AOB}$= 0.74 mg N L^{-1}) the model predictions indicate that nitrate accumulates in the effluent because NOB repression is not efficient (Table 5.3). When a higher oxygen affinity is considered for NOB $K_{O2,NOB}$ < $K_{O2,AOB,}$ (0.16 and 0.74 mg N L^{-1}, respectively), even a higher nitrate concentration was found with the model (Table 5.3). The simulation results indicated that if AOB oxygen affinity is equal or lower than that of NOB, nitrite oxidizing activity is not effectively repressed despite applying low DO/TAN concentration ratios in the bulk liquid, and nitrate is produced. In both cases (for $K_{O2,AOB}$ = 0.74 and 0.16 mg N L^{-1}) for long term simulations (i.e. steady state) NOB are nor washed out from the reactor, contrary to what is observed experimentally (Table 1) and when using $K_{O2,NOB}$ > $K_{O2,AOB}$.

Table 5.3. Effluent concentration of N-species on day 237 as predicted by the model for different values of the NOB oxygen half-saturation coefficient ($K_{O2,NOB}$) at 12.5ºC. NOB repression is efficient only for $K_{O2,NOB}$ > $K_{O2,AOB}$.

	$K_{O2,NOB}$ (mg N L^{-1})	**TAN (mg N L^{-1})**	**TNN (mg N L^{-1})**	**Nitrate (mg N L^{-1})**
$K_{O2,NOB}$ > $K_{O2,AOB}$ (model evaluation)	1.75	30	37	1.1
$K_{O2,NOB}$ = $K_{O2,AOB}$	0.74	30	19	19
$K_{O2,NOB}$ < $K_{O2,AOB}$	0.16	30	11	28

Although it is generally accepted that NOB have lower oxygen affinity than AOB (Sin et al., 2008), Liu and Wang (2013) recently demonstrated that NOB can become better oxygen competitor than AOB under long term low DO conditions and as a result, nitrate is produced. Also, Regmi et al. (2014) found that the NOB population in their nitrifying reactor had a lower DO half-saturation constant than that of AOB and could compete with AOB for oxygen uptake at low DO concentrations. Interestingly, both studies found that the dominant NOB genus in their systems was *Nitrospira* instead of *Nitrobacter*.

Therefore, a scenario in which NOB have higher oxygen affinity than that of AOB is possible if the NOB population is enriched in *Nitrospira* instead of *Nitrobacter* (Liu and Wang, 2013; Regmi et al., 2014). Thus we hypothesize that a key aspect for achieving stable partial nitritation at temperatures below 20ºC could be to select a NOB population composed mainly by *Nitrobacter* instead of *Nitrospira*.

5.3.4.3 Importance of ammonium excess for effective NOB repression

As previously described, the control strategy applied in this study is based on maintaining a very low value of the DO/TAN concentrations ratio in the bulk liquid, thus assuring strong limiting conditions required to obtain the NOB repression in the granules. The importance of the oxygen affinity has been demonstrated in the previous section but also the importance of the ammonium excess in the bulk liquid was assessed with the model.

A new dynamic simulation was run as to switch from the usual $[TAN]_{SP}$=30 mg N L^{-1} to 10 mg N L^{-1} and the ammonium and DO concentration profiles in the biofilm were investigated at these two different ammonium setpoint values. When decreasing the $[TAN]_{SP}$ to 10 mg N L^{-1}, ammonium was still in excess (see Figure 5.4B), but the corresponding Monod term of the kinetics changed importantly (Figures 5.5A and 5.5B).

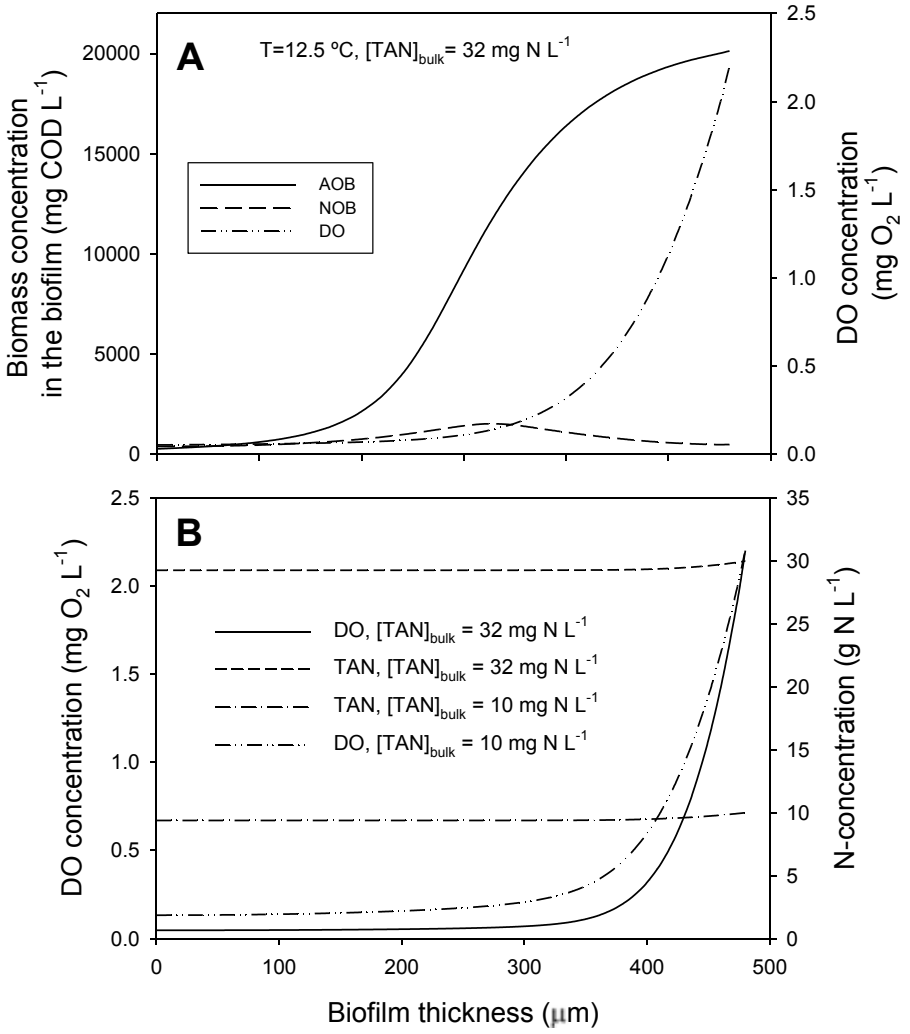

Figure 5.4. Results obtained with the model. (A) Simulated biomass and oxygen biofilm profiles in the granular sludge at 12.5 ºC, day 248 when NOB are repressed. (B) Simulated dissolved oxygen (DO) and total ammonia nitrogen (TAN) biofilm profiles in the granular sludge at 12.5ºC for a $[TAN]_{SP}$ of 32 and 10 mg N L^{-1}, corresponding to days 248, and 254 respectively in the dynamic simulation.

This was the major change since oxygen was kept constant in the bulk at 2.2 mg O_2 L^{-1}. At $[TAN]_{SP}$= 10 mg N L^{-1} the AOB specific growth rate in the biofilm was lower than that of NOB (see Figure 5.5D), reversing the previous trend found at $[TAN]_{SP}$=30 mg N L^{-1} (see Figure 5.5C). With the $[TAN]_{SP}$= 10 mg N L^{-1}, nitrate increased very fast in the reactor (in a period of only hours, see Figure 5.6), which would lead to a stable NOB development in the biofilm.

Therefore, despite partial nitritation can be achieved in granular reactors in oxygen limiting conditions when the AOB population has a higher affinity for DO than that of the NOB, a certain excess of ammonium in the bulk liquid is required to keep the specific AOB growth rate higher than that of NOB.

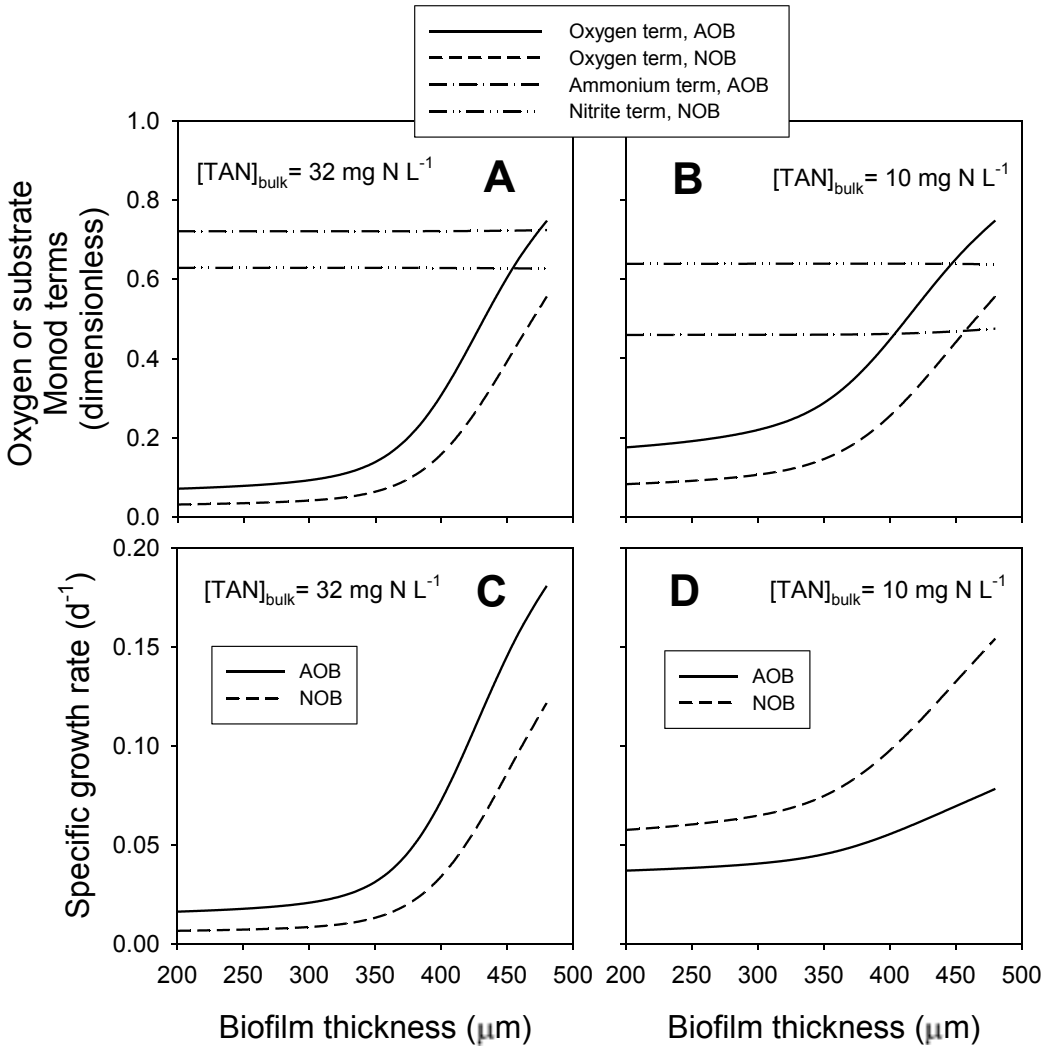

Figure 5.5. Results obtained with the model at 12.5ºC. Oxygen, ammonium and nitrite Monod terms in the granular sludge when maintaining the ammonium concentration in the bulk liquid at 32 mg N L-1 (A) and 10 mg N L-1 (B). Specific growth rate of AOB and NOB in the granular sludge at 32 mg N L-1 (C) and 10 mg N L-1 (D).

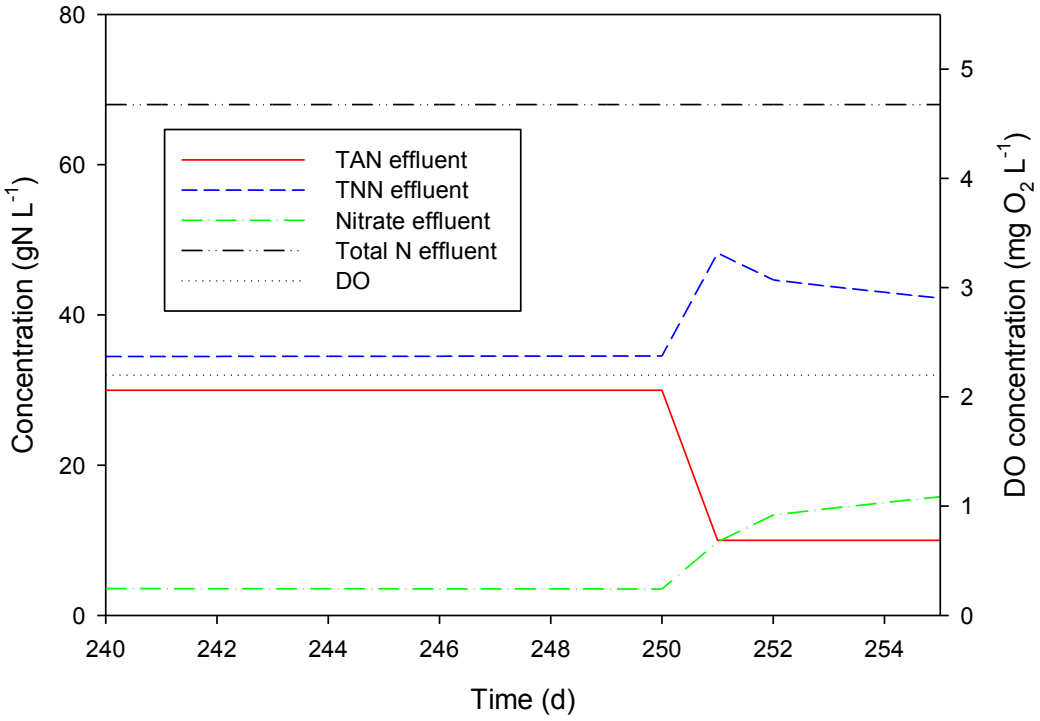

Figure 5.6. Simulations results obtained for a step down in the [TAN]SP from 30 to 10 mg N L-1 while DO was kept constant. Nitrate concentration increased very fast after the disturbance because NOB repression is not longer efficient.

5.3.5 Suitability of a two-stage autotrophic N-removal system for mainstream treatment

The strategy to split the N-removal in two different reactors has as main advantage that the anammox reactor can be operated anoxically, to avoid competition for nitrite by NOB, which is one of the main weak points of the use of an one-stage N-removal biofilm reactor to remove nitrogen in these conditions (de Clippeleir et al., 2013; Winkler et al., 2011b) (like genuinely proposed by Kartal et al. (2010)).

Additionally, since the effluent of the partial nitritation reactor should be fed to a subsequent anammox reactor, nitrite will be always in excess. This type of operation favors the selection of *Nitrobacter*-like bacteria (r-strategist) instead of *Nitrospira*-like bacteria (K-strategist), enhancing the stability of the partial nitritation process in granular reactors due to the lower oxygen affinity of *Nitrobacter* compared to that of *Nitrospira* (as discussed in section 5.3.4.2). Furthermore, the presence of *Nitrobacter* can inhibit the growth of *Nitrospira*, increasing the stability of partial nitritation (Ahn et al., 2011; Wagner et al., 2002).

The operation of anammox reactors treating pretreated municipal wastewater at temperatures below 20 ºC, as the one required in the two-stage N-removal system, has been previously demonstrated (Lotti et al., 2014). In that study, a NLR of 0.6 g N L^{-1} d^{-1} was achieved at 10 ºC using and upflow fluidized granular sludge reactor. Since the average NLR applied in our partial nitritation reactor at 12.5 ºC was 0.7±0.3 g N L^{-1} d^{-1} (Figure 5.2B), both processes could be easily integrated in series, in a two-stage autotrophic N-removal system.

5.4 Appendix

Table A5.1. Kinetic rate expressions

j	*Process*	*Process rate (d^{-1})*	*Reference*
1	Growth of X_{AOB}	$\mu_{\max,AOB} \cdot \frac{S_{O_2}}{K_{O_2,AOB} + S_{O_2}} \cdot \frac{S_{TAN}}{K_{S,TAN,AOB} + S_{TAN} + \frac{S_{TAN}^2}{K_{I,TAN,AOB}}} \cdot \frac{K_{I,TNN,AOB}}{K_{I,TNN,AOB} + S_{TNN}} \cdot X_{AOB}$	Jubany et al. (2008)
2	Decay of X_{AOB}	$b_{AER,AOB} \cdot \frac{S_{O_2}}{K_{O_2,AOB} + S_{O_2}} \cdot X_{AOB} + b_{ANAER,AOB} \cdot X_{AOB}$	Munz et al. (2011a)
3	Growth of X_{NOB}	$\mu_{\max,NOB} \cdot \frac{S_{O_2}}{K_{O_2,NOB} + S_{O_2}} \cdot \frac{S_{TNN}}{K_{S,TNN,NOB} + S_{TNN} + \frac{S_{TNN}^2}{K_{I,TNN,AOB}}} \cdot \frac{K_{I,TAN,NOB}}{K_{I,TAN,NOB} + S_{TAN}} \cdot X_{NOB}$	Jubany et al. (2008)
4	Decay of X_{NOB}	$b_{AER,NOB} \cdot \frac{S_{O_2}}{K_{O_2,NOB} + S_{O_2}} \cdot X_{NOB} + b_{ANAER,NOB} \cdot X_{NOB}$	Munz et al. (2011a)

Table A5.2. Stoichiometric Matrix

j	Process	S_{O2}	S_{TAN}	S_{TNN}	S_{NO3}	X_{AOB}	X_{NOB}	X_I
1	Growth of X_{AOB}	$-(3.43-Y_{AOB})/Y_{AOB}$	$-1/Y_{AOB}$	$1/Y_{AOB}$		1		
2	Decay of X_{AOB}					-1		1
3	Growth of X_{NOB}	$-(1.14-Y_{NOB})/Y_{NOB}$		$-1/Y_{NOB}$	$1/Y_{NOB}$		1	
4	Decay of X_{NOB}						-1	1
	Units	g O_2 m^{-3}	g N m^{-3}	g N m^{-3}	g N m^{-3}	g COD m^{-3}	g COD m^{-3}	g COD m^{-3}

Table A5.3. Kinetic parameters (12.5 ^{o}C and pH 8.0)

Symbol	Definition	Value	Unit	References
	Ammonia oxidizing bacteria (AOB)			
$\mu_{max,AOB}$	Maximum specific growth rate	0.36	d^{-1}	Jubany et al. (2008)
$b_{AER,AOB}$	Decay rate	0.11	d^{-1}	Munz et al. (2011)
$b_{ANAER,AOB}$	Anaerobic decay rate	0.005	d^{-1}	Munz et al. (2011)
Y_{AOB}	Growth yield	0.18	g COD g^{-1} N	Jubany et al. (2008)
$K_{O2,AOB}$	Affinity constant for oxygen	0.74	mg O_2 L^{-1}	Guisasola et al. (2005)
$K_{S,TAN}$	Affinity constant for TAN	11	mg TAN L^{-1}	Carrera et al. (2004)
	Nitrite-oxidizing bacteria (NOB)			
$\mu_{max,NOB}$	Maximum specific growth rate	0.47	d^{-1}	Jubany et al. (2008)
b_{NOB}	Decay rate	0.09	d^{-1}	Munz et al. (2011)
$b_{ANAER,NOB}$	Anaerobic decay rate	0.004	d^{-1}	Munz et al. (2011)
Y_{NOB}	Growth yield	0.08	g COD g^{-1} N	Jubany et al. (2008)
$K_{O2,NOB}$	Affinity constant for oxygen	1.75	mg O_2 L^{-1}	Guisasola et al. (2005)
$K_{S,TNN}$	Affinity constant for TNN	22	mg TNN L^{-1}	Ni et al. (2008a)

Table A5.4. Diffusivity coefficients

Parameter	Symbol	Value	Unit	References
Diffusivity of O_2 in water	D_{O2}	$2.2 \cdot 10^{-4}$	$m^2\ d^{-1}$	Picioreanu et al. (1997)
Diffusivity of NH_4^+ in water	D_{TAN}	$1.9 \cdot 10^{-4}$	$m^2\ d^{-1}$	Picioreanu et al. (1997)
Diffusivity of NO_2^- in water	D_{TNN}	$1.7 \cdot 10^{-4}$	$m^2\ d^{-1}$	Picioreanu et al. (1997)
Diffusivity of NO_3^- in water	D_{NO3}	$1.7 \cdot 10^{-4}$	$m^2\ d^{-1}$	Picioreanu et al. (1997)
Diffusivity of organic substrate in water	D_S	$1.0 \cdot 10^{-4}$	$m^2\ d^{-1}$	Picioreanu et al. (1997)
Diffusivity coefficient inside biofilm	E_{diff}	0.5	dimensionless	Assumed, in the range proposed by Bishop et al. (1995)

CHAPTER 6

MICROBIAL COMMUNITY SHIFTS ON AN ANAMMOX REACTOR AFTER A TEMPERATURE SHOCK USING 454-PYROSEQUENCING ANALYSIS

Part of this chapter is being prepared for publishing as:

Isanta, E., Bezerra, T., Suárez-Ojeda, M.E., Fernandez, I., Pérez, J., Carrera, J., 2013. Microbial community shifts on an anammox reactor after a temperature shock using 454-pyrosequencing analysis. *Bioresource Technol*.

6.1 Introduction

The anaerobic ammonium oxidation (anammox) is widely considered as the most economical and sustainable process for nitrogen removal from wastewater, due to its high nitrogen removal potential at reduced operating costs (Kartal et al., 2010; Lackner et al., 2014; Van Hulle et al., 2010). Compared to conventional nitrification-denitrification process, the anammox process does not require organic matter for nitrogen removal, and oxygen requirements are reduced since only ca. half ammonium needs to be oxidized into nitrite in a previous partial nitritation step (Lackner et al., 2014; Van Hulle et al., 2010).

The main disadvantage of the anammox process is, however, the very slow growth rate of the microbes responsible of this process, i.e. the "anammox bacteria". Due to this slow growth rate, anammox bacteria doubling times around 10-14 days have been typically reported at their optimum growth temperature, i.e. 35-40 ºC (Dosta et al., 2008; Strous et al., 1999). Also, anammox growth rate is reduced ca. 30-40% every 5 ºC of temperature decrease (Dosta et al., 2008; Strous et al., 1999). Perhaps for this reason, early anammox process implementations were generally at temperatures close to the optimum (Abma et al., 2010; Sliekers et al., 2003; van der Star et al., 2007; Wett, 2007), in order to minimize the slow growing characteristics of anammox bacteria. For some applications, anammox reactors are even heated to enhance the anammox growth, such as in some lab-scale rectors (Hu et al., 2013) or industrial reactors (Wett et al., 2013).

Although in natural environments, anammox growth has been reported to occur at temperatures as low as −2.5°C in sea ice (Rysgaard and Glud, 2004) and as high as 70°C in hot springs and hydrothermal vent areas (Byrne et al., 2009; Jaeschke et al., 2009), in wastewater treatment applications anammox growth is limited to a maximum temperature of 43ºC (Strous et al., 1999). In fact, Toh et al. (2002) could not cultivate thermophilic anammox biomass at 55ºC and Dosta et al. (2008) observed that the exposure of anammox biomass at a temperature of 45 ºC during a few hours resulted in a complete loss of activity and evidences of cell lysis (Dosta et al., 2008). Accordingly, temperature in anammox reactors should be carefully controlled bellow ca. 40ºC, especially in those reactors with temperature control using heaters (as abovementioned), or in reactors used for the treatment of industrial hot effluents (Lopez-Vazquez et al., 2014), to avoid the risk of overpassing the maximum permissible temperature of anammox bacteria which would lead to an anammox reactor failure. To the best of our knowledge, there is lack of information in the literature about the impact of a temperature shock over the performance of an anammox reactor.

Changes in environmental conditions, such as a temperature shock, have a direct impact in microbial communities. The study of these microbial communities and their changes provides valuable information to better understand the nutrient removal processes occurring in wastewater treatment ecosystems. Different molecular biology techniques, such as fluorescence in-situ hybridization (FISH) (Lotti et al., 2014), denaturing gradient gel electrophoresis (DGGE) (Park et al., 2010) or clone library (Hu et al., 2010) have been widely used for this purpose. Recently, the second generation of 454-pyrosequencing has been developed. This technique offers a high-throughput, fast and economical sequencing platform, with exceptional accuracy (Droege and Hill, 2008). With 454-pyrosequencing, thousands of operational taxonomic units (OTUs) can be identified in a reasonable period of time. Therefore, this technique can provide wider and more complete information about microbial community structures than previous conventional molecular biology techniques. For these reasons, 454-pyrosequencing has gained interest in the study of complex microbial communities such as those of wastewater treatment environments (Hu et al., 2012; Ma et al., 2012; Xie et al., 2013; Ye et al., 2011). Despite the potential of 454-pyrosequencing, the use of this novel technique with anammox reactors is still scarce (Costa et al., 2014; Pereira et al., 2014).

Hence, we present the performance of an anammox reactor before and after the occurrence of a high temperature shock (i.e. up to 46 ºC) which lasted for 8 days. The research was focused on exploring the microbial community structure changes during the N-removal recovery process of the anammox reactor. With that purpose, 454-pyrosequencing technique was used.

6.2 Materials and methods

6.2.1 Experimental set-up description

The anammox process was carried out in a sequencing batch reactor (SBR) with a working volume of 10 L, a diameter of 20 cm and a height of 61 cm. The SBR was operated in cycles of 6 h, divided in four phases: mixed filling (300 min), mixing (30 min), settling (20 min) and effluent withdrawal (10 min). The volumetric exchange ratio was of 25%. Biomass was mixed using a mechanical stirrer operated at rotating speed of 72 rpm. Nitrogen gas was flushed into the headspace at an average flow rate of 300 mL min^{-1}. The pH was not controlled but ranged between 7.5 – 8.5 during one cycle. The temperature before and after the temperature shock was maintained constant at 35 ºC.

The reactor was fed with a mineral medium containing (mg L^{-1}): $KHCO_3$ (100); H_2PO_4 (50); $CaCl_2 \cdot 2H_2O$ (100); $MgSO_4 \cdot 7H_2O$ (200); $FeSO_4$ (6.3); EDTA (6.3) and 1.25 mL L^{-1} of a trace elements

solution (van de Graaf et al., 1996). The required amounts of nitrite and ammonium in the form of $NaNO_2$ and $(NH_4)_2SO_4$ were added to this mineral medium (as specified in the Results and Discussion section, Figure 6.1).

The SBR was operated for more than 700 days previously to the temperature shock with nitrogen loading rate (NLR) ranging from 0.20 – 0.55 g N L^{-1} d^{-1}. The biomass had an average SAA of 0.40±0.05 g N g^{-1} VSS d^{-1}.

The temperatures shock lasted from days -8 to 0 and consisted in an increase of the temperature in the anammox SBR to 46ºC.

6.2.2 Analytical methods

Ammonium was measured by means of an ammonium analyzer (AMTAX, Hach Lange, Germany). Nitrate and nitrite concentrations were analyzed with ionic chromatography using an ICS-2000 Integrated Reagent-Free IC system (DIONEX Corporation, USA) which performs ion analyses using suppressed conductivity detection. Mixed liquor total suspended solids (TSS), mixed liquor volatile suspended solids (VSS) were measured according to Standard Methods (APHA, 2008).

Specific Anammox Activity (SAA) was determined in batch assays, measuring the overpressure produced by di-nitrogen gas production of anammox bacteria (adapted from Dapena-Mora et al. 2007).

Nitrifying activity was determined in an aerobic batch assay, measuring the ammonium, nitrite and nitrate concentration over time. DO concentration, pH and temperature were maintained in this assay at 0.5-1.0 mg O_2 L^{-1}, 7.5 ± 0.1 and 34 ± 1 ºC, respectively.

6.2.3 Granular sludge morphology

The Anammox granules for scanning electron microscope (SEM) observation were washed three times with water to remove impurities. For fixation, cells were immersed in 2.5% (vol/vol) glutaraldehyde (pH 7.4) for 2 h. The samples were then processed according to conventional electron microscopy methods as described in (Julián et al., 2010). Anammox granules were observed with an S-570 scanning electron microscope (Hitachi Ltd., Japan) at an accelerating voltage of 30 kV.

6.2.4 Microbial diversity analysis

6.2.4.1 DNA Isolation

DNA was extracted from samples using the MoBio PowerBiofilm™ DNA Isolation Kit (MoBio Laboratories, USA), following the manufacturer protocol, with the exception of solution BF3,

that was added to 200 mL instead of the 100 mL recommended by the manufacturer. The quality and quantity of extracted DNA were measured by using a NanoDrop 1000 Spectrophotometer (Thermo Fisher Scientific, USA). All DNA samples were adjusted to 25 ng mL^{-1} for tagged pyrosequencing.

6.2.4.2 Bacteria and anammox specific pyrosequencing for 16S rRNA

Purified community DNA samples were submitted to the Research and Testing Laboratory (Lubbock, TX, USA) for Bacterial Tag-Encoded FLX-Titanium Amplicon Pyrosequencing (bTEFAP) and data processing. Samples were amplified for pyrosequencing using a forward and reverse fusion primer. The forward primer was constructed with (5'-3') the Roche A linker (CCATCTCATCCCTGCGTGTCTCCGACTCAG), an 8bp barcode and the appropriated forward primer selected for bacteria diversity assay (530F: GTGCCAGCMGCNGCGG) or for anammox specific diversity assay (Amx368F: TTCGCAATGCCCGAAAGG; (Cornish Shartau et al., 2010). The reverse fusion primer was constructed with (5'-3') a biotin molecule, the Roche B linker (CCTATCCCCTGTGTGCCTTGGCAGTCTCAG), and the proper reverse primer for bacteria diversity assay (1100R: GGGTTNCGNTCGTTR) or for anammox specific diversity assay (Amx820R: AAAACCCCTCTACTTAGTGCCC; Cornish Shartau et al. (2010)). Amplifications were performed in 25 µl reactions with Qiagen HotStar Taq master mix (Qiagen Inc, Valencia, California), 1µl of each 5µM primer, and 1µl of template. Reactions were performed on ABI Veriti thermocyclers (Applied Biosytems, Carlsbad, California) under the following thermal profile: 95ºC for 5 min, then 35 cycles of 94ºC for 30 sec, 54ºC for 40 sec, 72ºC for 1 min, followed by one cycle of 72ºC for 10 min and 4ºC hold.

Amplification products were visualized with eGels (Life Technologies, Grand Island, New York). Products were then pooled equimolar and each pool was cleaned with Diffinity RapidTip (Diffinity Genomics, West Henrietta, New York), and size selected using Agencourt AMPure XP (BeckmanCoulter, Indianapolis, Indiana) following Roche 454 protocols (454 Life Sciences, Branford, Connecticut). Size selected pools were then quantified and 150 ng of DNA were hybridized to Dynabeads M-270 (Life Technologies) to create single stranded DNA following Roche 454 protocols (454 Life Sciences). Single stranded DNA was diluted and used in emPCR reactions, which were performed and subsequently enriched. Sequencing following established manufacture protocols (454 Life Sciences, Branford, Connecticut).

6.2.4.3 Biodiversity analysis and phylogenetic classification

Quality of data obtained from sequencing was evaluated and denoised and chimeras were removed from the data set at Research and Testing Laboratory. USEARCH was used for

dereplication, clustering (4% divergence) and consensus sequence generation and poor reads were then eliminated (Edgar, 2010). For general bacteria diversity analysis, reads shorter than 250 bps and larger than 673 bps were trimmed. The same was done for Anammox specific diversity analysis but for reads shorter than 274 bps and larger than 675 bps. Chimera detection and removal was performed by executing UCHIME (Edgar et al., 2011) in *de novo* mode on the clustered data. In order to determine the identity of each remaining sequence, the sequences must first be quality checked and then clustered into Operational Taxonomic Units using the UPARSE algorithm (Edgar, 2013). Each OTU is then identified using the USEARCH global alignment algorithm (Edgar, 2010) and a database of high quality sequences derived from NCBI maintained by Research and Testing Laboratory.

For each OTU, the top six matches from the high quality database were kept and confidence values were assigned to each taxonomic level by taking the number of taxonomic matches that agree with the best match at that level and dividing that by the number of high quality sequence matches that were found. Each OTU was then assigned taxonomic information using the lowest common taxonomic level whose confidence value was above 51%. OTUs that received no matches against the high quality sequences are identified as “no hit” After resolving the number of sequences per OTU, the percentage of each organism was individually calculated for each sample. Data obtained provided relative abundance information within and among individual samples. Relative abundances of reads were calculated by taxonomic level for each library. Values represent the percentage of reads of sequences obtained at each taxonomic identity (according to the degree that of similarity described above) within the total set of readings from the library.

Indices of biological diversity were calculated for both libraries (Table 6.1 and Figure A6.1-A6.3 in the Appendix of this chapter) indicating both libraries were comparable in terms of abundance percentages and that good coverage of diversity was reached.

6.2.4.4 Anammox doubling time estimation

An indirect estimation of the doubling time of the anammox biomass in the SBR was calculated from the variation rate of the nitrogen removal rate (NRR) (Park et al., 2010; van der Star et al., 2007). The variation rate of the NRR (μ_{NRR}) was determined with the least-squares method from the logarithm of NRR with respect to time:

$$\ln NRR_i = \ln NRR_0 + \mu_{NRR} \cdot t \qquad \text{Eq. (6.1)}$$

Where NRR_0 and NRR_i are the initial NRR and at time = t (d), respectively

Then, the doubling time was calculated as:

doubling time = $\ln(2)/\mu_{NRR}$ Eq. (6.2)

6.3 Results and discussion

6.3.1 Nitrogen removal recovery after the temperature shock

During the temperature shock (days -8 to 0 in Figure 6.1), a progressive accumulation of ammonium and nitrite was observed in the reactor. Simultaneously, the NRR decreased from 0.250 to 0.023 g N L^{-1} d^{-1}. The color of the supernatant at the end of the temperature shock (day 0) presented a slight orange color (data not shown), suggesting the lysis of anammox cells. On day 7, a SAA test was performed, but not measurable activity was obtained (Table 6.2). Similar results were found by Dosta et al. (2008) when, after performing two consecutive SAA tests at 45 ºC to an anammox culture, almost no activity was measured and the supernatant presented an slight orange color. These authors suggested that this orange color could be due to the release of cytochrome c after the lysis of anammox cells due to the temperature shock.

Table 2. Anammox activity of the biomass before and after the temperature shock event

	Day 7	Day 55	Day 166
NRR (g N L^{-1} d^{-1})	0	0.166	0.383
SAA (g N g^{-1} VSS d^{-1})	0*	0.150±0.005	0.381±0.040

*Below detection limit of the method

To enhance the anammox activity recovery, the ammonium and nitrite influent concentrations were decreased to minimize any substrate inhibition of the anammox bacteria (Jin et al., 2012). From day 7 onwards, a progressive increase of the NRR was observed in the reactor. As depicted in Figure 6.2, from days 0 to 22 the ratio of nitrate production to ammonium consumption showed higher values than the 0.26 g $N\text{-}NO_3^-$ g^{-1} $N\text{-}NH_4^+$ expected according to anammox stoichiometry (van de Graaf et al., 1996). However, from day 22 onwards the nitrate to ammonium stoichiometric ratio stabilized on 0.25±0.05 g $N\text{-}NO_3^-$ g^{-1} $N\text{-}NH_4^+$. The average nitrite to ammonium ratio was stable at 1.3±0.1 g $N\text{-}NO_2^-$ g^{-1} $N\text{-}NH_4^+$ during all the experimental period, including the temperature shock (Figure 6.2).

On day 40, nitrite effluent concentration was lower than 3 mg $N\text{-}NO_2$ L^{-1}, and NRR did not vary from days 32 to 40 (see Figure 6.1), which suggested that anammox growth rate was limited by low substrate concentration. Accordingly, the ammonium and nitrite influent concentrations were progressively increased, which allowed the NRR increase to 0.25 g N L^{-1} d^{-1} on day 70. This

NRR was similar to the obtained just before the temperature shock. Also on day 70, the SAA of the anammox granules was of 0.15 g N g^{-1} VSS d^{-1}. This SAA was lower than the average 0.40±0.05 g N g^{-1} VSS d^{-1} measured before the temperature shock. Similar SAA values to that obtained previous to the temperature shock (i.e. 0.38±0.04 g N g^{-1} VSS d^{-1}) could not be measured until day 166

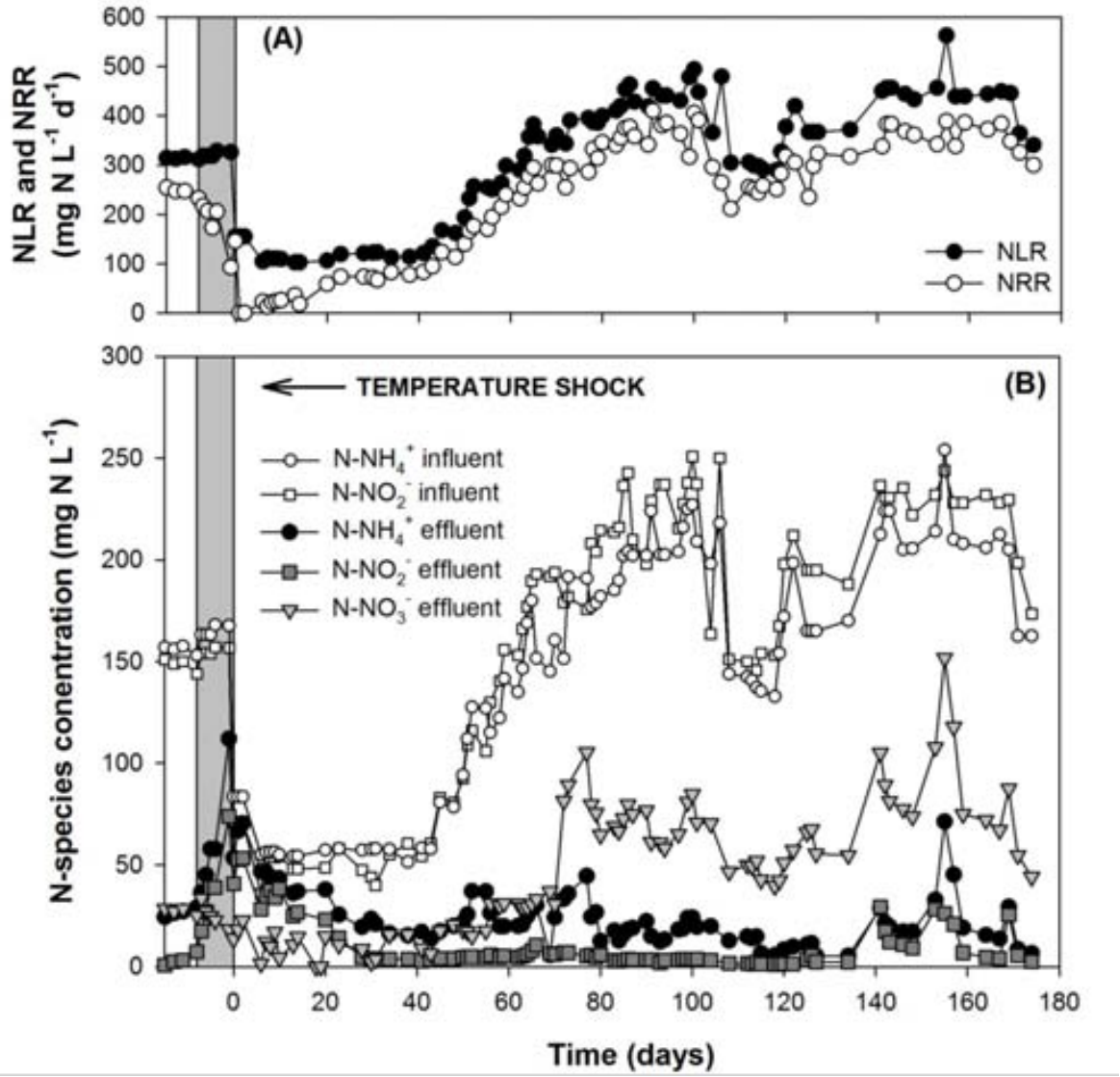

Figure 6.1. Time course of nitrogen removal performance measured in the anammox reactor before and after the temperature shock event (highlighted with a gray band). (A) nitrogen loading and removal rate; (B) influent and effluent ammonium, nitrite and nitrate concentration.

The doubling time of anammox biomass was calculated from NRR growth rate data. Two different doubling times could be calculated until day 70 (Figure 6.3). From days 10 to 38, the doubling time was 10.4 days (Figure 6.3), which is in the range of the 10 – 14 days of average

duplication time of anammox cells at 35ºC, as typically reported in the literature (Strous et al., 1999). In contrast, form day 31 to 70 the doubling time was 17.2 days, which is higher than that expected at 35ºC. Probably, on that second period the growth rate was slightly limited by substrate concentrations, since from day 31 onwards the effluent nitrite concentration was most of the time around 2-5 mg $N\text{-}NO_2^-$ L^{-1} (see Fig 6.4) .

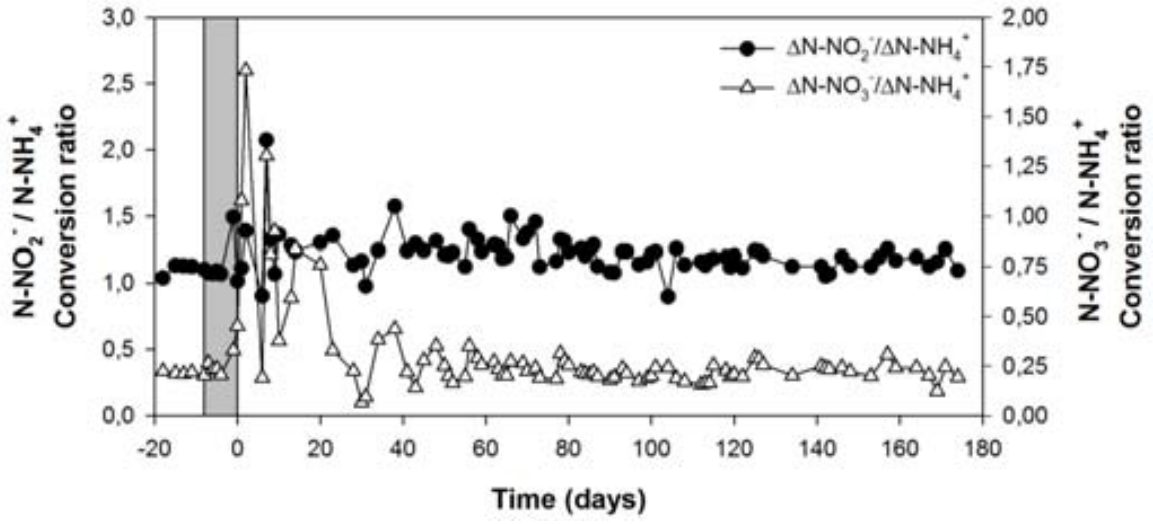

Figure 6.2. Time course of nitrite to ammonium and nitrate to ammonium conversion ratios in the anammox reactor calculated form effluent N-species concentration. The temperature shock event is highlighted with a gray band.

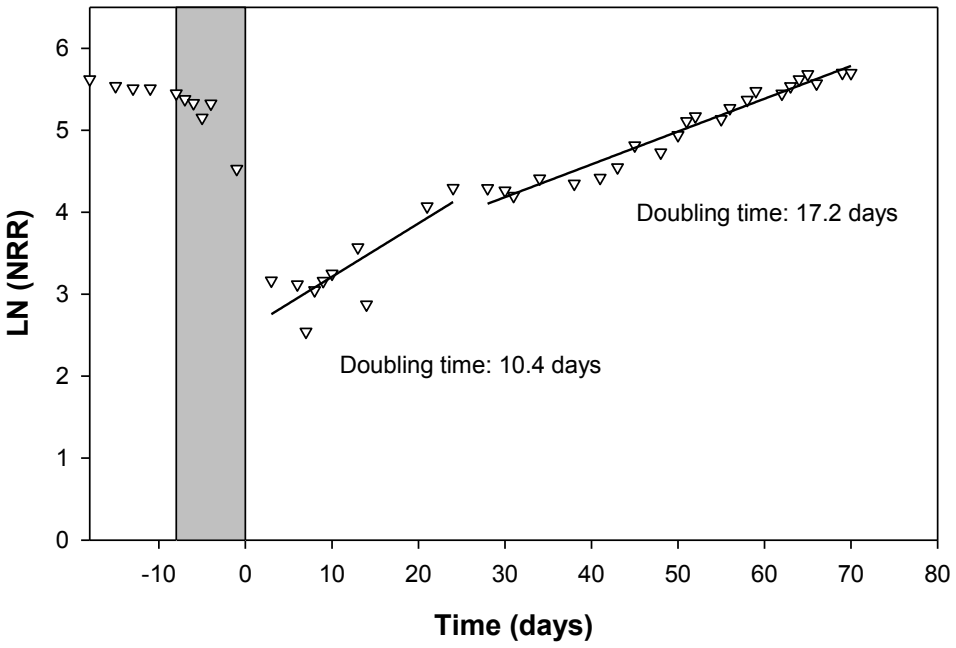

Figure 6.3. Indirect estimation of the anammox biomass average doubling time from nitrogen removal rate data.

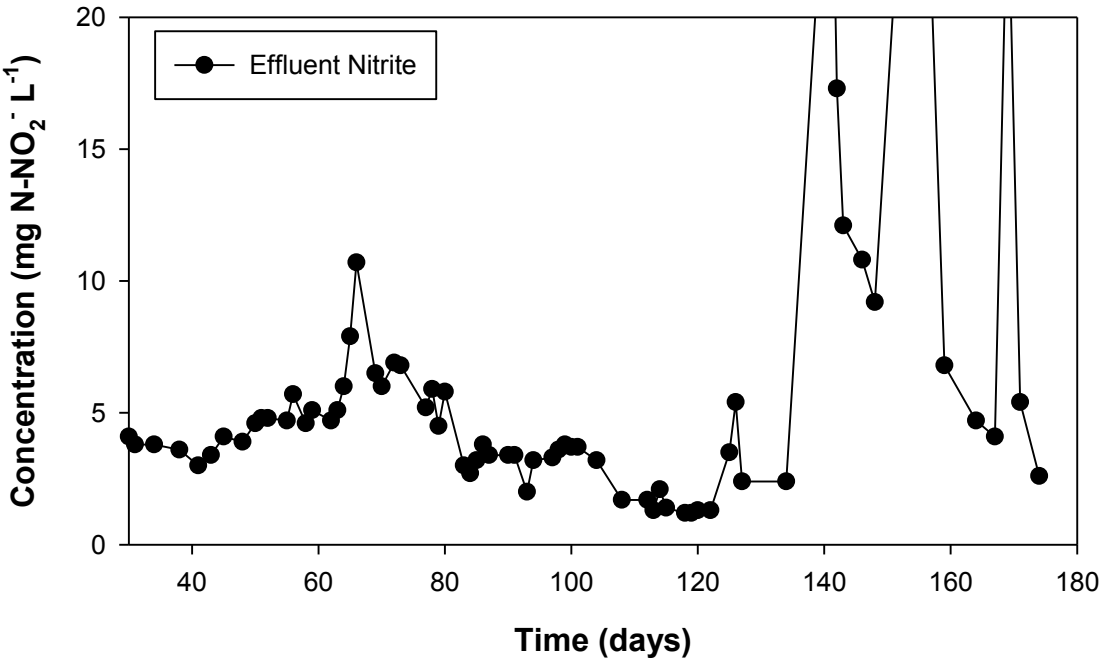

Figure 6.4. Effluent nitrite concentration from day 30 onwards

6.3.2 SEM images

The morphological differences between the anammox granules on days 13 and 42 after the temperature shock were inspected with SEM. Granules on day 13 presented a moderately rough surface (Figure 6.5A). When granules were inspected at a higher magnification, a consortium of rod, coccus and filamentous bacteria seemed to be growing over an apparently inert substratum (Figure 6.5C) without any colony structure.

For granules taken on day 42, a much rougher surface could be observed compared with granules from day 13 (Figure 6.5B). At a higher magnification, the bacteria in the image seemed to grow in colonies and the inert substratum was not observed (Figure 6.5D). It seems like the temperature shock killed most cells from the granule and then, new cells were growing in colonies over the structure of the old granule.

The small rounded cells could presumably be anammox cells, since they are typically visualized under the microscope as small coccoid cells with a diameter of about 0.8 µm (Kartal et al., 2013). If this is the case, the number of anammox cells in the picture taken on day 42 (Figure 6.5D) seemed to be greater than that in picture from day 13 (Figure 6.5C).

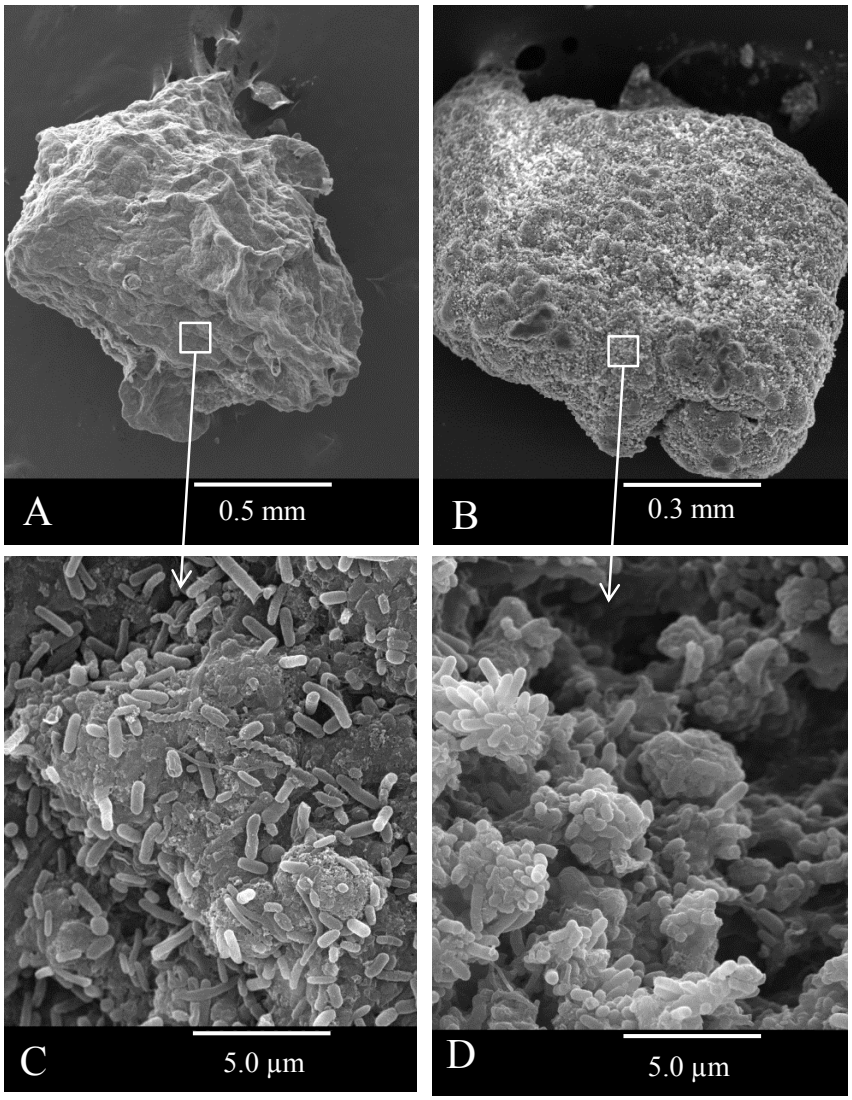

Figure 6.5. SEM images of the anammox granules on days 14 and 50 after the temperature shock.

6.3.3 Effect of temperature shock over microbial community diversity

6.3.3.1 Microbial diversity in anammox granules using 530F-1100R primers

The microbial community structure in the anammox reactor after the temperature shock was analyzed through the bTEFAP approach using the primers 530F-1100R. Three amplicon libraries, namely AMX_13, AMX_45 and AMX_166, were constructed with biomass samples obtained 13, 45 and 166 days after the temperature shock, respectively. A total of 17770 (AMX_13), 12568 (AMX_ 45) and 20940 (AMX_166) sequence reads were obtained. After quality analysis and removal of low quality sequences, 43964 sequences were annotated, corresponding to 14725 high-quality V4-V6 tags of the 16S rRNA-gene in library AMX_13, to 11200 in library AMX_45 and

to 18039 in AMX_166, with average lengths of 419, 411 and 504 bp per sequence, respectively. Later, unique OTUs were clustered in taxa and finally, 66 (AMX_13), 51 (AMX_45) and 24 (AMX_166) genera were estimated. Species similarities were found for a total of 1793 (AMX_13), 1297 (AMX_45) and 548 (AMX_166) clusters. Table A6.1 in the appendix of this chapter shows the complete results of relative abundance of bacteria at genus level obtained with pyrosequencing for AMX_13, AMX_45 and AMX_166.

Chao1, Shannon and E indexes estimated at 97% of similarity for the three biomass samples (see Table 6.1) showed a progressive diminution of microbial diversity as the reactor progressively recovered the anammox activity after the temperatures shock, since the values of these indexes in AMX_13 were higher than that of AMX_45, and much higher than in AMX_166. These results suggest that the temperature shock increased the microbial diversity in the reactor. Such increase of diversity of bacteria just after the temperature shock was reasonable, since many opportunistic bacteria could grow on lysis products from died cells during the temperature shock.

Table 6.1.Indexes of richness Chao1, diversity Shannon (H') and E of Eubacteria at 97% of similitude for libraries AMX_13, AMX_45 and AMX_166 and day at which biomass samples were obtained after the temperature shock.

Library	Day	Number of reads	Chao1	Shannon (H')	E
AMX_13	13	14725	2388	6.38	0.85
AMX_45	45	11200	1807	5.84	0.82
AMX_166	166	18039	630	3.56	0.56

In AMX_13 library, corresponding to the reactor just after the temperature shock, β-Proteobacteria was the most abundant group at class level with 14% of total sequences while Planctomycetia was only 7%, indicating a low anammox abundance (Figure 6.6). Other classes, such as Actinobacteria (7%), δ-Proteobacteria (6%) or Clostridia (4%), presented significant abundances showing a high microbial diversity after the temperature shock. As known, Planctomycetia class contains all known anammox bacteria, while β-proteobacteria class contains several groups of nitrifying, denitrifying and other N-cycle related microorganisms, among many others.

At genus level, any predominant group was observed, and a very diverse number of genera presented relative abundances between 1-7% (Figure 6.7). Many of these genera, (i.e. *Pelobacter, Zooglea, Eubacterium, Chlorflexus* or *Clostridium*, among others), contained bacteria capable of performing anaerobic metabolism, which could presumably degrade organic products

from cell lysis that took place during the temperature shock. Anammox bacteria genera *Brocadia* and *Candidatus Kuenenia* only had a 3% of abundance each (Figure 6.7). Two strictly aerobic genera, *Nitrospira* and *Derxia* had significant abundances, 4% and 7% respectively (Figure 6.7) in spite of the anoxic conditions of the reactor.

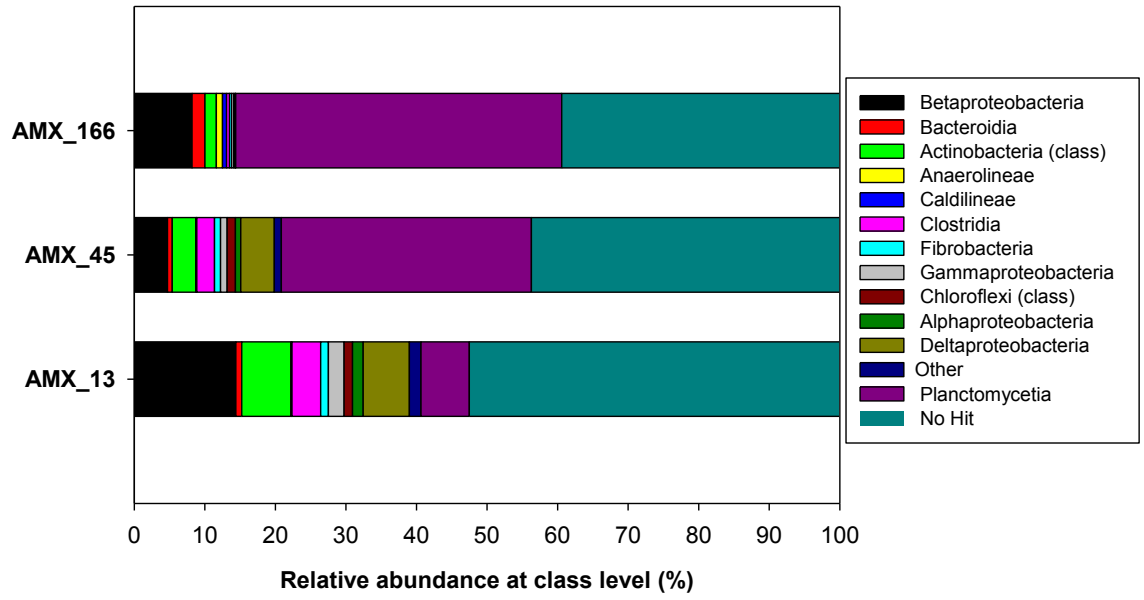

Figure 6.6. Microbial diversity at class level of libraries AMX_13, AMX_45 and AMX_166 obtained using primers 530F-1100F. Relative abundance is defined as the number of sequences affiliated with that taxon divided by the total number of sequences per sample (%). Classes making up less than 1% are defined as "Others".

In AMX_45, a similar community structure than that in AMX_13 was observed at both class and genus levels, with two main differences (Figures 6.6 and 6.7). On one side, the Planctomycetacia class increased its abundance from 7% on AMX_13 to 35% in AMX_45 (Figure 6.6). In fact, *Brocadia* genus represented 33% overall reads, indicating a clear anammox bacteria recovery from days 13 to 45 (Figure 6.7). On the other side, at both class and genus level, most of all the other groups presented lower abundances in AMX_45 than those observed in AMX_13 (Figures 6.6 and 6.7). The only non-anammox genus whose abundance increased from AMX_13 to AMX_45 was *Anaeromyxobacter* (2% overall reads in AMX_45), a group of anaerobic bacteria (Figure 6.7).

In AMX_166 library, corresponding to the fully recovered reactor, Planctomycetia was clearly the most abundant class, accounting for 46% of total reads, followed by β-proteobacteria with 9% of total reads (Figure 6.6). The clear the predominance of Planctomycetia class in AMX_166 suggested that the reactor was enriched in anammox bacteria (Figure 6.6).

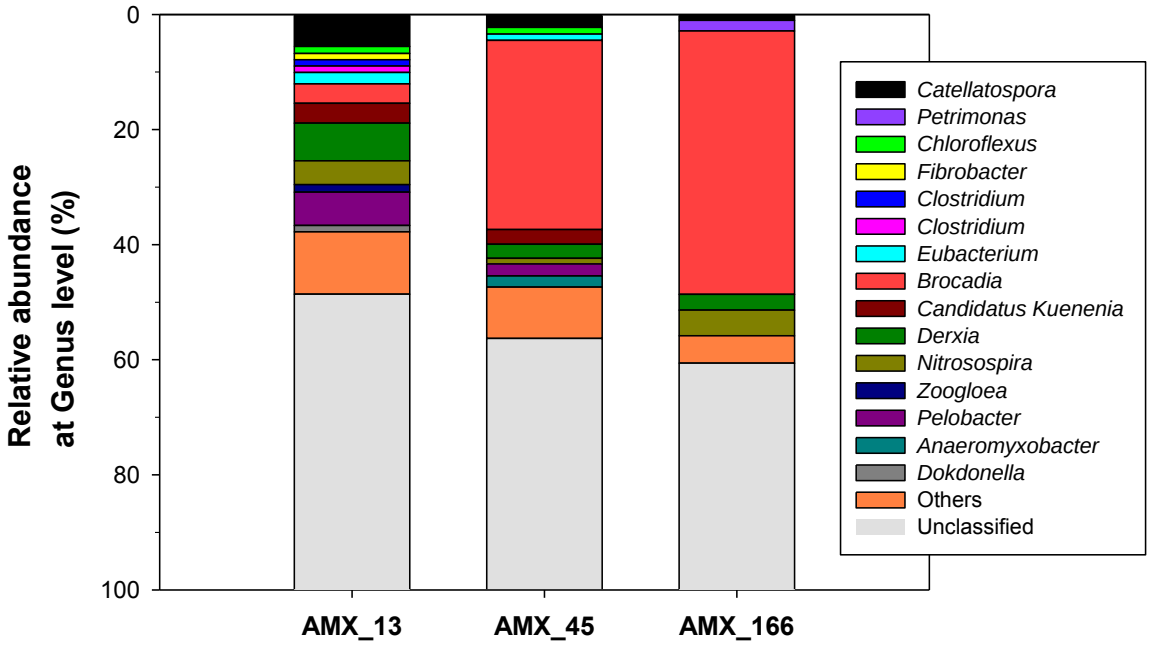

Figure 6.7. Microbial diversity at genus level of libraries AMX_13, AMX_45 and AMX_166 obtained using primers 530F-1100F. Relative abundance is defined as the number of sequences affiliated with that taxon divided by the total number of sequences per sample (%). Genera making up less than 1% are defined as "Others".

As shown in Figure 6.7, results at genus level confirmed the enrichment of the reactor in anammox biomass, since 99% of reads within Planctomycetia class corresponded to *Brocadia*, while the other 1% corresponded to *Candidatus Kuenenia*, both, two known anammox genera. Accordingly, 46% of total reads where identified as anammox bacteria. Apart from *Brocadia*, only genera *Nitrosospira* (4%) and *Derxia* (3%) and *Petrimonas* (2%), presented abundance above 1% of total sequences (Figure 6.6). *Nitrosospira* genus are ammonium-oxidising bacteria (AOB), while *Derxia* genus contains N-fixing microorganisms. Both, *Nitrosospira* and *Derxia* are strictly aerobic bacteria. *Petrimonas* genus are anaerobic fermentative bacteria.

Total AOB in AMX_166 accounted 6% of total sequences (as the sum of *Nitrosospira*, *Nitrosomonas* and *Nitrococcus* genera). However, the ammonium to nitrite stoichiometric ratios measured in the reactor (see Figure 6.2) were quite similar to those typically reported in the literatures for anammox reactors (Strous et al., 1998; van der Star et al., 2007), suggesting that AOB in the anammox granules were not very active. The AOB activity of the granular biomass from the anammox reactor was checked with a batch assay performed on day 160. During first 24h, a nitrite formation rate of 0.9 ± 0.4 mg N L^{-1} d^{-1} was measured while nitrate formation was not detected. The batch assay was left 24 additional hours and the AOB activity increased in the

range of one order of magnitude, to 10 ± 2 mg N L^{-1} d^{-1} while nitrite-oxidizing bacteria (NOB) activity remained undetected. These results confirmed, on one side, that AOB were present in the reactor with a very low activity whereas NOB were not present. But on the other side, the AOB activity test suggested that AOB could be rapidly reactivated if enough oxygen is supplied. The DO sources that allowed the growth of aerobic bacteria in the anammox reactor were the DO in the feeding (ca. 3-4 mg O_2 L^{-1}) and air entering the reactor during discharge phases. Probably, the N_2 flushed into the anammox reactor (ca. 0.3 L min^{-1}) was not enough to totally displace the oxygen entering the head-space volume of the reactor (10 L), preventing to maintain fully anaerobic conditions. In fact, an average and relatively constant DO concentration of 0.4 mg O_2 L^{-1} was measured during two different SBR cycles on days 150 and 160 using a DO probe (WTW, Germany) mounted on one of the free ports of the reactor. Despite oxygen presence, AOB activity did not probably go further in the reactor, unlike in the batch assay, due to strong external boundary layer resistance caused by the low stirring speed (72 rpm) in the anammox reactor. The presence of AOB in an anoxic anammox reactor has been reported previously (Kindaichi et al., 2007). These authors suggested that AOB could remain due to the ability of some AOB of reducing nitrite to N_2O or NO gases under oxygen-limiting conditions.

6.3.3.2 Anammox diversity in biomass samples using Amx368F-Amx820R

As shown in Figure 6.7, total anammox bacteria accounted for 7%, 35% and 46% of total sequences in libraries AMX_13, AMX_45 and AMX_166, respectively, indicating that the biomass in the reactor progressively enriched in anammox bacteria as the reactor recovered the N-removal capacity after temperature shock. These results were consistent with the N-removal capacity observed in the reactor, and with SAA measured in the anammox granules (Table 6.2).

An anammox-specific primer (Amx368F-Amx820R) was used to more precisely determine the anammox community in the biomass samples. Relative abundances at species level are shown in Figure 6.7. Sequence reads from the three biomass samples could be classified into 5 groups: *Brocadia anammoxidans, Brocadia fulgida, Brocadia sp., Candidatus Kuenenia sp.* and unclassified. As shown in Figure 6.6, *B. anammoxidans* was clearly identified as the most abundant anammox specie in the fully recovered reactor sample with 95% of total reads (Figure 6.8, AMX_166), as well as in AMX_45 library, with 93% of total reads (Figure 6.8, AMX_45). In contrast, in AMX_13 library, just after the temperature shock, *Ca. Kuenania sp*. was the most abundant specie (61%), while *B. anammoxidans* accounted for 32% of total sequences (Figure 6.8, AMX_13). Other 6% of sequences were classified as *B. fulgida* in AMX_13.

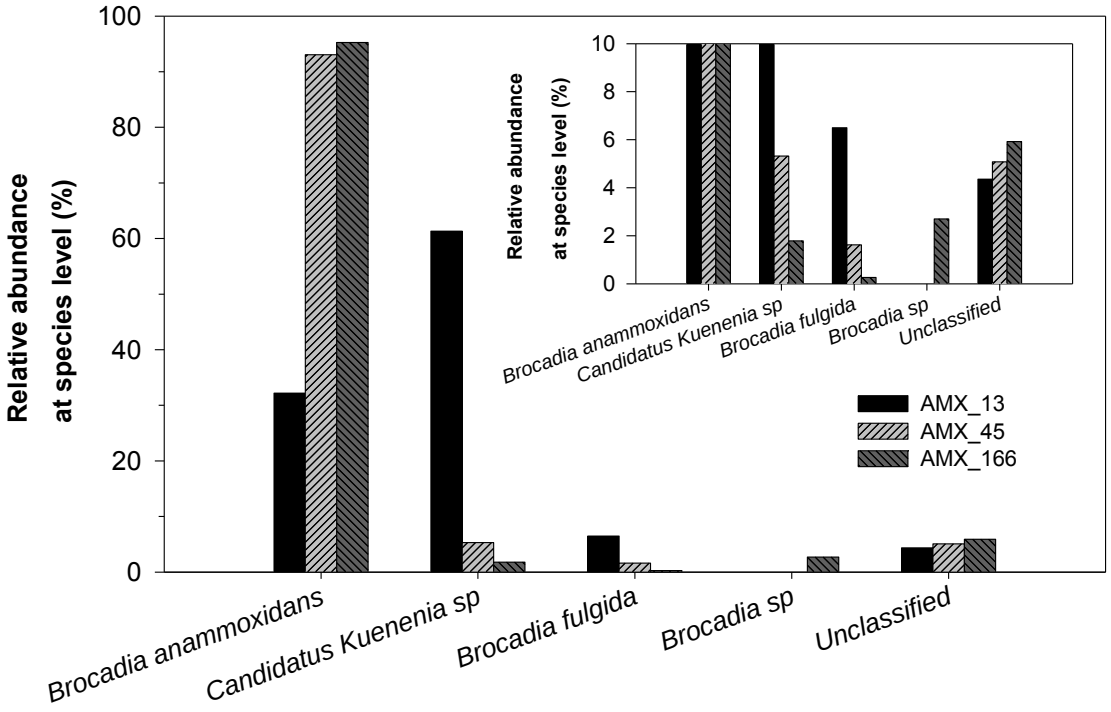

Figure 6.8. Relative abundance of anammox species for libraries AMX_13, AMX_45 and AMX_166 obtained using Amx368F-Amx820R specific primer. Relative abundance is defined as the number of sequences affiliated with that taxon divided by the total number of sequences per sample (%).

The niche differentiation between *Brocadia* and *Candidatus Kuenenia* genera is still not clear. According to several studies, the genus *Brocadia* would presumabily be an r-strategist (i.e., better growth rate but lower substrate affinity) (Oshiki et al., 2011; Puyol et al., 2013), while the genus *Candidatus Kuenenia* could be a K-strategist (i.e., lower growth rate but better substrate affinity) (van der Star et al., 2008). In this study, ammonium was clearly in excess during all the reactor operation. Nitrite was also not completely consumed during all the reactor operation (around 4.0±1.9 mg $N\text{-}NO_2$ L^{-1} from days 40 to 140, and higher than 4.0 mg $N\text{-}NO_2$ L^{-1} from day 140 to 166; see Figures 6.1 and 6.4 for further details). This continuous excess of substrate would favor the proliferation of a r-strategist population, i.e., a *Brocadia*-like anammox genus, as experimentally obtained. Also, the slight excess of nitrite at the end of the cycle could be an indication that the anammox population had a high nitrite half-saturation coefficient, which would be in accordance with the hypothesis that *Brocadia*-like populations are r-strategist. For example, Puyol et al., (2013) reported a nitrite half-saturation coefficient of 5 mg $N\text{-}NO_2$ L^{-1} for a *Brocadia* spp.-dominated anammox culture.

6.4 Conclusions

- The microbial community structure changed during the N-removal recovery process, from a very diverse microbial community just after the temperature shock, to an anammox enriched community in the fully recovered reactor.

- Anammox abundance results were in agreement with the N-removal performance results and SAA measured in the reactor during the recovery process.

- Anammox population shifted from Candidatus Kuenenia sp. just after the temperature shock to Brocadia anammoxidans. This population shift was in agreement with the hypothesis of different kinetic strategies (i.e. either r or K-strategist) of Brocadia and Candidatus Kuenenia genera, as shown in the literature.

6.5 Appendix

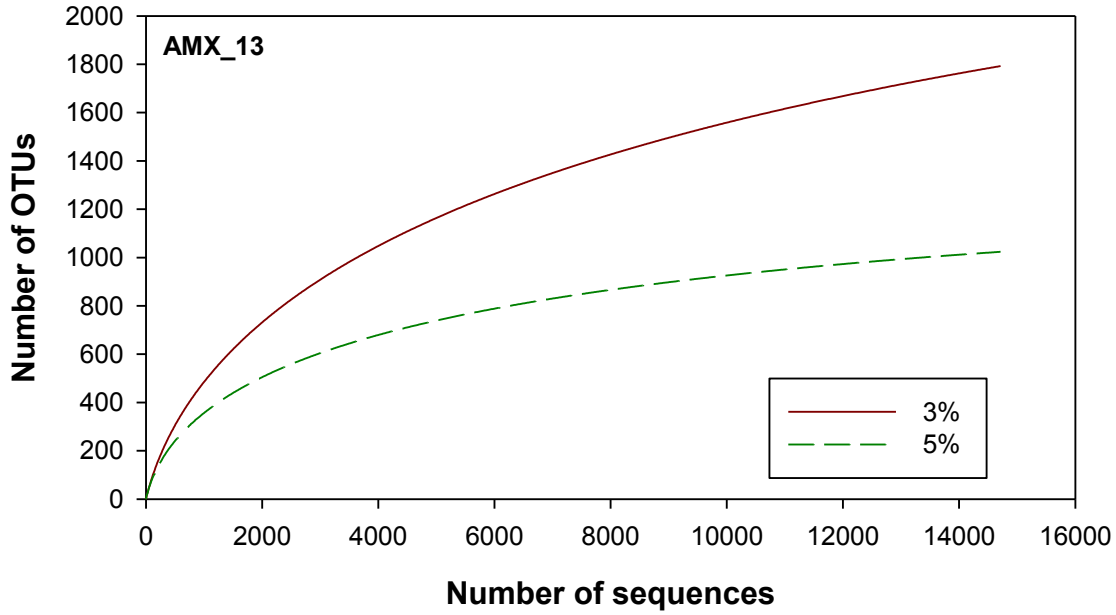

Figure A6.1. Rarefaction curves for libraries AMX_13. OTUs were defined at 3% and 5% distances, respectively.

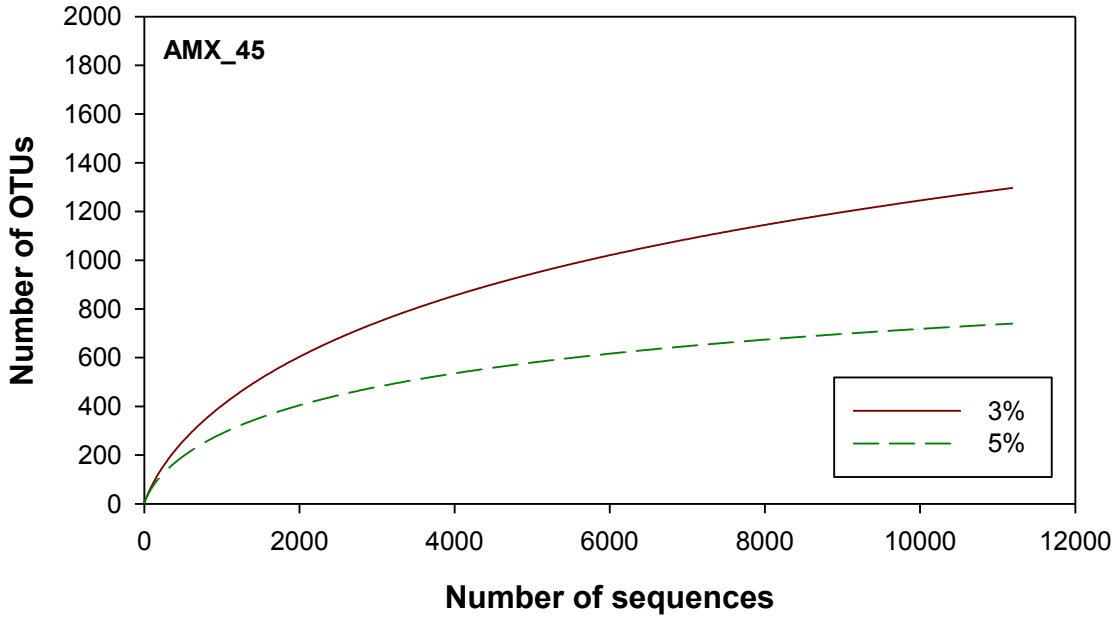

Figure A6.2. Rarefaction curves for libraries AMX_45. OTUs were defined at 3% and 5% distances, respectively.

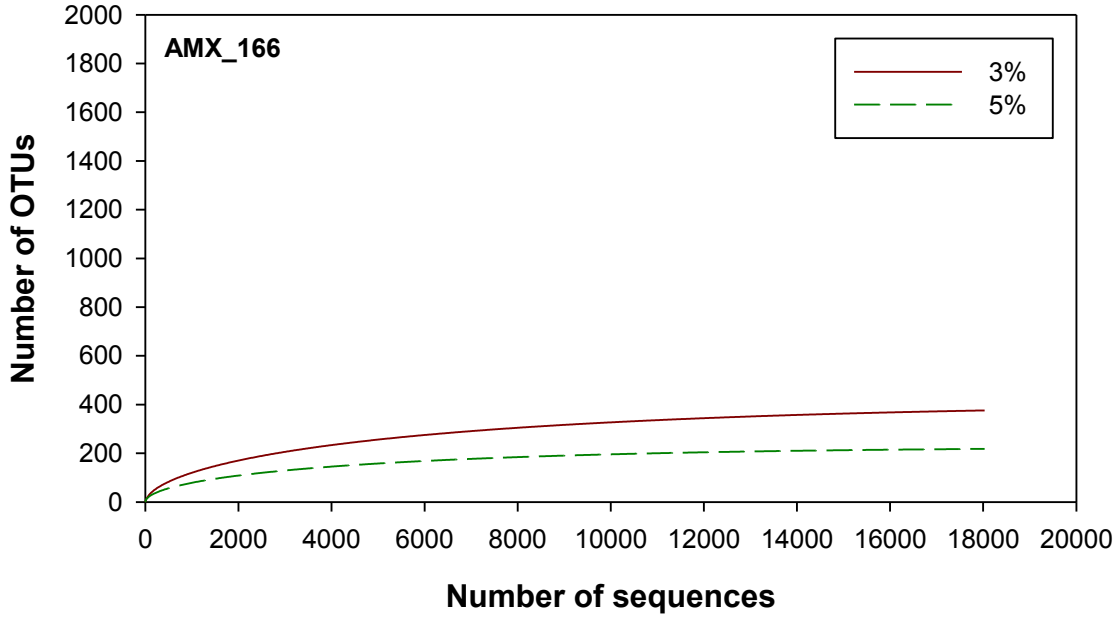

Figure A6.3. Rarefaction curves for libraries AMX_166. OTUs were defined at 3% and 5% distances, respectively.

Table S6.1. Relative abundance of bacteria at genus level for libraries AMX_13, AMX_45 and AMX_166. Relative abundance is defined as the number of sequences affiliated with that taxon divided by the total number of sequences per sample (%).

Kingdom	Phylum	Class	Order	Family	Genus	AMX_13	AMX_45	AMX_166
Bacteria	Acidobacteria	Holophagae	Holophagales	Holophagaceae	*Holophaga*	0.694494	0.398591	-
Bacteria	Acidobacteria	Solibacteres	Solibacterales	Solibacteraceae	*Solibacter*	0.077953	0.083426	-
Bacteria	Actinobacteria	Actinobacteria (class)	Actinomycetales	Frankiaceae	*Frankia*	0.23386	0.157582	-
Bacteria	Actinobacteria	Actinobacteria (class)	Actinomycetales	Micromonosporaceae	*Catellatospora*	5.570123	2.233964	1.030264
Bacteria	Actinobacteria	Actinobacteria (class)	Actinomycetales	Mycobacteriaceae	*Mycobacterium*	0.035433	0.037078	-
Bacteria	Actinobacteria	Actinobacteria (class)	Actinomycetales	Nocardiaceae	*Rhodococcus*	0.25512	0.037078	-
Bacteria	Actinobacteria	Actinobacteria (class)	Rubrobacterales	Rubrobacteraceae	*Rubrobacter*	0.800794	0.750834	0.57367
Bacteria	Actinobacteria	Actinobacteria (class)	Solirubrobacterales	Conexibacteraceae	*Conexibacter*	0.070867	0.111235	-
Bacteria	Actinobacteria	Actinobacteria (class)	Solirubrobacterales	Solirubrobacteraceae	*Solirubrobacter*	0.014173	0.037078	-
Bacteria	Bacteroidetes	Bacteroidia	Bacteroidales	Porphyromonadaceae	*Petrimonas*	0.836227	0.667408	1.832231
Bacteria	Bacteroidetes	Flavobacteriia	Flavobacteriales	Cryomorphaceae	*Owenweeksia*	0.035433	0.482017	-
Bacteria	Bacteroidetes	Flavobacteriia	Flavobacteriales	Flavobacteriaceae	*Flavobacterium*	0.59528	0.018539	0.011708
Bacteria	Bacteroidetes	Sphingobacteriia	Sphingobacteriales	Chitinophagaceae	*Flavisolibacter*	0.035433	-	-
Bacteria	Chloroflexi	Anaerolineae	Anaerolineales	Anaerolineaceae	*Anaerolinea*	0.070867	-	0.872212
Bacteria	Chloroflexi	Anaerolineae	Anaerolineales	Anaerolineaceae	*Levilinea*	0.014173	0.046348	-
Bacteria	Chloroflexi	Caldilineae	Caldilineales	Caldilineaceae	*Caldilinea*	0.070867	0.074156	0.579524
Bacteria	Chloroflexi	Chloroflexi (class)	Chloroflexales	Chloroflexaceae	*Chloroflexus*	1.204734	1.167964	0.175613
Bacteria	Chloroflexi	Thermomicrobia	Sphaerobacterales	Sphaerobacteraceae	*Sphaerobacter*	0.02126	0.018539	-
Bacteria	Fibrobacteres	Fibrobacteria	Fibrobacterales	Fibrobacteraceae	*Fibrobacter*	1.091347	0.84353	0.304396
Bacteria	Firmicutes	Bacilli	Bacillales	Bacillaceae	*Bacillus*	-	-	0.017561
Bacteria	Firmicutes	Clostridia	Clostridiales	Clostridiaceae	*Clostridium*	1.105521	0.973304	0.409764
Bacteria	Firmicutes	Clostridia	Clostridiales	Eubacteriaceae	*Eubacterium*	1.991354	1.103077	-
Bacteria	Firmicutes	Clostridia	Clostridiales	Peptococcaceae	*Desulforudis*	0.76536	0.287356	-

Table S6.1. (continued)

Kingdom	Phylum	Class	Order	Family	Genus	AMX_13	AMX_45	AMX_166
Bacteria	Firmicutes	Clostridia	Clostridiales	Syntrophomonadaceae	*Syntrophomonas*	0.19134	0.157582	-
Bacteria	Gemmatimonadetes	Gemmatimonadetes (class)	Gemmatimonadales	Gemmatimonadaceae	*Gemmatimonas*	-	-	0.017561
Bacteria	Nitrospirae	Nitrospira (class)	Nitrospirales	Nitrospiraceae	*Nitrospira*	0.14882	-	-
Bacteria	Planctomycetes	Planctomycetia	Brocadiales	Brocadiaceae	*Brocadia*	3.373255	32.86986	45.75309
Bacteria	Planctomycetes	Planctomycetia	Candidatus Brocadiales	Candidatus Brocadiaceae	*Candidatus Kuenenia*	3.444122	2.549129	0.450741
Bacteria	Planctomycetes	Planctomycetia	Planctomycetales	Planctomycetaceae	*Pirellula*	0.035433	0.018539	-
Bacteria	Proteobacteria	Alphaproteobacteria	Rhizobiales	Bradyrhizobiaceae	*Bradyrhizobium*	0.113387	0.027809	-
Bacteria	Proteobacteria	Alphaproteobacteria	Rhizobiales	Bradyrhizobiaceae	*Nitrobacter*	0.120473	-	-
Bacteria	Proteobacteria	Alphaproteobacteria	Rhizobiales	Hyphomicrobiaceae	*Hyphomicrobium*	0.304727	0.139043	0.04683
Bacteria	Proteobacteria	Alphaproteobacteria	Rhizobiales	Hyphomicrobiaceae	*Rhodoplanes*	0.226773	0.129774	-
Bacteria	Proteobacteria	Alphaproteobacteria	Rhizobiales	Methylobacteriaceae	*Methylobacterium*	-	0.083426	-
Bacteria	Proteobacteria	Alphaproteobacteria	Rhizobiales	Phyllobacteriaceae	*Mesorhizobium*	0.141733	0.074156	-
Bacteria	Proteobacteria	Alphaproteobacteria	Rhizobiales	Phyllobacteriaceae	*Parvibaculum*	0.120473	0.139043	-
Bacteria	Proteobacteria	Alphaproteobacteria	Rhizobiales	Rhizobiaceae	*Rhizobium*	0.028347	-	0.011708
Bacteria	Proteobacteria	Alphaproteobacteria	Rhodobacterales	Hyphomonadaceae	*Hyphomonas*	0.226773	0.157582	-
Bacteria	Proteobacteria	Alphaproteobacteria	Rhodobacterales	Rhodobacteraceae	*Paracoccus*	0.035433	-	-
Bacteria	Proteobacteria	Alphaproteobacteria	Rhodospirillales	Acetobacteraceae	*Gluconobacter*	0.04252	0.018539	-
Bacteria	Proteobacteria	Alphaproteobacteria	Sphingomonadales	Sphingomonadaceae	*Sphingobium*	0.08504	-	-
Bacteria	Proteobacteria	Alphaproteobacteria	Sphingomonadales	Sphingomonadaceae	*Sphingopyxis*	0.070867	-	-
Bacteria	Proteobacteria	Betaproteobacteria	Betaproteobacteria (order)	Betaproteobacteria (family)	*Denitrobacter*	0.02126	-	-
Bacteria	Proteobacteria	Betaproteobacteria	Betaproteobacteria (order)	Betaproteobacteria (family)	*Nitrotoga*	0.177167	0.037078	-
Bacteria	Proteobacteria	Betaproteobacteria	Burkholderiales	Alcaligenaceae	*Derxia*	6.562256	2.437894	2.745419
Bacteria	Proteobacteria	Betaproteobacteria	Burkholderiales	Burkholderiaceae	*Burkholderia*	0.155907	0.018539	0.076099
Bacteria	Proteobacteria	Betaproteobacteria	Burkholderiales	Burkholderiaceae	*Cupriavidus*	-	-	0.070245

Table S1. (continued)

Kingdom	Phylum	Class	Order	Family	Genus	AMX_13	AMX_45	AMX_166
Bacteria	Proteobacteria	Betaproteobacteria	Burkholderiales	Burkholderiaceae	*Pandoraea*	0.02126	-	-
Bacteria	Proteobacteria	Betaproteobacteria	Burkholderiales	Burkholderiaceae	*Ralstonia*	0.673234	0.231739	0.017561
Bacteria	Proteobacteria	Betaproteobacteria	Burkholderiales	Comamonadaceae	*Acidovorax*	0.077953	-	-
Bacteria	Proteobacteria	Betaproteobacteria	Burkholderiales	Comamonadaceae	*Comamonas*	0.070867	-	-
Bacteria	Proteobacteria	Betaproteobacteria	Burkholderiales	Comamonadaceae	*Polaromonas*	0.290553	0.148313	-
Bacteria	Proteobacteria	Betaproteobacteria	Hydrogenophilales	Hydrogenophilaceae	*Thiobacillus*	0.056693	0.00927	-
Bacteria	Proteobacteria	Betaproteobacteria	Nitrosomonadales	Nitrosomonadaceae	*Nitrosomonas*	0.48898	0.185391	0.784406
Bacteria	Proteobacteria	Betaproteobacteria	Nitrosomonadales	Nitrosomonadaceae	*Nitrosospira*	4.131529	1.001112	4.466429
Bacteria	Proteobacteria	Betaproteobacteria	Rhodocyclales	Rhodocyclaceae	*Denitratisoma*	0.155907	-	-
Bacteria	Proteobacteria	Betaproteobacteria	Rhodocyclales	Rhodocyclaceae	*Sterolibacterium*	0.219687	-	-
Bacteria	Proteobacteria	Betaproteobacteria	Rhodocyclales	Rhodocyclaceae	*Thauera*	-	-	0.035123
Bacteria	Proteobacteria	Betaproteobacteria	Rhodocyclales	Rhodocyclaceae	*Zoogloea*	1.289774	0.6396	-
Bacteria	Proteobacteria	Deltaproteobacteria	Desulfobacterales	Desulfobacteraceae	*Desulfobacter*	-	0.2132	-
Bacteria	Proteobacteria	Deltaproteobacteria	Desulfovibrionales	Desulfovibrionaceae	*Desulfovibrio*	0.2126	0.259548	-
Bacteria	Proteobacteria	Deltaproteobacteria	Desulfuromonadales	Geobacteraceae	*Geobacter*	0.248033	0.231739	-
Bacteria	Proteobacteria	Deltaproteobacteria	Desulfuromonadales	Pelobacteraceae	*Malonomonas*	0.06378	0.018539	-
Bacteria	Proteobacteria	Deltaproteobacteria	Desulfuromonadales	Pelobacteraceae	*Pelobacter*	5.796896	2.085651	-
Bacteria	Proteobacteria	Deltaproteobacteria	Myxococcales	Myxococcaceae	*Anaeromyxobacter*	0.2126	1.937338	-
Bacteria	Proteobacteria	Gammaproteobacteria	Chromatiales	Chromatiaceae	*Nitrosococcus*	0.70158	0.667408	0.275127
Bacteria	Proteobacteria	Gammaproteobacteria	Chromatiales	Chromatiaceae	*Rheinheimera*	0.077953	-	-
Bacteria	Proteobacteria	Gammaproteobacteria	Chromatiales	Ectothiorhodospiraceae	*Thioalkalivibrio*	-	-	0.023415
Bacteria	Proteobacteria	Gammaproteobacteria	Pseudomonadales	Pseudomonadaceae	*Pseudomonas*	0.177167	0.046348	-
Bacteria	Proteobacteria	Gammaproteobacteria	Xanthomonadales	Xanthomonadaceae	*Dokdonella*	1.112607	0.2132	-
Bacteria	Proteobacteria	Gammaproteobacteria	Xanthomonadales	Xanthomonadaceae	*Dyella*	0.092127	-	-
Bacteria	Proteobacteria	Gammaproteobacteria	Xanthomonadales	Xanthomonadaceae	*Thermomonas*	0.06378	0.00927	-
Bacteria	Verrucomicrobia	Verrucomicrobiae	Verrucomicrobiales	Verrucomicrobiaceae	*Verrucomicrobium*	0.049607	-	-
No Hit	No Hit	No Hit	No Hit	No Hit	Unclassified	52.49805	43.71524	39.41931

CHAPTER 7

GENERAL CONCLUSIONS

In this chapter, the overall conclusions and the main achievements of this research are presented.

For Granular Sequencing Batch Reactors:

- A pilot scale GSBR treating a low-strength wastewater was successfully started-up and operated during almost a year.
- Biological nutrient removal in the pilot scale GSBR was successfully achieved, and N-removal was mainly via nitrite.
- Mature granules with good properties could be maintained during more than 5 months. However, short COD overloading events and, probably, the accumulation inorganic particles in the core of the granules caused instability of the granular biomass.
- A novel control strategy that enhanced N-removal in a GSBR was proposed by means of model-based study. This control strategy was only based on online measurement of DO and ammonium at whatever values of granule size, influent C/N ratio or NLR. This control strategy was patented.

For an anammox-based urban wastewater treatment:

- Stable partial nitritation at low temperatures (i.e. 12.5 ºC) was demonstrated to be feasible using a granular airlift reactor applying a low DO/TAN concentrations ratio in the bulk liquid.
- Using a model-based study, the higher oxygen affinity of AOB compared to that of NOB was confirmed to be the key to obtain stable partial nitritation in granular reactors at low temperatures. Additionally, a certain excess of ammonium in the bulk liquid was demonstrated to be required to keep the specific AOB growth rate higher than that of NOB at the conditions of the study.
- The above described achievements open the door for applying a two-stage system (partial nitritation + anammox) in the mainstream treatment.
- Temperature shock in an anammox reactor caused an irreversible loss of activity.
- 454-pyrosequencing analysis was successfully used to monitor microbial community structure changes in the anammox reactor after the temperature shock. Pyrosequencing results were in accordance with macroscopic results in the reactor.

CHAPTER 8

REFERENCES

Abma, W.R., Driessen, W., Haarhuis, R., van Loosdrecht, M.C.M., 2010. Upgrading of sewage treatment plant by sustainable and cost-effective separate treatment of industrial wastewater. Water Sci. Technol. 61, 1715–1722.

Adav, S.S., Lee, D.-J., Lai, J.Y., 2007. Effects of aeration intensity on formation of phenol-fed aerobic granules and extracellular polymeric substances. Appl. Microbiol. Biotechnol. 77, 175–182.

Adav, S.S., Lee, D.-J., Lai, J.-Y., 2009. Biological nitrification-denitrification with alternating oxic and anoxic operations using aerobic granules. Appl. Microbiol. Biotechnol. 84, 1181–1189.

Adav, S.S., Lee, D.-J., Show, K.-Y., Tay, J.-H., 2008. Aerobic granular sludge: recent advances. Biotechnol. Adv. 26, 411–423.

Ahn, J.H., Kwan, T., Chandran, K., 2011. Comparison of partial and full nitrification processes applied for treating high-strength nitrogen wastewaters: microbial ecology through nitrous oxide production. Environ. Sci. Technol. 45, 2734–2740.

Ahn, Y.-H., 2006. Sustainable nitrogen elimination biotechnologies: A review. Process Biochem. 41, 1709–1721.

Amann, R.I., Binder, B.J., Olson, R.J., Chisholm, S.W., Devereux, R., Stahl, D. a, 1990. Combination of 16S rRNA-targeted oligonucleotide probes with flow cytometry for analyzing mixed microbial populations. Appl. Environ. Microbiol. 56, 1919–1925.

Anthonisen, A.C., Loehr, R.C., Prakasam, T.B.S., Srinath, E.G., 1976. Inhibition of nitrification by ammonia and nitrous acid. J. Water Pollut. Control Fed. 48, 835–852.

APHA, 2008. Standard methods for the examination of water and wastewater. American Water Association (Ed.), Washington, DC.

Arrojo, B., Figueroa, M., Mosquera-Corral, A., Campos, J.L., Méndez, R., 2008. Influence of gas flow-induced shear stress on the operation of the Anammox process in a SBR. Chemosphere 72, 1687–1693.

Arrojo, B., Mosquera-Corral, A., Garrido, J.M., Méndez, R., 2004. Aerobic granulation with industrial wastewater in sequencing batch reactors. Water Res. 38, 3389–3399.

Bartrolí, A., Carrera, J., Pérez, J., 2011. Bioaugmentation as a tool for improving the start-up and stability of a pilot-scale partial nitrification biofilm airlift reactor. Bioresour. Technol. 102, 4370–4375.

Bartrolí, A., Pérez, J., Carrera, J., 2010. Applying ratio control in a continuous granular reactor to achieve full nitritation under stable operating conditions. Environ. Sci. Technol. 44, 8930–8935.

Bernet, N., Sanchez, O., Cesbron, D., Steyer, J.-P., Delgenès, J.-P., 2005. Modeling and control of nitrite accumulation in a nitrifying biofilm reactor. Biochem. Eng. J. 24, 173–183.

Beun, J., Hendriks, A., van Loosdrecht, M., Morgenroth, E., Wilderer, P., Heijnen, J., 1999. Aerobic granulation in a sequencing batch reactor. Water Res. 33, 2283–2290.

Beun, J.J., Heijnen, J.J., van Loosdrecht, M.C., 2001. N-removal in a granular sludge sequencing batch airlift reactor. Biotechnol. Bioeng. 75, 82–92.

Beun, J.J., van Loosdrecht, M.C.M., Heijnen, J.J., 2002. Aerobic granulation in a sequencing batch airlift reactor. Water Res. 36, 702–712.

Bishop, P.L., Zhang, T.C., Yun-Chung, F., 1995. Effects of biofilm structure, microbial distributions and mass transport on biodegradation process. Water Sci. Technol. 31 (1), 143–152.

Blackburne, R., Vadivelu, V.M., Yuan, Z., Keller, J., 2007. Kinetic characterisation of an enriched Nitrospira culture with comparison to Nitrobacter. Water Res. 41, 3033–3042.

Bougard, D., Bernet, N., Dabert, P., Delgenes, J.P., Steyer, J.P., 2006. Influence of closed loop control on microbial diversity in a nitrification process. Water Sci. Technol. 53 (4-5), 85–93.

Brockmann, D., Morgenroth, E., 2010. Evaluating operating conditions for outcompeting nitrite oxidizers and maintaining partial nitrification in biofilm systems using biofilm modeling and Monte Carlo filtering. Water Res. 44, 1995–2009.

Byrne, N., Strous, M., Crépeau, V., Kartal, B., Birrien, J.-L., Schmid, M., Lesongeur, F., Schouten, S., Jaeschke, A., Jetten, M., Prieur, D., Godfroy, A., 2009. Presence and activity of anaerobic ammonium-oxidizing bacteria at deep-sea hydrothermal vents. ISME J. 3, 117–123.

Carrera, J., Baeza, J.A., Vicent, T., Lafuente, J., 2003. Biological nitrogen removal of high-strength ammonium industrial wastewater with two-sludge system. Water Res. 37, 4211–4221.

Cassidy, D.P., Belia, E., 2005. Nitrogen and phosphorus removal from an abattoir wastewater in a SBR with aerobic granular sludge. Water Res. 39, 4817–4823.

Chen, F., Liu, Y.-Q., Tay, J.-H., Ning, P., 2011. Operational strategies for nitrogen removal in granular sequencing batch reactor. J. Hazard. Mater. 189, 342–428.

Coma, M., Puig, S., Balaguer, M., Colprim, J., 2010. The role of nitrate and nitrite in a granular sludge process treating low-strength wastewater. Chem. Eng. J. 164, 208–213.

Coma, M., Verawaty, M., Pijuan, M., Yuan, Z., Bond, P.L., 2011. Enhancing aerobic granulation for biological nutrient removal from domestic wastewater. Bioresour. Technol. 103, 101–108.

Cornish Shartau, S.L., Yurkiw, M., Lin, S., Grigoryan, A. a, Lambo, A., Park, H.-S., Lomans, B.P., van der Biezen, E., Jetten, M.S.M., Voordouw, G., 2010. Ammonium concentrations in produced waters from a mesothermic oil field subjected to nitrate injection decrease through formation of denitrifying biomass and anammox activity. Appl. Environ. Microbiol. 76, 4977–4987.

Costa, M.C.M.S., Carvalho, L., Leal, C.D., Dias, M.F., Martins, K.L., Garcia, G.B., Mancuelo, I.D., Hipólito, T., Mac Conell, E.F.A., Okada, D., Etchebehere, C., Chernicharo, C.A.L., Araujo, J.C., 2014. Impact of inocula and operating conditions on the microbial community structure of two anammox reactors. Environ. Technol. 1–12.

Crocetti, G.R., Banfield, J.F., Keller, J., Bond, P.L., Blackall, L.L., 2002. Glycogen-accumulating organisms in laboratory-scale and full-scale wastewater treatment processes. Microbiology 148, 3353–3364.

Crocetti, G.R., Hugenholtz, P., Bond, P.L., Schuler, A., Keller, J., Jenkins, D., Blackall, L.L., 2000. Identification of Polyphosphate-Accumulating Organisms and Design of 16S rRNA-Directed Probes for Their Detection and Quantitation. Appl. Environ. Microbiol. 66, 1175–1182.

Daims, H., Brühl, A., Amann, R., Schleifer, K.H., Wagner, M., 1999. The domain-specific probe EUB338 is insufficient for the detection of all Bacteria: development and evaluation of a more comprehensive probe set. Syst. Appl. Microbiol. 22, 434–444.

Daims, H., Nielsen, J.L., Nielsen, P.H., Schleifer, K.H., Wagner, M., 2001. In situ characterization of Nitrospira-like nitrite-oxidizing bacteria active in wastewater treatment plants. Appl. Environ. Microbiol. 67, 5273–5284.

Dalsgaard, T., Thamdrup, B., 2002. Factors Controlling Anaerobic Ammonium Oxidation with Nitrite in Marine Sediments. Appl. Environ. Microbiol. 68, 3802–3808.

Dapena-Mora, A., Fernández, I., Campos, J.L., Mosquera-Corral, A., Méndez, R., Jetten, M.S.M., 2007. Evaluation of activity and inhibition effects on Anammox process by batch tests based on the nitrogen gas production. Enzyme Microb. Technol. 40, 859–865.

Dapena-Mora, A., Van Hulle, S.W., Luis Campos, J., Méndez, R., Vanrolleghem, P. a, Jetten, M., 2004. Enrichment of Anammox biomass from municipal activated sludge: experimental and modelling results. J. Chem. Technol. Biotechnol. 79, 1421–1428.

De Bruin, L.M.M., de Kreuk, M.K., van der Roest, H.F.R., Uijterlinde, C., van Loosdrecht, M.C.M., 2004. Aerobic granular sludge technology: an alternative to activated sludge? Water Sci. Technol. 49, 1–7.

De Clippeleir, H., Vlaeminck, S.E., De Wilde, F., Daeninck, K., Mosquera, M., Boeckx, P., Verstraete, W., Boon, N., 2013. One-stage partial nitritation/anammox at 15 °C on pretreated sewage: feasibility demonstration at lab-scale. Appl. Microbiol. Biotechnol. 97, 10199–10210.

De Kreuk, M.K., Heijnen, J.J., van Loosdrecht, M.C.M., 2005a. Simultaneous COD, nitrogen, and phosphate removal by aerobic granular sludge. Biotechnol. Bioeng. 90, 761–769.

De Kreuk, M.K., Kishida, N., van Loosdrecht, M.C.M., 2007a. Aerobic granular sludge – state of the art. Water Sci. Technol. 55, 75–81.

De Kreuk, M.K., Picioreanu, C., Hosseini, M., Xavier, J.B., van Loosdrecht, M.C.M., 2007b. Kinetic model of a granular sludge SBR: influences on nutrient removal. Biotechnol. Bioeng. 97, 801–815.

De Kreuk, M.K., Pronk, M., Tay, J., Schwarzenbeck, S.T.L., Wilderer, P.A., 2005b. Aerobic granular sludge (water and environmental management series). IWA Publishing, Munich.

De Kreuk, M.K., van Loosdrecht, M.C.M., 2004. Selection of slow growing organisms as a means for improving aerobic granular sludge stability. Water Sci. Technol. 49, 9–17.

De Kreuk, M.K., van Loosdrecht, M.C.M., 2006. Formation of Aerobic Granules with Domestic Sewage. J. Environ. Eng. 132, 694–697.

Desloover, J., De Clippeleir, H., Boeckx, P., Du Laing, G., Colsen, J., Verstraete, W., Vlaeminck, S.E., 2011. Floc-based sequential partial nitritation and anammox at full scale with contrasting N2O emissions. Water Res. 45, 2811–21.

Dosta, J., Fernández, I., Vázquez-Padín, J.R., Mosquera-Corral, A., Campos, J.L., Mata-Alvarez, J., Méndez, R., 2008. Short- and long-term effects of temperature on the Anammox process. J. Hazard. Mater. 154, 688–693.

Downing, L.S., Nerenberg, R., 2008. Effect of oxygen gradients on the activity and microbial community structure of a nitrifying, membrane-aerated biofilm. Biotechnol. Bioeng. 101, 1193–1204.

Droege, M., Hill, B., 2008. The Genome Sequencer FLX System--longer reads, more applications, straight forward bioinformatics and more complete data sets. J. Biotechnol. 136, 3–10.

Eberl, H.J., van Loosdrecht, M.C.M., Morgenroth, E., Noguera, D.R., Perez, J., Picioreanu, C., Rittmann, B.E., Schwarz, a O., Wanner, O., 2004. Modelling a spatially heterogeneous biofilm and the bulk fluid: selected results from benchmark problem 2 (BM2). Water Sci. Technol. 49, 155–162.

Edgar, R.C., 2010. Search and clustering orders of magnitude faster than BLAST. Bioinformatics 26, 2460–2461.

Edgar, R.C., 2013. UPARSE: highly accurate OTU sequences from microbial amplicon reads. Nat. Methods 10, 996–998.

Edgar, R.C., Haas, B.J., Clemente, J.C., Quince, C., Knight, R., 2011. UCHIME improves sensitivity and speed of chimera detection. Bioinformatics 27, 2194–2200.

Egli, K., Fanger, U., Alvarez, P.J., Siegrist, H., van der Meer, J.R., Zehnder, A.J., 2001. Enrichment and characterization of an anammox bacterium from a rotating biological contactor treating ammonium-rich leachate. Arch. Microbiol. 175, 198–207.

EPA, 2009. Nutrient Control Design Manual. Cincinnati, Ohio.

Fernández, I., Dosta, J., Fajardo, C., Campos, J.L., Mosquera-Corral, A., Méndez, R., 2012. Short- and long-term effects of ammonium and nitrite on the Anammox process. J. Environ. Manage. 95, S170–S174.

Figueroa, M., Val del Río, A., Campos, J.L., Mosquera-Corra, A., Méndez, R., 2011. Treatment of high loaded swine slurry in an aerobic granular reactor. Water Sci. Technol. 63, 1808–1814.

Furukawa, K., Lieu, P.K., Tokitoh, H., Fujii, T., 2006. Development of single-stage nitrogen removal using anammox and partial nitritation (SNAP) and its treatment performances. Water Sci. Technol. 53, 83–90.

Fux, C., Boehler, M., Huber, P., Brunner, I., Siegrist, H., 2002. Biological treatment of ammonium-rich wastewater by partial nitritation and subsequent anaerobic ammonium oxidation (anammox) in a pilot plant. J. Biotechnol. 99, 295–306.

Fux, C., Huang, D., Monti, A., Siegrist, H., 2004. Difficulties in maintaining long-term partial nitritation of ammonium-rich sludge digester liquids in a moving-bed biofilm reactor (MBBR). Water Sci. Technol. 49 (11-12), 53–60.

Garrido, J.M., van Benthum, W.A., van Loosdrecht, M.C.M., Heijnen, J.J., 1997. Influence of dissolved oxygen concentration on nitrite accumulation in a biofilm airlift suspension reactor. Biotechnol. Bioeng. 53, 168–178.

Gu, S., Wang, S., Yang, Q., Yang, P., Peng, Y., 2012. Start up partial nitrification at low temperature with a real-time control strategy based on blower frequency and pH. Bioresour. Technol. 112, 34–41.

Guerrero, J., Guisasola, A., Baeza, J.A., 2011. The nature of the carbon source rules the competition between PAO and denitrifiers in systems for simultaneous biological nitrogen and phosphorus removal. Water Res. 1–10.

Guisasola, A., Jubany, I., Baeza, J.A., Carrera, J., Lafuente, J., 2005. Respirometric estimation of the oxygen affinity constants for biological ammonium and nitrite oxidation. J. Chem. Technol. Biotechnol. 80, 388–396.

Gujer, W., 2010. Nitrification and me - a subjective review. Water Res. 44, 1–19.

Hao, X., Heijnen, J., van Loosdrecht, M.C.M., 2002a. Sensitivity analysis of a biofilm model describing a one-stage completely autotrophic nitrogen removal (CANON) process. Biotechnol. Bioeng. 77, 266–277.

Hao, X., Heijnen, J.J., Van Loosdrecht, M.C.M., 2002b. Model-based evaluation of temperature and inflow variations on a partial nitrification-ANAMMOX biofilm process. Water Res. 36, 4839–4849.

Hao, X.D., Cao, X.Q., Picioreanu, C., van Loosdrecht, M.C.M., 2005. Model-based evaluation of oxygen consumption in a partial nitrification- Anammox biofilm process. Water Sci. Technol. 52, 155–160.

Hao, X.D., van Loosdrecht, M.C.M., 2004. Model-based evaluation of COD influence on a partial nitrification-Anammox biofilm (CANON) process. Water Sci. Technol. 49, 83–90.

Hellinga, C., Schellen, A., Mulder, J., van Loosdrecht, M., Heijnen, J., 1998. The SHARON process: an innovative method for nitrogen removal from ammonium-rich waste water. Water Sci. Technol. 37, 135–142.

Helmer, C., Kunst, S., Juretschko, S., Schmid, M., Schleifer, K., Wagner, M., 1999. Nitrogen loss in a nitrifying biofilm system. Water Sci. Technol. 39, 13–21.

Helmer, C., Schmid, M., Filipov, E., Gaul, T., Hippen, A., Rosenwinkel, K.H., Seyfried, C.F., Wagner, M., Kunst, S., 2002. Deammonification in biofilm systems: population structure and function. Water Sci. Technol. 46, 223–231.

Henze, M., Gujer, W., Mino, T., van Loosdrecht, M.C.M., 2000. Activated sludge models ASM1, ASM2, ASM2d and ASM3. IWA Publishing, London.

Hickey, R.F., Wu, W.M., Veiga, M.C., Jones, R., 1991. Start-up, operation, monitoring and control of high-rate anaerobic treatment systems. Water Sci. Technol. 24, 207–255.

Hippen, A., Helmer, C., Kunst, S., Rosenwinkel, K.H., Seyfried, C.F., 2001. Six years' practical experience with aerobic/anoxic deammonification in biofilm systems. Water Sci. Technol. 44, 39–48.

Hippen, A., Rosenwinkel, K., Baumgarten, G., Seyfried, C.F., 1997. Aerobic deammonification: a new experience in the treatment of waste waters. Water Sci. Technol. 35, 111–120.

Hu, B., Zheng, P., Tang, C., Chen, J., van der Biezen, E., Zhang, L., Ni, B., Jetten, M.S.M., Yan, J., Yu, H.-Q., Kartal, B., 2010. Identification and quantification of anammox bacteria in eight nitrogen removal reactors. Water Res. 44, 5014–5020.

Hu, M., Wang, X., Wen, X., Xia, Y., 2012. Microbial community structures in different wastewater treatment plants as revealed by 454-pyrosequencing analysis. Bioresour. Technol. 117, 72–79.

Hu, Z., Lotti, T., de Kreuk, M., Kleerebezem, R., van Loosdrecht, M.C.M., Kruit, J., Jetten, M.S.M., Kartal, B., 2013. Nitrogen removal by a nitritation-anammox bioreactor at low temperature. Appl. Environ. Microbiol. 79, 2807–2812.

Hunik, J.H., Bos, C.G., van den Hoogen, M.P., De Gooijer, C.D., Tramper, J., 1994. Co-immobilized Nitrosomonas europaea and Nitrobacter agilis cells: validation of a dynamic model for simultaneous substrate conversion and growth in kappa-carrageenan gel beads. Biotechnol. Bioeng. 43, 1153–1163.

Isaka, K., Sumino, T., Tsuneda, S., 2007. High nitrogen removal performance at moderately low temperature utilizing anaerobic ammonium oxidation reactions. J. Biosci. Bioeng. 103, 486–490.

Isanta, E., Suárez-Ojeda, M.E., Val del Río, Á., Morales, N., Pérez, J., Carrera, J., 2012. Long term operation of a granular sequencing batch reactor at pilot scale treating a low-strength wastewater. Chem. Eng. J. 198-199, 163–170.

Jaeschke, A., Op den Camp, H.J.M., Harhangi, H., Klimiuk, A., Hopmans, E.C., Jetten, M.S.M., Schouten, S., Sinninghe Damsté, J.S., 2009. 16S rRNA gene and lipid biomarker evidence for anaerobic ammonium-oxidizing bacteria (anammox) in California and Nevada hot springs. FEMS Microbiol. Ecol. 67, 343–350.

Jaroszynski, L.W., Oleszkiewicz, J.A., 2011. Autotrophic ammonium removal from reject water: partial nitrification and anammox in one-reactor versus two-reactor systems. Environ. Technol. 32, 289–294.

Jemaat, Z., Bartrolí, A., Isanta, E., Carrera, J., Suárez-Ojeda, M.E., Pérez, J., 2013. Closed-loop control of ammonium concentration in nitritation: convenient for reactor operation but also for modeling. Bioresour. Technol. 128, 655–663.

Jin, R.-C., Ma, C., Yu, J.-J., 2013. Performance of an Anammox UASB reactor at high load and low ambient temperature. Chem. Eng. J. 232, 17–25.

Jin, R.-C., Yang, G.-F., Yu, J.-J., Zheng, P., 2012. The inhibition of the Anammox process: A review. Chem. Eng. J. 197, 67–79.

Joss, A., Derlon, N., Cyprien, C., Burger, S., Szivak, I., Traber, J., Siegrist, H., Morgenroth, E., 2011. Combined nitritation-anammox: advances in understanding process stability. Environ. Sci. Technol. 45, 9735–9742.

Joss, A., Salzgeber, D., Eugster, J., König, R., Rottermann, K., Burger, S., Fabijan, P., Leumann, S., Mohn, J., Siegrist, H., 2009. Full-scale nitrogen removal from digester liquid with partial nitritation and anammox in one SBR. Environ. Sci. Technol. 43, 5301–5306.

Jubany, I., Carrera, J., Lafuente, J., Baeza, J.A., 2008. Start-up of a nitrification system with automatic control to treat highly concentrated ammonium wastewater: Experimental results and modeling. Chem. Eng. J. 144, 407–419.

Jubany, I., Lafuente, J., Baeza, J.A., Carrera, J., 2009a. Total and stable washout of nitrite oxidizing bacteria from a nitrifying continuous activated sludge system using automatic control based on Oxygen Uptake Rate measurements. Water Res. 43, 2761–2772.

Jubany, I., Lafuente, J., Carrera, J., Baeza, J.A., 2009b. Automated thresholding method (ATM) for biomass fraction determination using FISH and confocal microscopy. J. Chem. Technol. Biotechnol. 84, 1140–1145.

Julián, E., Roldán, M., Sánchez-Chardi, A., Astola, O., Agustí, G., Luquin, M., 2010. Microscopic cords, a virulence-related characteristic of Mycobacterium tuberculosis, are also present in nonpathogenic mycobacteria. J. Bacteriol. 192, 1751–1760.

Jungles, M.K., Figueroa, M., Morales, N., Val del Río, Á., da Costa, R.H.R., Campos, J.L., Mosquera-Corral, A., Méndez, R., 2011. Start up of a pilot scale aerobic granular reactor for organic matter and nitrogen removal. J. Chem. Technol. Biotechnol. 86, 763–768.

Kaelin, D., Manser, R., Rieger, L., Eugster, J., Rottermann, K., Siegrist, H., 2009. Extension of ASM3 for two-step nitrification and denitrification and its calibration and validation with batch tests and pilot scale data. Water Res. 43, 1680–1692.

Kartal, B., de Almeida, N.M., Maalcke, W.J., Op den Camp, H.J.M., Jetten, M.S.M., Keltjens, J.T., 2013. How to make a living from anaerobic ammonium oxidation. FEMS Microbiol. Rev. 37, 428–461.

Kartal, B., Kuenen, J.G., van Loosdrecht, M.C.M., 2010. Sewage treatment with anammox. Science 328, 702–703.

Kim, D.-J., Kim, S.-H., 2006. Effect of nitrite concentration on the distribution and competition of nitrite-oxidizing bacteria in nitratation reactor systems and their kinetic characteristics. Water Res. 40, 887–94.

Kindaichi, T., Tsushima, I., Ogasawara, Y., Shimokawa, M., Ozaki, N., Satoh, H., Okabe, S., 2007. In situ activity and spatial organization of anaerobic ammonium-oxidizing (anammox) bacteria in biofilms. Appl. Environ. Microbiol. 73, 4931–4939.

Kishida, N., Kim, J., Tsuneda, S., Sudo, R., 2006. Anaerobic/oxic/anoxic granular sludge process as an effective nutrient removal process utilizing denitrifying polyphosphate-accumulating organisms. Water Res. 40, 2303–2310.

Koch, G., Kuhni, M., Gujer, W., 2000. Calibration and validation of Activated Sludge Model No. 3 for Swiss municipal wastewater. Water Res. 34, 3580–3590.

Kong, Y., Nielsen, J.L., Nielsen, P.H., 2005. Identity and ecophysiology of uncultured actinobacterial polyphosphate-accumulating organisms in full-scale enhanced biological phosphorus removal plants. Appl. Environ. Microbiol. 71, 4076–4085.

Kuai, L., Verstraete, W., 1998. Ammonium removal by the oxygen-limited autotrophic nitrification-denitrification system. Appl. Environ. Microbiol. 64, 4500–4506.

Kuenen, J.G., 2008. Anammox bacteria: from discovery to application. Nat. Rev. Microbiol. 6, 320–326.

Lackner, S., Gilbert, E.M., Vlaeminck, S.E., Joss, A., Horn, H., van Loosdrecht, M.C.M., 2014. Full-scale partial nitritation/anammox experiences--an application survey. Water Res. 55, 292–303.

Lee, D.-J., Chen, Y.-Y., Show, K.-Y., Whiteley, C.G., Tay, J.-H., 2010. Advances in aerobic granule formation and granule stability in the course of storage and reactor operation. Biotechnol. Adv. 28, 919–934.

Lettinga, G., van Velsen, A.F.M., Hobma, S.W., de Zeeuw, W., Klapwijk, A., 1980. Use of the upflow sludge blanket (USB) reactor concept for biological wastewater treatment, especially for anaerobic treatment. Biotechnol. Bioeng. 22, 699–734.

Li, Y., Liu, Y., Shen, L., Chen, F., 2008. DO diffusion profile in aerobic granule and its microbiological implications. Enzyme Microb. Technol. 43, 349–354.

Lin, Y.-M., Liu, Y., Tay, J.-H., 2003. Development and characteristics of phosphorus-accumulating microbial granules in sequencing batch reactors. Appl. Microbiol. Biotechnol. 62, 430–435.

Liu, G., Wang, J., 2013. Long-term low do enriches and shifts nitrifier community in activated sludge. Environ. Sci. Technol. 47, 5109–17.

Liu, Q.S., Tay, J.H., Liu, Y., 2003. Substrate concentration-independent aerobic granulation in sequential aerobic sludge blanket reactor. Environ. Technol. 24, 1235–1242.

Liu, Y., Liu, Q.-S., 2006. Causes and control of filamentous growth in aerobic granular sludge sequencing batch reactors. Biotechnol. Adv. 24, 115–127.

Liu, Y., Moy, B., Kong, Y., Tay, J.H., 2010. Formation, physical characteristics and microbial community structure of aerobic granules in a pilot-scale sequencing batch reactor for real wastewater treatment. Enzyme Microb. Technol. 46, 520–525.

Liu, Y., Tay, J.-H., 2004. State of the art of biogranulation technology for wastewater treatment. Biotechnol. Adv. 22, 533–563.

Liu, Y., Wang, Z.-W., Qin, L., Liu, Y.-Q., Tay, J.-H., 2005. Selection pressure-driven aerobic granulation in a sequencing batch reactor. Appl. Microbiol. Biotechnol. 67, 26–32.

Liu, Y., Yang, S.-F., Tay, J.-H., Liu, Q.-S., Qin, L., Li, Y., 2004. Cell hydrophobicity is a triggering force of biogranulation. Enzyme Microb. Technol. 34, 371–379.

López-Palau, S., Pinto, a., Basset, N., Dosta, J., Mata-Álvarez, J., 2012. ORP slope and feast–famine strategy as the basis of the control of a granular sequencing batch reactor treating winery wastewater. Biochem. Eng. J. 68, 190–198.

Lopez-Vazquez, C.M., Kubare, M., Saroj, D.P., Chikamba, C., Schwarz, J., Daims, H., Brdjanovic, D., 2014. Thermophilic biological nitrogen removal in industrial wastewater treatment. Appl. Microbiol. Biotechnol. 98, 945–956.

Lotti, T., Kleerebezem, R., van Erp Taalman Kip, C., Hendrickx, T., Kruit, J., van Loosdrecht, M.C.M., 2014. Anammox growth on pretreated municipal wastewater. Environ. Sci. Technol. In Press.

Lotti, T., van der Star, W.R.L., Kleerebezem, R., Lubello, C., van Loosdrecht, M.C.M., 2012. The effect of nitrite inhibition on the anammox process. Water Res. 46, 2559–2569.

Ma, B., Peng, Y., Zhang, S., Wang, J., Gan, Y., Chang, J., Wang, S., Wang, S., Zhu, G., 2013. Performance of anammox UASB reactor treating low strength wastewater under moderate and low temperatures. Bioresour. Technol. 129, 606–611.

Ma, B., Zhang, S., Zhang, L., Yi, P., Wang, J., Wang, S., Peng, Y., 2011. The feasibility of using a two-stage autotrophic nitrogen removal process to treat sewage. Bioresour. Technol. 102, 8331–8334.

Ma, J., Wang, Z., Yang, Y., Mei, X., Wu, Z., 2012. Correlating microbial community structure and composition with aeration intensity in submerged membrane bioreactors by 454 high-throughput pyrosequencing. Water Res. 47, 859–869.

Mañas, A., Biscans, B., Spéerandio, M., 2011. Biologically induced phosphorus precipitation in aerobic granular sludge process. Water Res. 45, 3776–3786.

Matějů, V., Čižinská, S., Krejčí, J., Janoch, T., 1992. Biological water denitrification—A review. Enzyme Microb. Technol. 14, 170–183.

Maurer, M., Abramovich, D., Siegrist, H., 1999. Kinetics of biologically induced phosphorus precipitation in waste-water treatment. Water Res. 33, 484–493.

McSwain, B.S., Irvine, R.L., 2008. Dissolved oxygen as a key parameter to aerobic granule formation. Water Sci. Technol. 58, 781–787.

McSwain, B.S., Irvine, R.L., Wilderer, P.A., 2004. The effect of intermittent feeding on aerobic granule structure. Water Sci. Technol. 49, 19–25.

Mino, T., van Loosdrecht, M.C.M., Heijnen, J.J., 1998. Microbiology and biochemistry of the enhanced biological phosphate removal process. Water Res. 32, 3193–3207.

Mishima, K., Nakamura, M., 1991. Self-Immobilization of Aerobic Activated Sludge--A Pilot Study of the Aerobic Upflow Sludge Blanket Process in Municipal Sewage Treatment. Water Sci. Technol. 23, 981–990.

Mobarry, B.K., Wagner, M., Urbain, V., Rittmann, B.E., Stahl, D.A., 1996. Phylogenetic probes for analyzing abundance and spatial organization of nitrifying bacteria. Appl. Environ. Microbiol. 62, 2156–2162.

Morgenroth, E., Sherden, T., van Loosdrecht, M., Heijnen, J., Wilderer, P., 1997. Aerobic granular sludge in a sequencing batch reactor. Water Res. 31, 3191–3194.

Mosquera-Corral, A., de Kreuk, M.K., Heijnen, J.J., van Loosdrecht, M.C.M., 2005. Effects of oxygen concentration on N-removal in an aerobic granular sludge reactor. Water Res. 39, 2676–2686.

Moy, B.Y.-P., Tay, J.-H., Toh, S.-K., Liu, Y., Tay, S.T.-L., 2002. High organic loading influences the physical characteristics of aerobic sludge granules. Lett. Appl. Microbiol. 34, 407–412.

Munz, G., Lubello, C., Oleszkiewicz, J. a, 2011a. Modeling the decay of ammonium oxidizing bacteria. Water Res. 45, 557–564.

Munz, G., Lubello, C., Oleszkiewicz, J.A., 2011b. Factors affecting the growth rates of ammonium and nitrite oxidizing bacteria. Chemosphere 83, 720–725.

Ni, B.-J., Fang, F., Xie, W.-M., Yu, H.-Q., 2008a. Growth, maintenance and product formation of autotrophs in activated sludge: taking the nitrite-oxidizing bacteria as an example. Water Res. 42, 4261–4270.

Ni, B.-J., Xie, W.-M., Liu, S.-G., Yu, H.-Q., Wang, Y.-Z., Wang, G., Dai, X.-L., 2009. Granulation of activated sludge in a pilot-scale sequencing batch reactor for the treatment of low-strength municipal wastewater. Water Res. 43, 751–61.

Ni, B.J., Yu, H.Q., 2010. Modeling and simulation of the formation and utilization of microbial products in aerobic granular sludge. AIChE J. 56, 546–559.

Ni, B.-J., Yu, H.-Q., Sun, Y.-J., 2008b. Modeling simultaneous autotrophic and heterotrophic growth in aerobic granules. Water Res. 42, 1583–1594.

Oehmen, A., Lemos, P.C., Carvalho, G., Yuan, Z., Keller, J., Blackall, L.L., Reis, M. a M., 2007. Advances in enhanced biological phosphorus removal: from micro to macro scale. Water Res. 41, 2271–2300.

Olsson, G., 2012. ICA and me--a subjective review. Water Res. 46, 1585–1624.

Oshiki, M., Shimokawa, M., Fujii, N., Satoh, H., Okabe, S., 2011. Physiological characteristics of the anaerobic ammonium-oxidizing bacterium “Candidatus Brocadia sinica”. Microbiology 157, 1706–1713.

Park, H., Rosenthal, A., Jezek, R., Ramalingam, K., Fillos, J., Chandran, K., 2010. Impact of inocula and growth mode on the molecular microbial ecology of anaerobic ammonia oxidation (anammox) bioreactor communities. Water Res. 44, 5005–5013.

Pereira, A.D., Leal, C.D., Dias, M.F., Etchebehere, C., Chernicharo, C.A.L., de Araújo, J.C., 2014. Effect of phenol on the nitrogen removal performance and microbial community structure and composition of an anammox reactor. Bioresour. Technol. 166, 103–111.

Pérez, J., Costa, E., Kreft, J.-U., 2009. Conditions for partial nitrification in biofilm reactors and a kinetic explanation. Biotechnol. Bioeng. 103, 282–295.

Pérez, J., Picioreanu, C., van Loosdrecht, M., 2005. Modeling biofilm and floc diffusion processes based on analytical solution of reaction-diffusion equations. Water Res. 39, 1311–1323.

Picioreanu, C., van Loosdrecht, M., Heijnen, J., 1997. Modelling the effect of oxygen concentration on nitrite accumulation in a biofilm airlift suspension reactor. Water Sci. Technol. 36 (1), 147–156.

Picioreanu, C., van Loosdrecht, M.C., Heijnen, J.J., 2000. Effect of diffusive and convective substrate transport on biofilm structure formation: a two-dimensional modeling study. Biotechnol. Bioeng. 69, 504–515.

Pijuan, M., Werner, U., Yuan, Z., 2009. Effect of long term anaerobic and intermittent anaerobic/aerobic starvation on aerobic granules. Water Res. 43, 3622–3632.

Puyol, D., Carvajal-Arroyo, J.M., Garcia, B., Sierra-Alvarez, R., Field, J. a, 2013. Kinetic characterization of Brocadia spp.-dominated anammox cultures. Bioresour. Technol. 139, 94–100.

Pynaert, K., Smets, B.F., Wyffels, S., Beheydt, D., Siciliano, S.D., Verstraete, W., 2003. Characterization of an Autotrophic Nitrogen-Removing Biofilm from a Highly Loaded Lab-Scale Rotating Biological Contactor. Appl. Environ. Microbiol. 69, 3626–3635.

Regmi, P., Miller, M.W., Holgate, B., Bunce, R., Park, H., Chandran, K., Wett, B., Murthy, S., Bott, C.B., 2014. Control of aeration, aerobic SRT and COD input for mainstream nitritation/denitritation. Water Res. 57, 162–171.

Reichert, P., 1998. AQUASIM 2.0 - Computer program for the identification and simulation of aquatic systems. Swiss Federal Institute of Environmental Science and Technology (EAWG), Switzerland.

Reichert, P., Borchardt, D., Henze, M., Rauch, W., Shanahan, P., Somlyódy, L., Vanrolleghem, P., 2001. River Water Quality Model no. 1 (RWQM1): II. Biochemical process equations. Water Sci. Technol. 43, 11–30.

Ren, T.T., Mu, Y., Liu, L., Li, X.Y., Yu, H.Q., 2009. Quantification of the shear stresses in a microbial granular sludge reactor. Water Res. 43, 4643–4651.

Rosenwinkel, K.-H., Cornelius, A., 2005. Deammonification in the Moving-Bed Process for the Treatment of Wastewater with High Ammonia Content. Chem. Eng. Technol. 28, 49–52.

Rysgaard, S., Glud, R.N., 2004. Anaerobic N2 production in Arctic sea ice. Limnol. Oceanogr. 49, 86–94.

Sáez, P.B., Rittmann, B.E., 1988. Improved pseudoanalytical solution for steady-state biofilm kinetics. Biotechnol. Bioeng. 32, 379–385.

Schmid, M.C., Maas, B., Dapena, A., van de Pas-Schoonen, K., van de Vossenberg, J., Kartal, B., van Niftrik, L., Schmidt, I., Cirpus, I., Kuenen, J.G., Wagner, M., Sinninghe Damsté, J.S., Kuypers, M., Revsbech, N.P., Mendez, R., Jetten, M.S.M., Strous, M., 2005. Biomarkers for in situ detection of anaerobic ammonium-oxidizing (anammox) bacteria. Appl. Environ. Microbiol. 71, 1677–84.

Schmidt, I., Sliekers, O., Schmid, M., Bock, E., Fuerst, J., Kuenen, J.G., Jetten, M.S.M., Strous, M., 2003. New concepts of microbial treatment processes for the nitrogen removal in wastewater. FEMS Microbiol. Rev. 27, 481–492.

Schramm, A., De Beer, D., Gieseke, A., Amann, R., 2000. Microenvironments and distribution of nitrifying bacteria in a membrane-bound biofilm. Environ. Microbiol. 2, 680–686.

Seka, a M., Van De Wiele, T., Verstraete, W., 2001. Feasibility of a multi-component additive for efficient control of activated sludge filamentous bulking. Water Res. 35, 2995–3003.

Seviour, R.J., Mino, T., Onuki, M., 2003. The microbiology of biological phosphorus removal in activated sludge systems. FEMS Microbiol. Rev. 27, 99–127.

Sin, G., Guisasola, A., De Pauw, D.J.W., Baeza, J. a, Carrera, J., Vanrolleghem, P. a, 2005. A new approach for modelling simultaneous storage and growth processes for activated sludge systems under aerobic conditions. Biotechnol. Bioeng. 92, 600–613.

Sin, G., Kaelin, D., Kampschreur, M.J., Takács, I., Wett, B., Gernaey, K. V, Rieger, L., Siegrist, H., van Loosdrecht, M.C.M., 2008. Modelling nitrite in wastewater treatment systems: a discussion of different modelling concepts. Water Sci. Technol. 58, 1155–1171.

Sliekers, a O., Haaijer, S.C.M., Stafsnes, M.H., Kuenen, J.G., Jetten, M.S.M., 2005. Competition and coexistence of aerobic ammonium- and nitrite-oxidizing bacteria at low oxygen concentrations. Appl. Microbiol. Biotechnol. 68, 808–817.

Sliekers, A.O., Third, K.., Abma, W., Kuenen, J.., Jetten, M.S.., 2003. CANON and Anammox in a gas-lift reactor. FEMS Microbiol. Lett. 218, 339–344.

Stephanopoulos, G., 1984. Chemical process control: an introduction to theory and practice. Prentice-Hall, New Jersey.

Strous, M., Heijnen, J.J., Kuenen, J.G., Jetten, M.S.M., 1998. The sequencing batch reactor as a powerful tool for the study of slowly growing anaerobic ammonium-oxidizing microorganisms. Appl. Microbiol. Biotechnol. 50, 589–596.

Strous, M., Jetten, M., 1997. Effects of Aerobic and Microaerobic Conditions on Anaerobic Ammonium-Oxidizing (Anammox) Sludge 63, 2446–2448.

Strous, M., Kuenen, J.G., Jetten, M.S., 1999. Key physiology of anaerobic ammonium oxidation. Appl. Environ. Microbiol. 65, 3248–3250.

Strous, M., Van Gerven, E., Zheng, P., Kuenen, J.G., Jetten, M.S.M., 1997. Ammonium removal from concentrated waste streams with the anaerobic ammonium oxidation (Anammox) process in different reactor configurations. Water Res. 31, 1955–1962.

Su, K.-Z., Ni, B.-J., Yu, H.-Q., 2013. Modeling and optimization of granulation process of activated sludge in sequencing batch reactors. Biotechnol. Bioeng. 110, 1312–1322.

Su, K.-Z., Yu, H.-Q., 2006. A generalized model for aerobic granule-based sequencing batch reactor. 1. Model development. Environ. Sci. Technol. 40, 4703–4708.

Tang, C.-J., Zheng, P., Wang, C.-H., Mahmood, Q., Zhang, J.-Q., Chen, X.-G., Zhang, L., Chen, J.-W., 2011. Performance of high-loaded ANAMMOX UASB reactors containing granular sludge. Water Res. 45, 135–144.

Tay, J., Liu, Q., Liu, Y., 2004. The effect of upflow air velocity on the structure of aerobic granules cultivated in a sequencing batch reactor. Water Sci. Technol. 49, 35–40.

Tay, J.H., Liu, Q.S., Liu, Y., 2001a. The effects of shear force on the formation, structure and metabolism of aerobic granules. Appl. Microbiol. Biotechnol. 57, 227–233.

Tay, J.H., Liu, Q.S., Liu, Y., 2001b. Microscopic observation of aerobic granulation in sequential aerobic sludge blanket reactor. J. Appl. Microbiol. 91, 168–75.

Tchobanoglous, G., Burton, F.L., Stensel, H.D., 2003. Wastewater Engineering: Treatment and Reuse. McGraw-Hill Professional, New York City.

Thanh, B., Visvanathan, C., Aim, R., 2009. Characterization of aerobic granular sludge at various organic loading rates. Process Biochem. 44, 242–245.

Third, K., Sliekers, A., Kuenen, J., Jetten, M.S.., 2001. The CANON system (completely autotrophic nitrogen-removal over nitrite) under ammonium limitation: interaction and competition between three groups of bacteria. Syst. Appl. Microbiol. 24, 588–596.

Toh, S.K., Webb, R.I., Ashbolt, N.J., 2002. Enrichment of autotrophic anaerobic ammonium-oxidizing consortia from various wastewaters. Microb. Ecol. 43, 154–167.

Tokutomi, T., 2004. Operation of a nitrite-type airlift reactor at low DO concentration. Water Sci. Technol. 49 (5-6), 81–88.

Torà, J.A., Lafuente, J., Garcia-Belinchón, C., Bouchy, L., Carrera, J., Baeza, J. a., 2014. High-throughput nitritation of reject water with a novel ammonium control loop: Stable effluent generation for anammox or heterotrophic denitritation. Chem. Eng. J. 243, 265–271.

Torà, J.A., Moliné, E., Carrera, J., Pérez, J., 2013. Efficient and automated start-up of a pilot reactor for nitritation of reject water: From batch granulation to high rate continuous operation. Chem. Eng. J. 226, 319–325.

Tsushima, I., Kindaichi, T., Okabe, S., 2007. Quantification of anaerobic ammonium-oxidizing bacteria in enrichment cultures by real-time PCR. Water Res. 41, 785–794.

Van de Graaf, A.A., de Bruijn, P., Robertson, L.A., Jetten, M.S.M., Kuenen, J.G., 1996. Autotrophic growth of anaerobic ammonium-oxidizing micro-organisms in a fluidized bed reactor. Microbiology 142, 2187–2196.

Van der Star, W.R.L., Abma, W.R., Blommers, D., Mulder, J.-W., Tokutomi, T., Strous, M., Picioreanu, C., van Loosdrecht, M.C.M., 2007. Startup of reactors for anoxic ammonium oxidation: experiences from the first full-scale anammox reactor in Rotterdam. Water Res. 41, 4149–4163.

Van der Star, W.R.L., Miclea, A.I., van Dongen, U.G.J.M., Muyzer, G., Picioreanu, C., van Loosdrecht, M.C.M., 2008. The membrane bioreactor: a novel tool to grow anammox bacteria as free cells. Biotechnol. Bioeng. 101, 286–294.

Van Hulle, S.W.H., Vandeweyer, H.J.P., Meesschaert, B.D., Vanrolleghem, P. a., Dejans, P., Dumoulin, A., 2010. Engineering aspects and practical application of autotrophic nitrogen removal from nitrogen rich streams. Chem. Eng. J. 162, 1–20.

Van Loosdrecht, M., Pot, M., Heijnen, J., 1997. Importance of bacterial storage polymers in bioprocesses. Water Sci. Technol. 35, 41–47.

Vangsgaard, A.K., Mauricio-Iglesias, M., Gernaey, K. V, Smets, B.F., Sin, G., 2012. Sensitivity analysis of autotrophic N removal by a granule based bioreactor: Influence of mass transfer versus microbial kinetics. Bioresour. Technol. 123, 230–241.

Vázquez-Padín, J.R., Mosquera-Corral, A., Campos, J.L., Méndez, R., Carrera, J., Pérez, J., 2010. Modelling aerobic granular SBR at variable COD/N ratios including accurate description of total solids concentration. Biochem. Eng. J. 49, 173–184.

Visvanathan, C., Aim, R. Ben, Parameshwaran, K., 2000. Membrane Separation Bioreactors for Wastewater Treatment. Crit. Rev. Environ. Sci. Technol. 30, 1–48.

Volcke, E.I.P., Picioreanu, C., De Baets, B., van Loosdrecht, M.C.M., 2010. Effect of granule size on autotrophic nitrogen removal in a granular sludge reactor. Environ. Technol. 31, 1271–1280.

Volcke, E.I.P., Picioreanu, C., De Baets, B., van Loosdrecht, M.C.M., 2012. The granule size distribution in an anammox-based granular sludge reactor affects the conversion--implications for modeling. Biotechnol. Bioeng. 109, 1629–1636.

Wagner, M., Loy, A., Nogueira, R., Purkhold, U., Lee, N., Daims, H., 2002. Microbial community composition and function in wastewater treatment plants. Antonie Van Leeuwenhoek 81, 665–680.

Wagner, M., Rath, G., Koops, H., Flood, J., Amann, R., 1996. In situ analysis of nitrifying bacteria in sewage treatment plants. Water Sci. Technol. 34, 237–244.

Wang, J., Yang, N., 2004. Partial nitrification under limited dissolved oxygen conditions. Process Biochem. 39, 1223–1229.

Wang, S.-G., Liu, X.-W., Gong, W.-X., Gao, B.-Y., Zhang, D.-H., Yu, H.-Q., 2007. Aerobic granulation with brewery wastewater in a sequencing batch reactor. Bioresour. Technol. 98, 2142–2147.

Wanner, O., Eberl, H., Morgenroth, E., Nogueira, R., Picioreanu, C., Rittmann, B.E., van Loosdrecht, M.C.M., 2006. Mathematical modeling of biofilms. IWA Publishing, Fairford.

Wanner, O., Reichert, P., 1996. Mathematical modeling of mixed-culture biofilms. Biotechnol. Bioeng. 49, 172–184.

Watson, S.W., Bock, E., Harms, H., Koops, H.P., Hooper, A., 1989. Bergey's manual of systematic bacteriology. The Willians & Wilkins Co., Baltimore.

Weissenbacher, N., Takacs, I., Murthy, S., Fuerhacker, M., Wett, B., 2010. Gaseous nitrogen and carbon emissions from a full-scale deammonification plant. Water Environ. Res. 82, 169–175.

Wett, B., 2007. Development and implementation of a robust deammonification process. Water Sci. Technol. 56, 81–88.

Wett, B., Hell, M., Nyhuis, G., Puempel, T., Takacs, I., Murthy, S., 2010. Syntrophy of aerobic and anaerobic ammonia oxidisers. Water Sci. Technol. 61, 1915–1922.

Wett, B., Omari, A., Podmirseg, S.M., Han, M., Akintayo, O., Gómez Brandón, M., Murthy, S., Bott, C., Hell, M., Takács, I., Nyhuis, G., O'Shaughnessy, M., 2013. Going for mainstream deammonification from bench to full scale for maximized resource efficiency. Water Sci. Technol. 68, 283–289.

Wiesmann, U., 1994. Biological nitrogen removal from wastewater. Adv. Biochem. Eng. Biotechnol. 51, 113–54.

Winkler, M.K.H., Bassin, J.P., Kleerebezem, R., de Bruin, L.M.M., van den Brand, T.P.H., van Loosdrecht, M.C.M., 2011a. Selective sludge removal in a segregated aerobic granular biomass system as a strategy to control PAO-GAO competition at high temperatures. Water Res. 45, 3291–3299.

Winkler, M.K.H., Kleerebezem, R., Kuenen, J.G., Yang, J., van Loosdrecht, M.C.M., 2011b. Segregation of biomass in cyclic anaerobic/aerobic granular sludge allows the enrichment of anaerobic ammonium oxidizing bacteria at low temperatures. Environ. Sci. Technol. 45, 7330–7337.

Winkler, M.K.H., Kleerebezem, R., van Loosdrecht, M.C.M., 2012. Integration of anammox into the aerobic granular sludge process for main stream wastewater treatment at ambient temperatures. Water Res. 46, 136–144.

Wyffels, S., Boeckx, P., Pynaert, K., Zhang, D., Van Cleemput, O., Chen, G., Verstraete, W., 2004. Nitrogen removal from sludge reject water by a two-stage oxygen-limited autotrophic nitrification denitrification process. Water Sci. Technol. 49, 57–64.

Xavier, J.B., de Kreuk, M.K., Picioreanu, C., van Loosdrecht, M.C.M., 2007. Multi-scale individual-based model of microbial and bioconversion dynamics in aerobic granular sludge. Environ. Sci. Technol. 41, 6410–7.

Xie, B., Lv, Z., Hu, C., Yang, X., Li, X., 2013. Nitrogen removal through different pathways in an aged refuse bioreactor treating mature landfill leachate. Appl. Microbiol. Biotechnol. 97, 9225–9234.

Yamamoto, T., Takaki, K., Koyama, T., Furukawa, K., 2006. Novel partial nitritation treatment for anaerobic digestion liquor of swine wastewater using swim-bed technology. J. Biosci. Bioeng. 102, 497–503.

Yang, W., Cicek, N., Ilg, J., 2006. State-of-the-art of membrane bioreactors: Worldwide research and commercial applications in North America. J. Memb. Sci. 270, 201–211.

Ye, L., Shao, M., Zhang, T., Tong, A.H.Y., Lok, S., 2011. Analysis of the bacterial community in a laboratory-scale nitrification reactor and a wastewater treatment plant by 454-pyrosequencing. Water Res. 45, 4390–4398.

Yilmaz, G., Lemaire, R., Keller, J., Yuan, Z., 2008. Simultaneous nitrification, denitrification, and phosphorus removal from nutrient-rich industrial wastewater using granular sludge. Biotechnol. Bioeng. 100, 529–541.

Yuan, Q., Oleszkiewicz, J.A., 2011. Low temperature biological phosphorus removal and partial nitrification in a pilot sequencing batch reactor system. Water Sci. Technol. 63, 2802–2807.

Yuan, X., Gao, D., 2010. Effect of dissolved oxygen on nitrogen removal and process control in aerobic granular sludge reactor. J. Hazard. Mater. 178, 1041–1045.

Zheng, Y.-M., Yu, H.-Q., Liu, S.-J., Liu, X.-Z., 2006. Formation and instability of aerobic granules under high organic loading conditions. Chemosphere 63, 1791–1800.